

AROMATIZATION OF LIGHT NAPHTHA

BY

MOHAMMED OSAMA JUMAH ELLOUH

A Thesis Presented to the
DEANSHIP OF GRADUATE STUDIES

KING FAHD UNIVERSITY OF PETROLEUM & MINERALS
DHAHRAN, SAUDI ARABIA

In Partial Fulfillment of the
Requirements for the Degree of

MASTER OF SCIENCE

In

CHEMICAL ENGINEERING

DECEMBER 2019

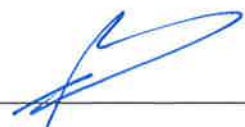
KING FAHD UNIVERSITY OF PETROLEUM & MINERALS
DHAHRAN- 31261, SAUDI ARABIA
DEANSHIP OF GRADUATE STUDIES

This thesis, written by **MOHAMMED OSAMA JUMAH ELLOUH** under the direction of his thesis advisor and approved by his thesis committee, has been presented and accepted by the Dean of Graduate Studies, in partial fulfillment of the requirements for the degree of **MASTER OF SCIENCE IN CHEMICAL ENGINEERING**.


Dr. Hassan Al-Asiri
(Advisor)


Dr. Mamdouh Al-Harthi
Department Chairman


Dr. Ziyauddin Qureshi
(Member)


Dr. Salam A. Zummo
Dean of Graduate Studies




Dr. Mohammed Hossain
(Member)

24/12/19
Date

© Mohammed Ellouh

2019

[It is an honest appreciativeness and genuine regard that this work is dedicated to my beloved family without whom this dissertation would have been completed.]

ACKNOWLEDGMENTS

First of all, my honest gratitude goes to Almighty Allah who has provided me all needed to complete this work magnificently. All over this entire study, he provided me with knowledge, health; strength and patience to successfully finish this study. Many thanks are to King Fahd University of Petroleum and Minerals (KFUPM) and Chemical Engineering department for their unlimited support throughout these last couple of years as undergraduate and graduate student.

All thanks, support, guidance, valuable comments and mentorship to my advisor Professor Hassan Al-Asiri is extremely appreciated. It is important to know that you are a necessary piece in this puzzle and your comments and recommendations do not go unnoticed. Your service and dedication is highly valued, and others do know too. Moreover, I wish to thank my committee members Professor Mohammed Hossain and Ziauddin Qureshi who were extremely generous with their knowledge and priceless time and their appreciated contribution of this study.

Special thanks go to the members of Centre of Refining and Petrochemicals (CRP) for their persistent support and allowing me to utilize the facilities available in the CRP in the meantime of the lab work. Also, I would like to thank Dr. Abdullah Aitani, , Dr. Muhammed Akhtar, Dr. Shakeel Ahmad, Dr. Sayed Ali, Dr. Jassir E.A and Dr. Rajish Theravalappil for their contribution and counsels and assisting me in my lab work and study. In addition, all the technical support from Mr. Saad Al-Qahtani , Mr. Tanimu Gazali and Mr. Roy Villarmino are greatly respected.

I am very grateful and appreciative to my parents, my brothers (Mahmoud, Ahmad and Anas), our neighbors and my whole family for their unlimited support, inspiration and prayers.

Finally, I want to thank my friends and colleagues Mr. Salem Boraik, Mr. Hussain Al-Saggaf, Mr. Mohammed Al-Joffery, Mr. Abdullah Al-Mashhour, Mr. Hamed Al-Saggaf , Mr. Amre Al-Amri, Mr. Akram AL-Absi, Mr. Mohammed Al-Tairi, Mr. Mahfoudh Jubran, Mr. Kareem Zahr, Mr. Mohammed Al-Koriami and Mr. Abdullah Atta.

TABLE OF CONTENTS

ACKNOWLEDGMENTS	V
TABLE OF CONTENTS.....	VII
LIST OF TABLES.....	XI
LIST OF FIGURES.....	XIII
LIST OF ABBREVIATIONS.....	XVI
ABSTRACT.....	XVII
ملخص الرسالة.....	XIX
CHAPTER 1 INTRODUCTION.....	1
1.1 Background.....	1
1.2 Aromatics Demand and Production	4
1.3 Aromatization of Light Naphtha.....	12
1.4 Thesis Objectives	14
1.5 Thesis Scope.....	15
1.6 References	16
CHAPTER 2 LITERATURE REVIEW	18
2.1 Background.....	18
2.2 Types of Catalysts	18
2.2.1 Background on Zeolites	19
2.2.2 Metal Supported Catalysts Performance Summary	22
2.3 Catalyst Synthesis	28
2.3.1 Synthesis of Conventional (Micro) H-ZSM-5	28

2.3.2	Synthesis of Metal Supported on Different Zeolites	29
2.4	Chemistry and Mechanisms of Aromatization of Light Naphtha	29
2.5	Characterization Techniques of Catalysts	32
2.5.1	Power X-ray Diffraction (XRD) Test	33
2.5.2	Temperature Programed Desorption (TPD) Test	34
2.5.3	Temperature Programed Reduction (TPR) Test	36
2.5.4	Surface Area (BET) Test	36
2.5.5	Infrared Spectroscopy (FT-IR) Test	38
2.6	References.....	39
CHAPTER 3 MATERIALS AND METHODS.....		44
3.1	Background	44
3.2	Feed.....	44
3.3	Catalyst Synthesis.....	45
3.3.1	Preparation of Metal Supported Catalyst by Wet Co- Impregnation Method.....	45
3.3.2	Nano ZSM-5 Synthesis.....	46
3.4	Catalysts	46
3.5	Evaluation of the Catalyst.....	47
3.6	References.....	48
CHAPTER 4 EFFECT OF $\text{SiO}_2/\text{Al}_2\text{O}_3$ MOLAR RATIO OF MFI-TYPE		
ZEOLITE CATALYST ON LIGHT NAPHTHA AROMATIZATION		49
4.1	Background	49
4.2	Introduction	49
4.3	Experimental	51
4.3.1	Reagents.....	51

4.3.2	Catalyst Preparation and Light Straight Run Naphtha Feed	51
4.3.3	Catalyst Characterization	52
4.3.4	Catalyst Evaluation	53
4.4	Results and Discussion	54
4.4.1	Catalyst Characterization	54
4.4.2	Catalyst Evaluation	59
4.5	References	62

CHAPTER 5 AROMATIZATION OF LIGHT NAPHTHA OVER BIMETALLIC

	MO-M/ZSM-5 MODIFIED CATALYSTS	64
5.1	Background	64
5.2	Introduction	64
5.3	Experimental.....	67
5.3.1	Catalyst Synthesis	67
5.3.2	Catalyst Characterization	68
5.3.3	Catalyst Evaluation	69
5.4	Results and Discussion	70
5.4.1	Catalyst Characterization	70
5.4.2	Catalytic Performance.....	76
5.4.3	Effect of Time-On-Stream	78
5.5	References	82

CHAPTER 6 AROMATIZATION OF LIGHT PARAFFINIC NAPHTHA OVER

	PT-M/ZSM-5 TRI-COMPOSITED CATALYSTS	87
6.1	Background	87
6.2	Introduction.....	87

6.3	Experimental	91
6.3.1	Catalyst Preparation	91
6.3.2	Catalyst Characterization	92
6.3.3	Catalyst Characterization	93
6.3.4	Catalyst Evaluation	94
6.4	Results and Discussion.....	96
6.4.1	Catalyst Characterization	96
6.4.2	Catalyst Evaluation	103
6.4.3	Effect of Time-on-Stream	107
6.5	References.....	109
 CHAPTER 7 CONCLUSIONS AND RECOMMNDATIONS.....		 114
7.1	Background	114
7.2	Conclusions.....	114
7.3	Recommendations.....	116
 VITAE.....		 117

LIST OF TABLES

CHAPTER 2

Table 2.1: Summary of industrial synthesized zeolites with some properties [7] a: catalyst number b: pore size c: maximum free sphere diameter d: maximum included sphere diameter e: ICP analysis	21
Table 2.2: Zinc performance summary for aromatization of light naphtha	23
Table 2.3: Platinum performance summary for aromatization of light naphtha	24
Table 2.4: Gallium performance summary for aromatization of light naphtha.	25
Table 2.5: Other metals performance summary for aromatization of light naphtha	26
Table 2.6: Mixture performance summary for aromatization of light naphtha	27

CHAPTER 3

Table 3.1: Composition of light straight run naphtha feed	44
---	----

CHAPTER 4

Table 4.1: Composition of light straight run naphtha feed	52
Table 4.2: Textural properties of the MFI samples catalysts	54
Table 4.3: NH ₃ TPD profiles for MFI samples with SiO ₂ /Al ₂ O ₃ (23, 30, 50, 280, and 1500) molar ratios	57
Table 4.4: Catalytic performance of thermal and parent MFI with SiO ₂ /Al ₂ O ₃ (23, 30, 50, 280, and 1500) ratios catalysts (Reaction conditions: Catalyst= 0.5 g, Feed= LSRN, Temp. = 550 oC, WHSV= 1 h ⁻¹ , N ₂ = 10 mL/min)	61

CHAPTER 5

Table 5.1: Composition of light naphtha feed (100% Total).....	70
Table 5.2: Textural properties of ZSM-5 and bi-metallic modified catalysts.....	72
Table 5.3: (NH ₃ -TPD) and strong acidic sites for parent and modified ZSM-5.....	74
Table 5.4: Catalytic performance of parent ZSM-5 and bi-metal modified ZSM-5 (Reaction conditions: Catalyst= 0.5 g, Feed= LSRN, Temp. = 550 °C, WHSV= 1 h ⁻¹ , N ₂ = 10 mL/min).....	80

CHAPTER 6

Table 6.1: Composition of light straight run naphtha feed (wt. %).....	94
Table 6.2: Textural properties of parent and modified ZSM-5 catalysts.....	96
Table 6.3: Total acidity and acid strength distribution of the parent and Pt or Pt-M modified ZSM-5 catalysts from NH ₃ -TPD.....	101
Table 6.4: Catalytic performance of parent and modified ZSM-5 (Reaction conditions: Catalyst= 0.5 g, Feed= LSRN, Temp. = 550 °C, WHSV= 1 h ⁻¹ , N ₂ = 10 mL/min).	105

LIST OF FIGURES

CHAPTER 1

Figure 1.1: Oil raffinate composition.....	3
Figure 1.2: Expected petrochemicals growth for 2020 and 2030 aromatics (BTX) [10] ...	4
Figure 1.3: BTX consumptions: a) Benzene, b) Toluene, c) Xylenes	5
Figure 1.4: The consumption of benzene by derivative in west European region 2013 [11].....	6
Figure 1.5: BTX usage in petrochemical industry [14]	7
Figure 1.6: Aromatics main sources [13]	8
Figure 1.7: Aromatics region distributions [13]	9
Figure 1.8: Trend of diesel and gasoline main structures [13]	10
Figure 1.9: Aromatics production different routes [13].....	11
Figure 1.10: nC ₆ Aromatization using acidic and metal zeolites [19]	13

CHAPTER 2

Figure 2.1: Different zeolites structure with varying pore sizes [5]	20
Figure 2.2: Aromatization of light naphtha three main mechanism steps [31].....	30
Figure 2.3: Aromatization of nC ₆ over bifunctional catalyst possible mechanism route [11].....	32
Figure 2.4: XRD sample's intensity curves [36]	34
Figure 2.5: TPD Example with NH ₃ [37]	35
Figure 2.6: Brønsted and Lewis Paths in zeolites with NH ₃ [38]	35
Figure 2.7: Langmuir's model equation and layers appearance [42].....	38

CHAPTER 3

Figure 3.1: Micro fixed bed reactor set up scheme.....	48
--	----

CHAPTER 4

Figure 4.1: Nitrogen adsorption-desorption isotherms of the MFI zeolite samples with SiO ₂ /Al ₂ O ₃ (23, 30, 50, 280, and 1500) molar ratios.....	55
Figure 4.2: BJH pore size of the MFI zeolite samples with SiO ₂ /Al ₂ O ₃ (23, 30, 50, 280, and 1500) ratios	55
Figure 4.3: XRD patterns of the MFI zeolite samples with SiO ₂ /Al ₂ O ₃ (23, 30, 50, 280, and 1500) molar ratios	56
Figure 4.4: NH ₃ -TPD curves for the parent MFI zeolite samples with SiO ₂ /Al ₂ O ₃ (23, 30, 50, 280, and 1500) ratios	57
Figure 4.5: The SEM images of MFI zeolite samples with several SiO ₂ /Al ₂ O ₃ (23, 30, 50, 280, and 1500) ratios	58
Figure 4.6: The effect of SiO ₂ /Al ₂ O ₃ (23, 30, 50, 280, and 1500) molar ratios catalysts, in the conversion of LSRN at 550 °C and 1.0 h ⁻¹ WHSV, Atmospheric pressure (a) Liquid yield, (b) Gas yield.....	60

CHAPTER 5

Figure 5.1: XRD patterns of H-ZSM-5 and other metal modified catalysts.....	71
Figure 5.2: N ₂ adsorption-desorption isotherms for parent and modified ZSM-5.....	72
Figure 5.3: BJH pore size distribution for parent and modified ZSM-5.....	73
Figure 5.4: NH ₃ -TPD patterns for ZSM-5 and bi-metallic modified catalysts.....	74
Figure 5.5: SEM images for parent Z30 and modified Mo/Z30 and Mo-Zn/Z30	75
Figure 5.6: Elemental mapping for modified Mo-Zn/Z30 catalyst.....	75
Figure 5.7: The effect of the parent and Mo or Mo-M modified Z30 catalysts, prepared by the co-impregnation method, in the conversion of LSRN at 550 °C and 1.0 h ⁻¹ WHSV. (a) Liquid yield, (b) Gas yield.....	77
Figure 5.8: Time-on-stream for aromatization of LSRN over the Mo-Zn/Z30 liquid and gaseous product distribution (WHSV= 1h ⁻¹ , feed=0.01 mL/min, N ₂ = 10 mL/min, T=550 °C). (a) Liquid yield, (b) Gas yield.....	79
Figure 5.9: Reproducibility test for Mo-Zn/Z30 a) liquid Yield b) Gas yield	81

CHAPTER 6

Figure 6.1: Nitrogen adsorption-desorption isotherms of parent and modified ZSM-5(30) catalysts.....	97
Figure 6.2: The BJH pore size of parent and modified ZSM-5(30) catalysts.....	98
Figure 6.3: XRD patterns of the parent and modified ZSM-5(30) catalysts	99
Figure 6.4: The SEM images of (a) Z30, (b) Pt/Z30, (c) Pt-Zn/Z30, (d) Pt-La/Z30, (e) Pt-Ga/Z30, and (f) Pt-Fe/Z30 catalysts	100
Figure 6.5: The homogeneous elemental dispersion of (a) O (b) Al, (c) Si, (d) Ga and (e) Pt in Z30 revealed by EDXS mapping of the Pt-Ga/Z30 catalyst ...	100
Figure 6.6: NH ₃ -TPD curves obtained for the parent and modified ZSM-5(30) catalysts.....	102
Figure 6.7: The effect of the parent and Pt or Pt-M modified Z30 catalysts, prepared by the co-impregnation method, in the conversion of LSRN at 550 °C and 1.0 h ⁻¹ WHSV. (a) Liquid yield, (b) Gas yield.....	104
Figure 6.8: Repeociability results for Pt-Ga/Z30 a) liquid b) gas yield	106
Figure 6.9: Time-on-stream for aromatization of LSRN over the Pt-Ga/Z30 liquid and gaseous product distribution (WHSV=1 h ⁻¹ , feed=0.01 mL/min, N ₂ =10 mL/min, T=550 °C). (a) Liquid yield, (b) Gas yield	108

LIST OF ABBREVIATIONS

ZSM-5 (MFI)	:	Zeolite Socony Mobil Five
LSRN	:	Light Straight Run Naphtha.
XRD	:	X-Ray Diffraction.
BET	:	Brunauer-Emmett-Teller
BJH	:	Barrett Joyner Halenda
WHSV	:	Weight Hour Space Velocity
BTEX	:	Benzene, Toluene, Ethylbenzene, Xylene
SEM	:	Scanning Electron Microscopy
TPD	:	Temperature Programmed Desorption
SAR	:	Silica Alumina Ratio
TOS	:	Time On Stream.
PIONA	:	Paraffin, Iso paraffins, Olefins, Naphthenes, Aromatics
TPR	:	Temperature Programmed Reduction
DHA GC	:	Detailed Hydrocarbons Analysis Gas Chromatograph
EDX	:	Energy Dispersion X-ray
FID	:	Flame Ionization Detector

ABSTRACT

Full Name : [Mohammed Osama Jumah Ellouh]

Thesis Title : [Aromatization of Light Naphtha]

Major Field : [Chemical Engineering]

Date of Degree : [December 2019]

The aromatization of light paraffinic naphtha (C_5 - C_6) was investigated over 1.0 wt. % Pt-M/ZSM-5 (MFI) [Si/2Al=30] and 2 wt. % Mo-M/ZSM-5[Si/2Al=30] (modifier M= 1 wt. % Zn, 2 wt. % of Fe, Ce, La, and Ga) tri-composited catalysts prepared using wet-impregnation method. The effects of (Pt , Mo) and modifier M on light naphtha conversion, yields and selectivity towards aromatics (benzene, toluene, xylenes, C_9+ aromatics) were studied using fixed-bed flow-type reactor at 550 °C, atmospheric pressure, and WHSV: 1 h⁻¹. The catalytic performances of Pt/ZSM-5 and Pt-M/ZSM-5 catalysts were compared with the conventional ZSM-5 catalyst. While the yield of total aromatics over Pt/ZSM-5 di-composited catalyst compared with the ZSM-5 sole catalyst was slightly increased from 32 wt. % to 37 wt. % and for Mo/ZSM-5 enhanced in a similar manner from 32 wt. % to 42 wt. %. The value for Pt-Ga/ZSM-5 tri-composited catalyst was significantly improved to 60 wt. % and for Mo-Ga/ZSM-5, Mo-Zn/ZSM-5 around 62 wt. %. The higher selectivity towards aromatics is due to the dehydrogenation activity of M added species. The species associated with platinum and molybdenum is effective in the conversion of light paraffinic naphtha to the olefins, which later converted into aromatics by secondary reactions: cracking, isomerization and dimerization.

Different characterization techniques are used to describe the nature and the behavior of the samples such as XRD, BET, NH₃-TPD and SEM. The Pt-Ga/ZSM-5 and Mo-Zn/ZSM-5 tri-composited catalyst also showed a good stability toward the selective production of aromatics.

Furthermore, the effect of SiO₂/Al₂O₃ of ZSM-5 (MFI) of light alkanes conversion to aromatics is studied. Relationships are attainable between the light naphtha conversion and aromatics yield, as the conversion relies on SiO₂/Al₂O₃ ratio of MFI zeolite. Varying SiO₂/Al₂O₃ ratio affects the acidity of the MFI zeolite and hence the production of aromatics. MFI zeolite with SiO₂/Al₂O₃ 30 zeolites attained the high yield of aromatics 59 wt. %.

ملخص الرسالة

الاسم الكامل: محمد أسامة جمعة اللوح

عنوان الرسالة: تعطير المركبات الهيدروكربونية الخفيفة

التخصص: الهندسة الكيميائية

تاريخ الدرجة العلمية: ديسمبر 2019

تعتبر المركبات العطرية من أهم المركبات الكيميائية التي تدخل في بعض الصناعات الكيميائية. تمت دراسة تحويل المركبات الهيدروكربونية الخفيفة (C_5-C_6) إلى مركبات عطرية بواسطة فحص كمية مئوية واحدة من البلاتينيوم والمحفز الزيولايت (نسبة السليكا إلى الألومينا 30) إضافة إلى بعض المعادن M. تم تحضير المحفز ثلاثي التركيب Pt-M/ZSM-5 باستخدام عملية التثريب. في حين تم فحص العوامل المؤثرة على عملية تعطير المركبات الهيدروكربونية الخفيفة عند درجة حرارة $550C^{\circ}$ و ضغط جوي 1atm باستخدام مفاعل مستمر التدفق. عند مقارنة المحفزين Pt/ZSM-5 و الزيولايت وُجدَ أن المحفز Pt/ZSM-5 ينتج مايقارب 37% من المواد العطرية بينما المحفز الزيولايت ينتج مانسبته 32% وفي الجهة المقابلة وُجدَ أن المحفز الثلاثي Pt-Ga/ZSM-5 ينتج كمية قدرها 60%، في حين وُجدَ أن المحفز Mo-Zn/ZSM-5 ينتج 62% من المركبات العطرية. يعزى سبب هذه الزيادة في المواد العطرية إلى عاملين مؤثرين هما الوسط الحمضي و عملية إزالة الهيدروجين، إذ إنَّ المحفز الزيولايت يحتوي على الوسط الحمضي ، والمعادن المضافة على المحفز الزيولايت تساعد على إزالة الهيدروجين بشكل أكبر. فعلى سبيل المثال نشاهد أن المعادن المرتبطة بكلٍ من (Pt , Mo) فعّالان في تحويل المركبات الهيدروكربونية الخفيفة (الألكانات) إلى ألكينات التي بدورها تتحول إلى مركبات عطرية باستخدام تفاعلات ثنائية إضافية مثل التكسير، التكوين و ثنائية التكوين. بالإضافة الى ما تم ذكره آنفاً فقد تم استخدام عدة طرق لوصف سلوك هذه المحفزات بواسطة عدة وسائل علمية مثل (XRD, BET, NH_3 -TPD, SEM). علاوة على ماسبق فقد تمت دراسة الثبات التفاعلي لبعض المحفزات الناجحة في تكوين المركبات العطرية بنسبة كبيرة. تعتبر نسبة السليكا إلى الألومينا عامل مهم جداً في تحويل و انتاج المواد العطرية حيث تم الوصول إلى علاقات مؤثرة. تؤثر نسبة زيادة نسبة السليكا إلى

الألومينا على درجة الحموضة عكسيا حيث أن زيادة النسبة تقل درجة الحموضة وبالتالي يقل إنتاج المواد العطرية. حقق المحفز الزيولايت الذي يحتوي مانسبته 30 من نسبة السليكا إلى الألومينا أعلى إنتاجية في المركبات العطرية.

CHAPTER 1

INTRODUCTION

1.1 Background

In the recent petrochemical industry, large quantities of the light alkanes are getting a significant interest due to the extraordinary impact in the industry. The main source of light naphtha is the distillation from the crude oil, natural gas condensate and some special processes such as Fischer-Tropsch that consists of (C₅-C₆). The boiling point and the Reid vapor pressure are (30-90) °C, 13 psi respectively. An important and beneficial product is the conversion of these light alkanes into primarily aromatics. These aromatic compounds are classified as benzene, toluene and xylenes which have abundant applications in the chemical industry [1]. Currently, light alkanes are used as feed to produce isomers and aromatics by isomerization and naphtha catalytic reforming correspondingly. Although the naphtha reforming is considered effective route to produce aromatics and its derivative, it is not economically perfect. This is due to the lack of converting the light hydrocarbons into valuable products [2]. The first process that was used to convert light naphtha to aromatics (BTX) was conducted by Csicsery in 1970 called as dehydrocyclodimerization [3]. In addition, conditions of this process require elevated temperatures and bimetallic catalyst. However, Csicsery catalytic reaction had benefit in comparison with catalytic reforming due to the transformation of more paraffin

into aromatic for dehydrocyclodimerization process. Two types of catalysts were used Platinum (Pt) and Chromium (Cr) supported on Alumina (Al_2O_3). The disadvantages of these catalysts were basically coke formation and fast deactivation. As consequence, tremendous studies were conducted to establish better performance catalysts. After that, special type of zeolites especially H-ZSM-5 were highly considered due to its superior properties. The silica and alumina that contained in the zeolite prevent coke formation and the shape of zeolite provides selective properties that allow special products and prevents other. Accordingly, the usage of H-ZSM-5 (MFI) decreases the development of coke (carbon) and residues active for a long time. Recently, Mobil Company proposed a process that is known as M₂-Forming in such a way that light naphtha is converted into blending gasoline aromatics over unmodified H-ZSM-5 and ZSM-11 [4]. This unmodified zeolite tends to crack that produce considerable amount of (C_1 and C_2) and deactivates very fast. On the other hand, this obstacle is solved by adding stimulating metals like (Ga, Ni, Pt, Cu, Zn, and Cr) and other working metals [5]. The role of these metals is to add beneficial frame work to assist the dehydrogenation purpose [6]. Among the metals, only specific type of metals appears to work toward the production of the aromatics such as Gallium (Ga), Platinum (Pt) and Zinc (Zn) [7]. Although the platinum shows superior performance into transforming light alkanes into aromatics, it deactivates very fast. Though, there are many sub reaction complemented by the aromatization reaction such as Methane and Ethane productions, olefins and De-alkylation reactions [8]. Similarly, light alkanes aromatization catalyzed by zeolites produces Hydrogen gas as byproduct that is extremely valuable in the chemical industry which can be used in some process such as Diesel Hydro-Treating (DHDT)/Diesel Hydro-Desulfurization

(DHDS). The addition of the framework types is the main reason to increase the selectivity and activity. As a result, commercial application of other significant processes is possible and brings attention in the petrochemical industry such as cyclor process which is made by UOP, British Petroleum (BP) and other petrochemical companies. The Aromatics (Benzene, Toluene, EthylBenzene and Xylenes) (BTEX) are the building blocks in the petrochemical industry. In oil business aromatic combinations and blenders are used as flavorings in petrol for the improvement of the research and motor octane number for the gasoline. These aromatic compounds are as well considered as raw resources in other Petrochemical productions. For example, they are used in the manufacturing products like medicines, agricultural goods, explosives manufacturing and detergents. In addition, aromatics are incorporated in the polymer industry as they are considered building units and monomers in polyester engineering productions and polystyrene [9] [2]. Figure 1.1 shows the composition of oil raffinate and the significance presence of light naphtha.

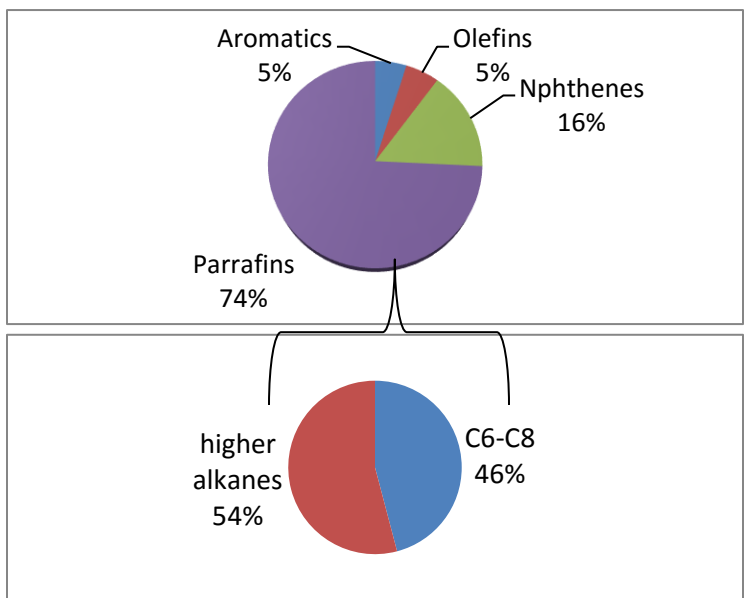


Figure 1.1: Oil raffinate composition

1.2 Aromatics Demand and Production

As recognized, aromatics (BTX) are the indispensable building blocks for one of the biggest petrochemical products in Nowadays industry. They are used and consumed to produce and contribute in the majority of the modern recent life styles products like polymers. The rate of growth is estimated to increase considerably in the future. As a result a supply gap is expected and alternative methods should be applied and creative solutions are highly suggested. Figure 1.2 shows the expected growth for the aromatics in 2020 and 2030 [10].

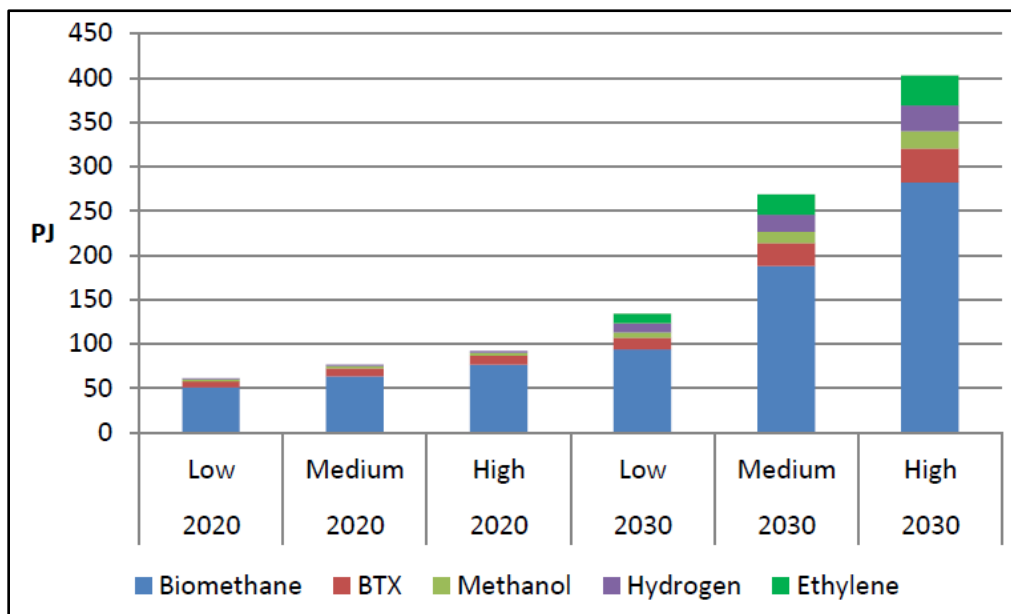


Figure 1.2: Expected petrochemicals growth for 2020 and 2030 aromatics (BTX) [10]

Because of its industrial importance, the international market of aromatic compounds is growing dramatically by (5-10) % per annum [11]. For instance, the claim of aromatics in the US was 21 million Tons per year in 2010 [12]. However, the BTX compounds are consumed by 40 million ton per year [13]. Figure 1.3 a, b and c shows the consumption of benzene, toluene and xylene in the 2018 respectively [13]. These figures estimate the consumption to 3.5 % per year through 2020 [13].

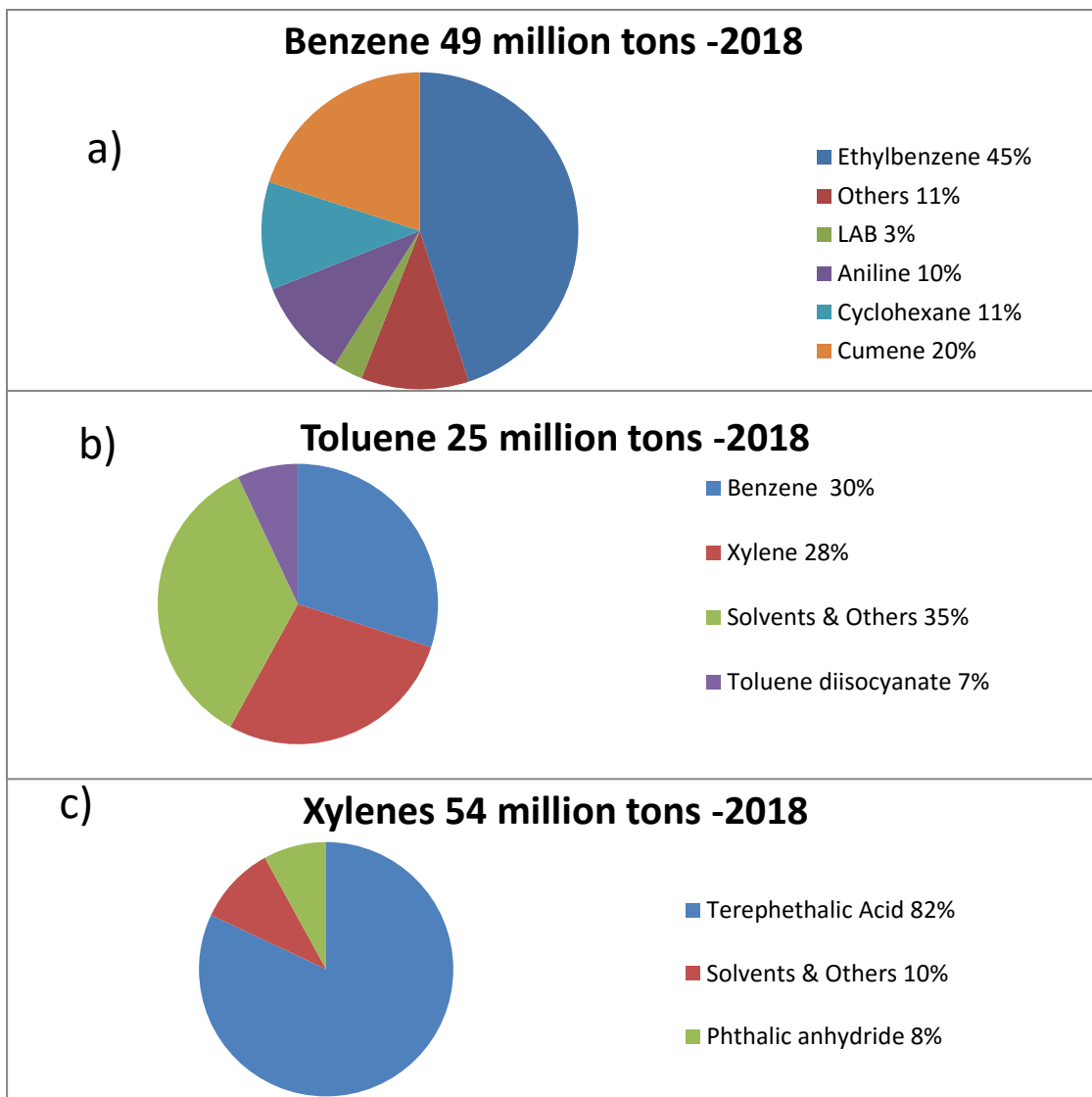


Figure 1.3: BTX consumptions: a) Benzene, b) Toluene, c) Xylenes

As predicted, the demand of aromatics will still increasing worldwide in the chemical industry due to its enormous applications in daily life basis of all BTEX compounds. Moreover, the consumption of benzene in the West European region in 2013 was 7,636 kilotons, the benzene fabrication was approximately 6,800 kilotons, while the benzene manufacture capacity was almost 10,000 kilotons as presented in Figure 1.4 [11].

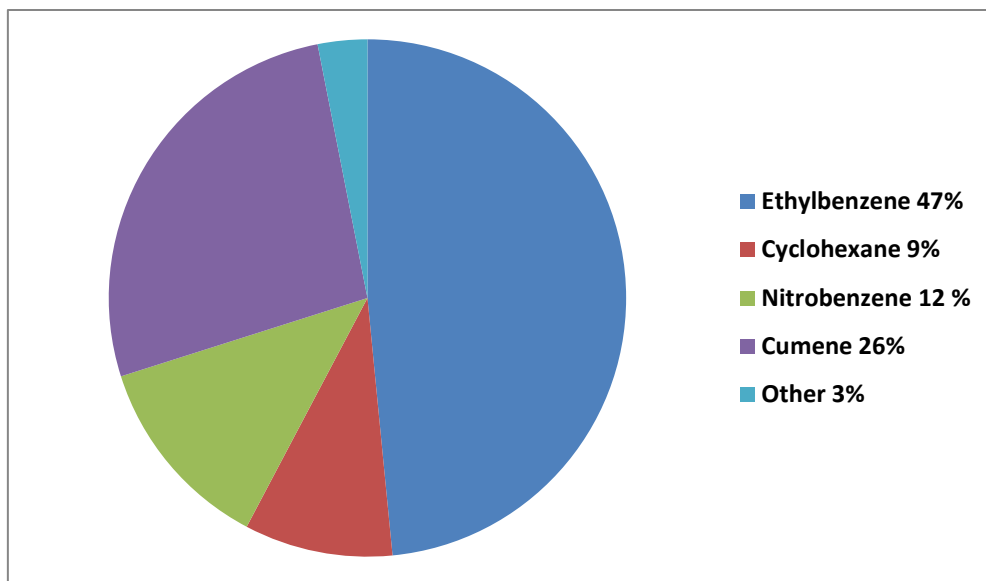


Figure 1.4: The consumption of benzene by derivative in west European region 2013 [11]

Benzene is generally used up for industrialized polystyrene (PS) by means of EthylBenzene. Also, xylenes are frequently shaped for creating polyethylene terephthalate (PET) by the use of terephthalic acid. Moreover, Toluene works as a solvent and manufacture of toluene di-isocyanine (TDI) in which it is a building block for polyurethanes. Figure 1.5 shows Aromatics usage summary. Usually the Toluene is converted into benzene using the catalytic trans-alkylation process. In recent years, the growth of polymers will increase so the volume and the amount of BTX volumes.

The BTX commands are produced in the large scale of industry with total volume by 95 million per year in 2012 [13].

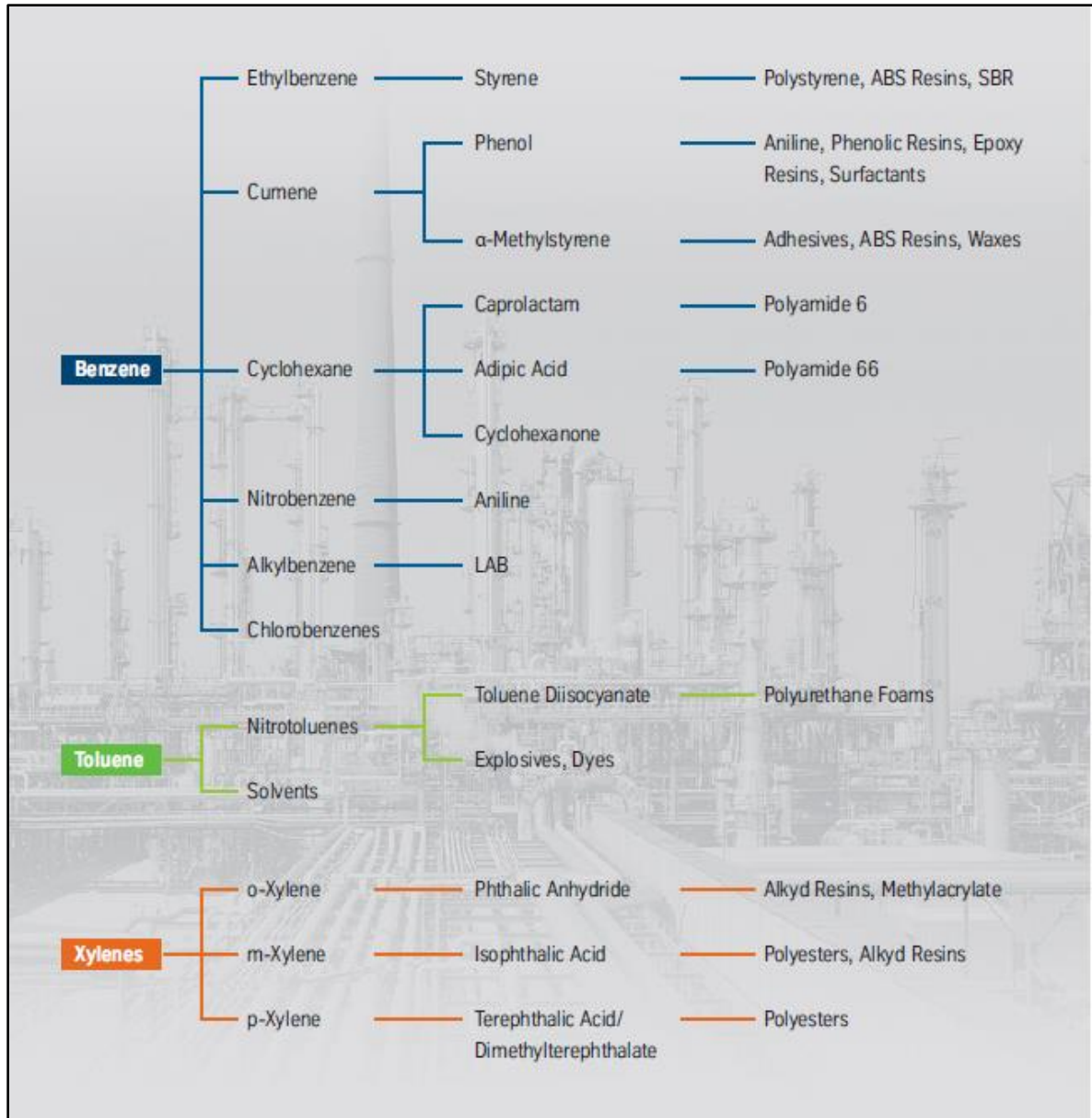


Figure 1.5: BTX usage in petrochemical industry [14]

There are three fundamental different sources for the supply of aromatics: catalytic reforming, steam cracking of naphtha and coke oven light oil (COLO). Catalytic reforming produces approximately half of the worldwide production capacity and steam catalytic cracking of naphtha is the main petrochemical source of BTEX compounds. A resourceful and optimistic process that is the COLO process in which the coal is transformed coke. However, COLO is not permanently applied to recover aromatics and tends toward the coke and total production of aromatics is small compared to the demand in the global market. Globally, Asia Pacific is the dominant region to use products manufactured from the aromatics and as a result leads demands and supply in the market for blending components.

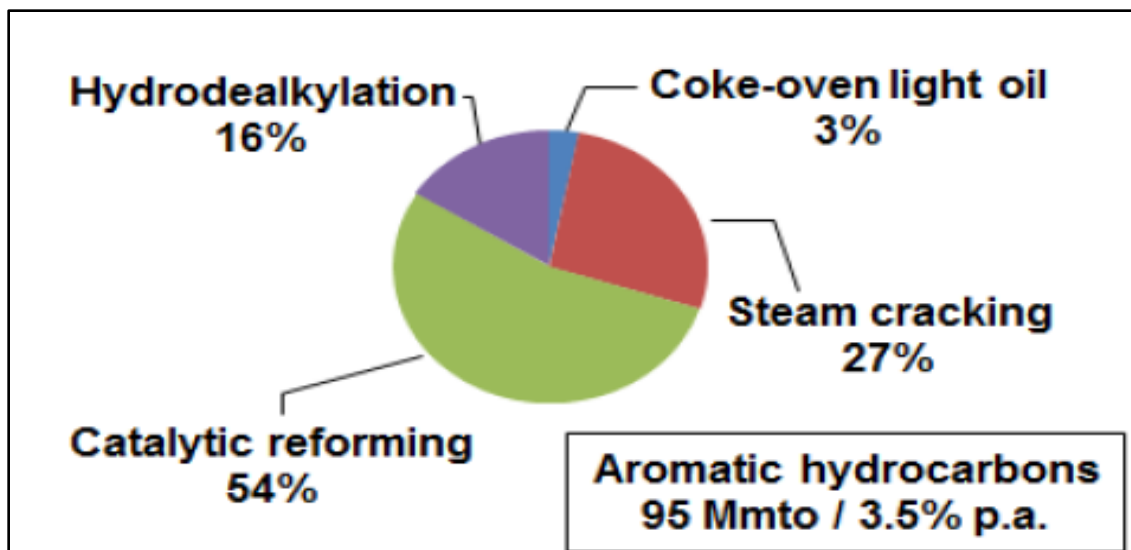


Figure 1.6: Aromatics main sources [13]

Also, the Middle East is increasing in the demand and in the future with development of superior processes such as aromatization will lead the global market of aromatics while demand is reduced in Europe due to shut-down in the refineries. In addition, great naphtha in shale oil will resource the global market with additional capacities of feedstock for the aromatics fabrication in steam crackers and catalytic reformers. Figures 1.6 and 1.7, shows pie charts of the processes that produces aromatics and the region distributions [13].

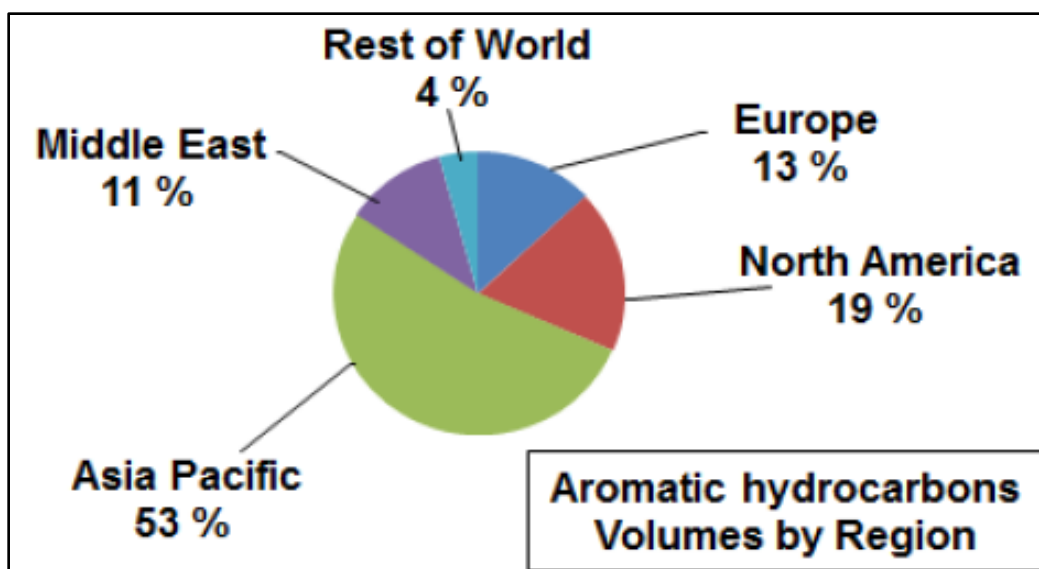


Figure 1.7: Aromatics region distributions [13]

Light naphtha consists of hydrocarbons from 5 to 6 carbon atoms and is handled primarily by steam cracking with (265 Mmto p.a.). Thermal steam cracking of light naphtha produces generally olefins besides a blend of aromatics with (53 Mmto P.a) that can be added to the feed in order to recover aromatics [13]. This process is known by pyrolysis of gasoline blending components.

On the other hand, heavy Naphtha (+C₇) is created as side product from the crude oil distillation is used as feed to execute catalytic reforming. After that, combination of dehydrogenation and cyclization reactions of some cyclic paraffin maintains high octane blending gasoline products. Furthermore, BTX production is (175 Mmto p.a.) from heavy naphtha feedstock of volume of (460 Mmto p.a.) [13]. Also, the perfect diesel composites are linear paraffin, whereas gasoline perfectly has a great amount of (BTEX) complexes as shown in Figure 1.8.

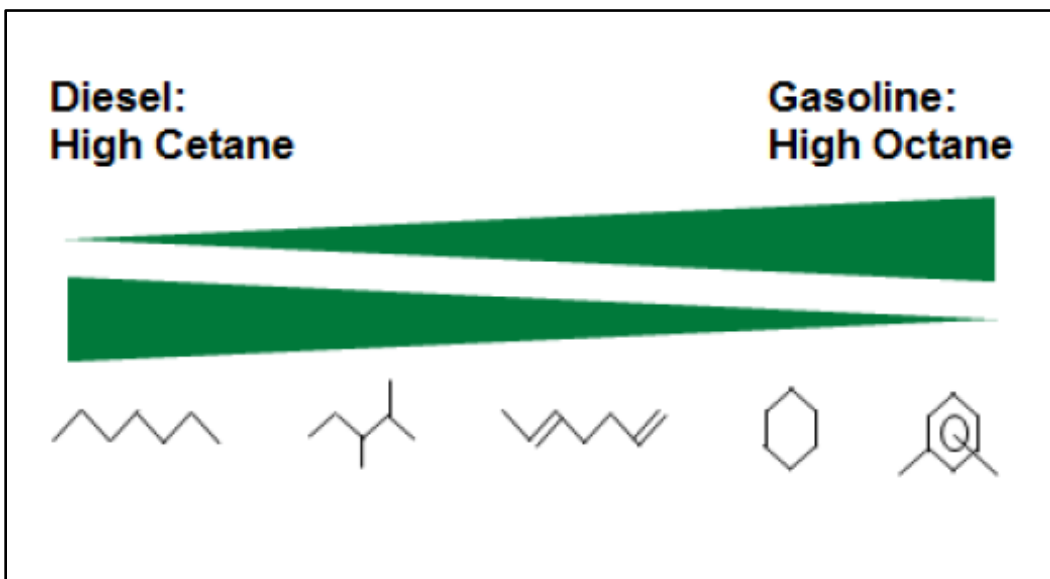


Figure 1.8: Trend of diesel and gasoline main structures [13]

In summary, Figure 1.9 presents the obvious obtainability of aromatic compounds relies basically on two specifics, specifically the development rate of crude oil source and the additional handling of light and heavy naphtha accounts into development of high octane blending complex. Knowledge for the optimization of manufactured article from steam cracking and catalytic reforming are applicable but will not maintain pointedly to the necessary aromatics supply.

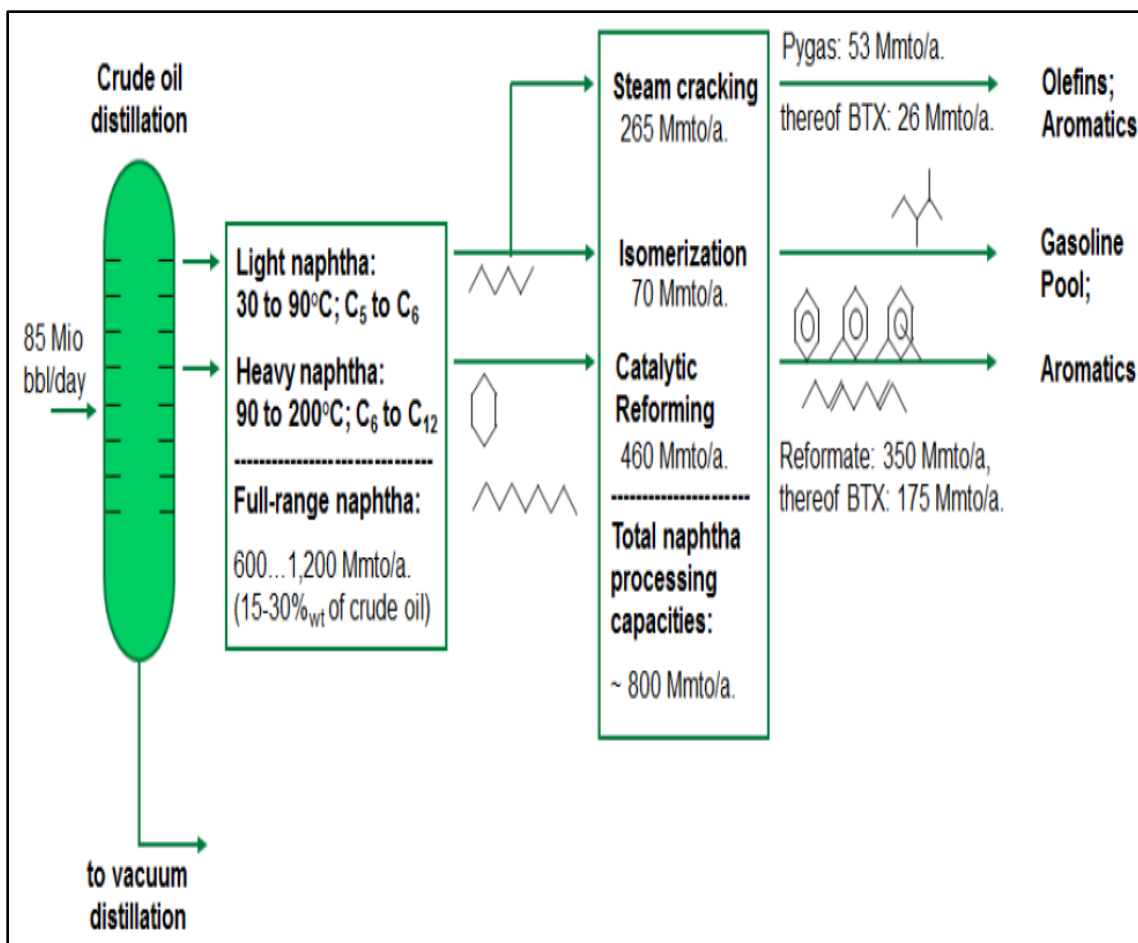


Figure 1.9: Aromatics production different routes [13]

1.3 Aromatization of Light Naphtha

Currently, light naphtha (alkanes) is transformed to isomerizes and aromatic complexes through isomerization and catalytic reforming reactions correspondingly. Yet, it is perceived that normal pentane ($n\text{-C}_5$) hydrocarbons in light alkanes are challenging to reform. A proposed route is to convert these low hydrocarbons into blending gasoline products and useful solvents and it is called aromatization. In addition, more research and development to increase the selectivity towards the aromatics and valuable hydrocarbons and this leads to zeolites that enhance the selectivity such as ZSM-5, ZSM-11 and other zeolites. These types of zeolites have been used in different petrochemical reactions such as conversion of Alcohols into aromatics alkylation and isomerization aromatics. Researches have shown that H-ZSM-5 is the best and suitable support and catalyst for the aromatization of light alkanes. This is due to several important reasons, superior pore size, and shape selective, strong and narrow acid catalyst and simple kinetic path [15]. Moreover, addition of metal on the zeolite supports increases the yield of aromatics. The light naphtha (C_6) as feed can be transformed into a large diversity of hydrocarbons including $\text{C}_1\text{-C}_4$ compounds, iso-paraffins, cycloalkanes, and BTEX compounds. There are different factors that control the selectivity towards the previous products like the acidity of the support, carbon deposition metal addition and dispersion, and reaction parameters. According to Mériaudeau research about the aromatization of light alkanes, C_6 olefin losing hydrogen first into diene and triene, and then naphthenes transformed into benzene rather than the opposite route [16]. Moreover, Rao et al investigated the aromatization of pentane and hexane to observe the yield of aromatics. It was summarized that the change in product distribution configuration was because of the

change in kinetics reaction pathways of alkanes transformation into aromatics [17]. Studies show that heavy Naphtha and long chain hydrocarbons might be without difficulty aromatized than light naphtha and aromatics were formed in superior quantities [18]. Figure 1.9 shows different products and plausible routes of the C₆ aromatization using acidic and metal zeolites.

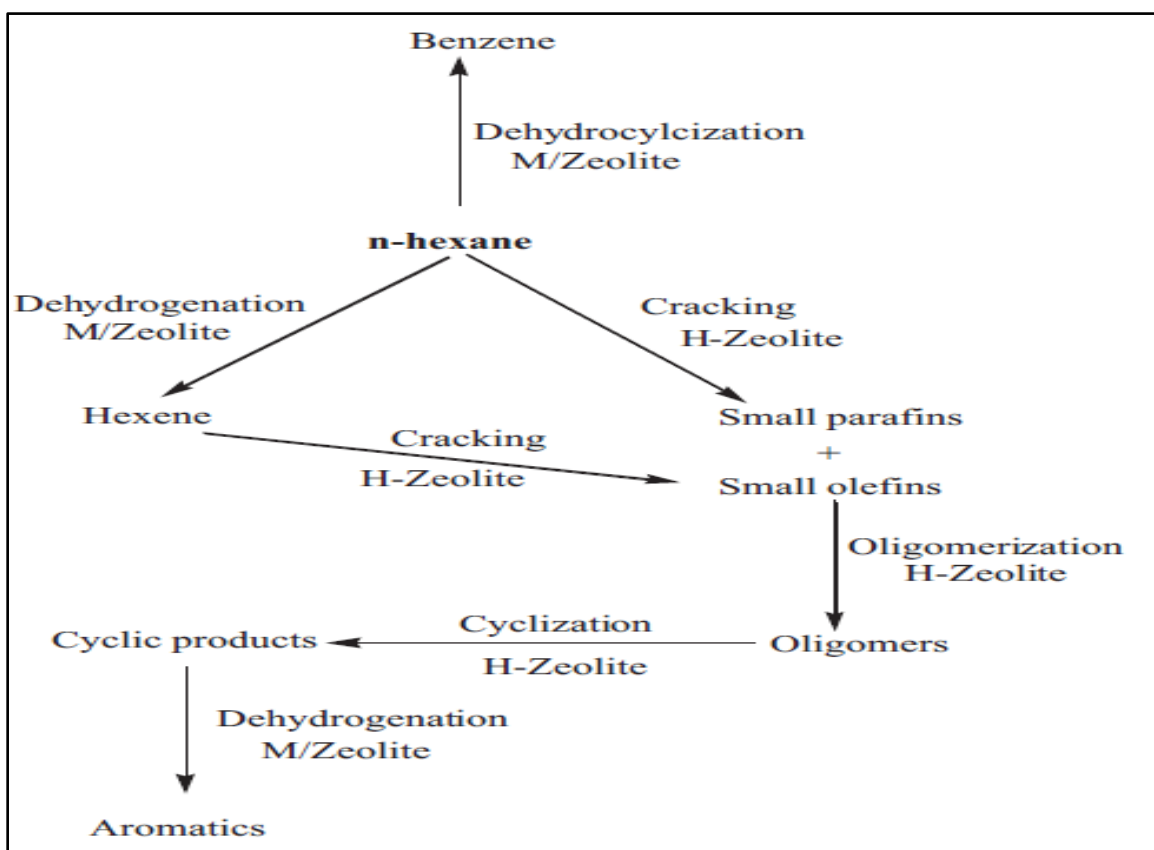


Figure 1.10: nC₆ Aromatization using acidic and metal zeolites [19]

1.4 Thesis Objectives

In the last couple of years, the oil industry faced a significant drop in prices and this fluctuation of the price of the crude oil affected the petrochemical industry. This is because crude oil and coal depletion are the sources for chemical industry. So, developments and researches are going on to improve and find economical methods and other sources that might be incorporated in generating gasoline, diesel and other essential elements that could be of decent usage in the petrochemical business. The catalytic transformation of light Naphtha into anticipated blending gasoline complexes is one encouraging method which can be utilized in improving the financial state of the chemical business.

The overall objective of the research is to examine the effect of $\text{SiO}_2 / \text{Al}_2\text{O}_3$ of ZSM-5 (MFI) type of zeolite and to investigate the effect bimetallic impregnation over ZSM-5 support on light naphtha aromatization. Further, the study will intend to:

1. Synthesize different types of mono and bi metal supported zeolites.
2. Apply characterization techniques such as XRD, TPD, TPR, BET and FT-IR.
3. Evaluate the aromatization of light naphtha reaction at various parameters such as WHSV and temperature.
4. Investigate the stability and reproducibility of the catalysts and their life time.

1.5 Thesis Scope

In the second chapter, literature review is prepared about the aromatization process and gives useful ideas and background about the catalysts and some additives that are used in the process. Furthermore, catalyst performance for some catalyst will be tabulated and summarized. Also, characterizations tests that are conducted in the literature are provided. In addition, chemistry and mechanisms of the aromatization process are present in such a way it elaborates the specific routes of the reactions.

In the Third chapter, specific information and overview about the feedstock for the aromatization reaction that used in this study is summarized. Also, Catalysts that are used in this work with it synthesis steps either the support or metal supported catalysts are presented.

Fourth chapter shows a simple case study about the effect of $\text{SiO}_2/\text{Al}_2\text{O}_3$ on the performance of the aromatization reaction of light paraffinic naphtha. Several characterizations techniques are carried out such as XRD, SEM, NH_3 -TPD and BET surface area.

Fifth and sixth chapters present the effects of both bimetallic Pt-M/MFI and Mo-M-MFI supported catalysts prepared by wetness co-impregnation method. The aromatization reaction activity of light alkanes is evaluated in a micro-fixed reactor at 550 °C, atmospheric pressure, and $\text{WHSV } 1\text{h}^{-1}$. It also demonstrates some characterizations techniques such as XRD, BET, SEM and NH_3 -TPD. In addition, stability of selective bimetallic catalyst towards the production of aromatics is presented.

Seventh chapter sum up findings of this research study and provides some recommendations for forthcoming work.

1.6 References

- [1] L. Cheng, H. Guo, X. Guo, H. Liu and G. Li, *Catal. Commun.*, 8 (2007) 416.
- [2] W.J.H. Dehertog and G.F. Fromen, *Appl. Catal. A: General*, 189 (1999) 63.
- [3] S.M. Ciscsery, *J. Catal.*, 17 (1970) 207.
- [4] Y. Xu and L. Lin, *Appl. Catal.*, 188 (1999) 53.
- [5] Y. Shu and M. Ichikawa, *Catal. Today.*, 71 (2001) 55.
- [6] Y. Xu, X. Bao and L. Lin, *J. Catal.*, 216 (2003) 386.
- [7] M.G. Sanchez, *Characterization of Gallium-containing Zeolites for Catalytic Application*, PhD Thesis, Eindhoven University of Technology, Netherlands, 2003.
- [8] P. Meriaudead and C. Naccache, *Catal. Rev-Sci. Eng.*, 39 (1997) 5.
- [9] J. L. Hodala et al., “Aromatization of C₅-rich Light Naphtha Feedstock over Tailored Zeolite Catalysts: Comparison with Model Compounds (n-C₅ - n-C₇),” *ChemistrySelect*, vol. 1, no. 10, pp. 2515–2521, 2016.
- [10] Bauen, A. et al. (2009): *Bioenergy – a sustainable and reliable energy source*. IEA Bioenergy: ExCO: 2009:06
- [11] B. S2Biom, “Market analysis of biomethane, BTX, methanol, hydrogen, ethylene, and mixed alcohols,” November, 2015.
- [12] Bioref-Integ (2010): *Identification and market analysis of most promising added-value products to be co-produced with the fuels*. May 2010.
- [13] M. Bender, “Global Aromatics Supply -Today and Tomorrow,” 2013.

- [14] T. Krupp, "World Market Leader in Aromatics Extraction," 2014.
- [15] X. Wang, H. Carabineiro, F. Lemos, M.A.N.D.A Lemos and F. Ramona Riberio, *J. Mol. Catal. A: Chemical*, 216 (2004)131.
- [16] Gallium based MFI zeolites for the aromatization of propane, P. Mériaudeau, C. Naccache, *Catal. Today.*, 31 (1996) 265 – 273.
- [17] Modification of catalytic functions of ZSM-5 with special reference to aromatization and NTGG process, T. S. R. Prasada Rao, *Stud. Surf. Sci. Catal.*, 113 (1998) 3 – 26.
- [18] Cracking and aromatization properties of some metal modified ZSM-5 catalysts for light alkane conversions, N. Viswanadham, G. Muralidhar, T. S. R. Prasada Rao, *J. Mol. Catal. A.*, 223 (2004) 269 – 274.
- [19] M. N. Akhtar, N. Al-Yassir, S. Al-Khattaf, and J. Čejka, "Aromatization of alkanes over Pt promoted conventional and mesoporous gallosilicates of MEL zeolite," *Catal. Today*, vol. 179, no. 1, pp. 61–72, 2012. |

CHAPTER 2

LITERATURE REVIEW

2.1 Background

In this section, a brief summary about the catalyst that is applicable in the process from the literature. Also, synthesis of the catalysts and different supports used in the literature and the chemistry of the aromatization reaction will be summarized. Moreover, some information about the metal loaded on several supports will be summarized. It explains how the chemistry and thermodynamics of the reaction take place for the aromatization reaction. Furthermore, characterizations techniques will be presented to explain and elaborate why this performance is achieved.

2.2 Types of Catalysts

There are many types of catalysts and supports that are associated with the aromatization process. In this section a summary from the literature review about these catalysts and their performance.

2.2.1 Background on Zeolites

Zeolites are one of the best famous and well known supports and catalysts in the petrochemical industry. The history of zeolites took place in the middle of the 16th century by the scientist Cronsted for material known as stilbite [1]. The word zeolite came from greek prefix Zeo that means to boil and Lithos which means stones. This specific naming comes from the activities of the mineral when exposed to a heating source and loss of water content and thus boil [2]. Alumino-silicate $(\text{SiO}_2)_n (\text{Al}_2\text{O}_3)_m \cdot x\text{H}_2\text{O}$ framework of natural zeolites that contains structure of water filled channels and some cations such as hydrogen ion and alkaline and earth alkaline ions. The reason of the water presence in the channels is to move the cations move freely and for the ion exchange process to happen at lower temperatures (less than 100°C). Also, loss of water happens at high temperatures (250°C) and regenerated again at ambient temperature [3]. However, zeolites are considered to be known as a porous material and regular arrays channels and cavities (3 to 15 Å) on the molecular scale and they are significant properties [4]. As a matter of fact, the main constructing units are the TO_4 tetrahedral structure and T stands for either Si or Al particles. These atoms are held together by oxygen bonds as T-O-T and framework ratio of $\text{O}/(\text{Si}+\text{Al})$.

As a result, varying the order and the number of the tetrahedral structure will form different sizes of rings. These very small rings are extremely important to guarantee the crystalline channels. For instance, ZSM-5 has 10 membered rings pore size and other secondary units that might vary the pore sizes in other zeolites as Figure 2.1 presents different zeolites structure with varying pore sizes.

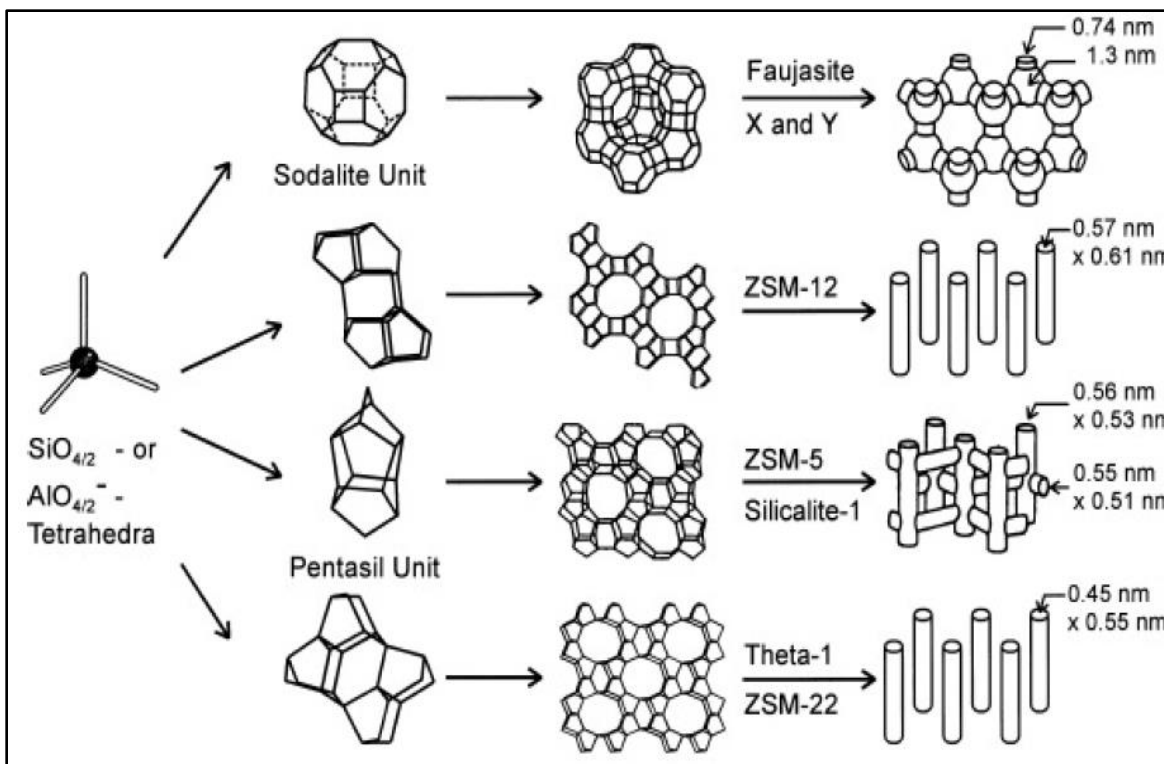


Figure 2.1: Different zeolites structure with varying pore sizes [5]

Moreover, there are many examples of zeolites with different physical and chemical properties. One example is Y zeolite (faujasite) that is formed from the built secondary units with specific linkage. Y zeolite is a significant catalyst in the heterogeneous catalysis due to its unique pore size and spherical super cages that linked together Tetrahedrally to form 12 membered ring pores. Another example is ZSM-5 which contains 10 membered ring pore size and also has both straight and Sinusoidal paths while ZSM-11 contains only straight path [5]. Furthermore, these zeolites have distinctive features in comparison other solid supports or catalysts such as uniform diameters and pore sizes as IUPAC classified them as micro-porous materials [6]. Table 2.1 shows summary of industrial synthesized zeolites with some properties [7].

Table 2.1: Summary of industrial synthesized zeolites with some properties [7] a: catalyst number b: pore size c: maximum free sphere diameter d: maximum included sphere diameter e: ICP analysis

No. ^a	Zeolite	nD^b	d_{\max}^c /nm	D_i^d /nm	ICP ^e		²⁹ Si MAS NMR	Concentration of H ⁺ /10 ⁻³ mol g ⁻¹	Crystal shape, average crystal size/ μ m
					$\frac{\text{SiO}_2}{\text{Al}_2\text{O}_3}$	or $\frac{\text{Si}}{(\text{Si} + \text{Al} + \text{P})}$			
10-MRs zeolite									
1	SAPO-41	1	0.501	0.537		0.024	—	0.38 ^f	Cuboids, 0.5-1
2	SAPO-11	1	0.457	0.558		0.047	—	0.41 ^f	Rectangular prism, 0.2-0.5
3	ZSM-22	1	0.505	0.565		56	59	0.44 ^g	Rod-like crystal, 0.05 \times 0.3
4	ZSM-23	1	0.501	0.613		74	88	0.31 ^g	Radial fin shaped rods, 0.2 \times 2
5	ZSM-5(24)	3	0.464	0.630		21	24	1.0 ^g	Rice kernel shaped particles, 0.5-1.5
	ZSM-5(39)	3	0.464	0.630		35	39	0.66 ^g	Rice kernel shaped particles, 0.5-1
	ZSM-5(55)	3	0.464	0.630		52	55	0.53 ^g	Overlapped rectangular plate, 1-1.5
	ZSM-5(69)	3	0.464	0.630		67	69	0.45 ^g	Overlapped rectangular plate, 1-2
	ZSM-5(120)	3	0.464	0.630		120	120	0.37 ^g	Cuboids, 0.5-1
	ZSM-5(1900)	3	0.464	0.630		1900	190	0.017 ^g	Cuboids, 0.5-1
6	Nu-87	2	0.501	0.698		29	31	0.86 ^g	Rectangular rods, 1-2
7	ZSM-11	3	0.513	0.766		45	48	0.63 ^g	Rectangular prism, 1-2
8	MCM-22	2	0.486	0.963		71	79	0.76 ^f	Overlapped platelets, 2-3
12-MRs zeolite									
9	SAPO-31	1	0.543	0.568		0.015	—	0.23 ^f	Hexagonal rods, 0.3 \times 5
10	ZSM-12	1	0.562	0.602		51	60	0.48 ^f	Rhombohedral, 0.5
11	MCM-68	3	0.500	0.703		16	—	0.35 ^f	Cuboids, 0.2
12	CIT-1	3	0.554	0.739		57	—	0.31 ^f	Octahedron, decahedron, 1-2
13	SAPO-5	1	0.736	0.824		0.45	—	0.37 ^f	Rhombohedral, 2
14	Y	3	0.729	1.118		2.9	4.2	4.0 ^g	Octahedron, 0.5-2

2.2.2 Metal Supported Catalysts Performance Summary

Generally, the combination of metals such as gallium and zinc implemented to catalysts improved the activity and aromatics yield through the enrichment of the dehydrogenation reaction activity. Still, high loaded metals may decrease the activity as reported in the literature and the preparation method also can influence the behavior and the performance of different zeolites support. The metal side is to remove hydrogen from alkanes to form alkenes in such a way it is considered the rate law determining step for the aromatization reaction. It is determined that the aromatization of light alkanes (C_5-C_6) controlled by a dual function mechanism path. These following tables show summary of some metal performance from the literature.

Table 2.2: Zinc performance summary for aromatization of light naphtha

Zn								
#	Feed	Catalyst Types	Reactor Type	Temperature (°C)	Conversion (%)	Aromatics Yield (%)	References	[#]
1	n(C ₆) in N ₂	Zn/ZSM-5	Fixed Bed	480	79.9	55.13	Smieskova 2004	[8]
2	n(C ₆)	Zn/ZSM-5	Fixed Bed	550	92.2	34.2	T.Thabala 2015	[9]
3	n(C ₅) in He	Zn/ZSM-5	Fixed Bed	500	16	31	Tamiyakul 2016	[10]
4	n(C ₆) in N ₂	Zn/ZSM-5	Fixed Bed	500	99.5	53.9	Hodala 2016	[11]
5	n(C ₇) in CH ₄	Zn/ZSM-5	Fixed Bed	400	96.83	51.17	Li 2018	[12]
6	n-Octene	Zn/ZSM-5	Fixed Bed	350	95.8	23.5	Long 2014	[13]
7	(C ₂ -C ₄)	Zn/ZSM 5	Fixed Bed	600	57.2	26.1	Lapidus 2009	[14]
8	n(C ₅) in He	Zn/ZSM-5	Fixed Bed	550	41.2	15.5	Park 1997	[15]

In Table 2.2, Zinc is added to ZSM-5 and the performance evaluated at various temperatures. The best conversion and yield are 99.5 % from Hodala and 55% from Smieskova. Also, the evaluation is carried out in a fixed bed reactor. Although some reactions have good conversions, the yields are very low. Usually, the aromatization reaction accompanied with Nitrogen, Hydrogen and Helium as a carrier gas.

Table 2.3: Platinum performance summary for aromatization of light naphtha

Pt								
#	Feed	Catalyst Types	Reactor Type	Temperature (°C)	Conversion (%)	Aromatics Yield (%)	References	[#]
1	n(C ₆) in H ₂	Pt/KL	Fixed Bed	500	41.2	28.8	Azzam 2010	[16]
2	n(C ₆) in H ₂	Pt/KL	Fixed Bed	450	50	36.3	Song 2015	[17]
3	n(C ₆) in H ₂	Pt/KL-14	Fixed Bed	500	95.6	64.7	Xu 2017	[18]
4	n(C ₆) in H ₂	PtMCM-41	Fixed Bed	450	25	6.3	Blanchard 2002	[19]
5	(C ₃) in He	Pt/ZSM-5	Fixed Bed	550	98	38.8	Maggiore 1991	[20]

Table 2.3 illustrates the performance of the platinum with different feed and zeolites supports such as ZSM-5, KL, and MCM. The best conversion for C₆ obtained is 95.6% and also the yield with a value of 64% for KL zeolite support. Moreover, most platinum reactions are accompanied with Hydrogen as a carrier gas.

Table 2.4: Gallium performance summary for aromatization of light naphtha.

Ga								
#	Feed	Catalyst Types	Reactor Type	Temperature (°C)	Conversion (%)	Arom. Yield (%)	References	[#]
1	n(C ₆)	Ga/ZSM-5	Fixed Bed	550	96.4	43.2	Thabala 2015	[9]
2	n(C ₅) in He	Ga/AT-AHFS-Z	Fixed Bed	550	98	68	Lee 2017	[21]
3	n(C ₆)in N ₂	Ga-ZSM-5	Fixed Bed	500	99.9	58.5	Hodala 2016	[11]
4	n(C ₇) in CH ₄	Ga/ZSM-5	Fixed Bed	400	97.71	52.3	Li 2018	[12]
5	n(C ₆)in N ₂	GaZSM-11	Fixed Bed	540	29.6	8.45	Akhtar 2012	[22]
6	n(C ₅)	GaZSM-5	Fixed Bed	500	99	94	Ntipan 2012	[23]
7	n(C ₁₆ H ₃₄)	Al ₂ O ₃ /GaAlMFI	Fixed Bed	550	91.7	10.36	Asoka 2012	[24]
8	n(C ₅)in He	GaZSM-5	Fixed Bed	550	92.1	48.2	<i>Park 1997</i>	[15]

For Gallium metal, Table 2.4 shows the performance is quite similar to Zn in the conversion and yield. From the literature, zeolite supports are used for the Aromatization reaction such as ZSM-5 and ZSM-11 with temperatures ranges in between (400-550) °C. The best conversion is 99.9 % for Hodala's research while the best yield is 94 % for Nipitans. Interesting results are obtained with Methane as a carrier gas.

Table 2.5: Other metals performance summary for aromatization of light naphtha

Other Metals								
#	Feed	Catalyst Types	Reactor Type	Temperature (°C)	Conversion (%)	Aromatics Yield (%)	References	[#]
1	n(C ₅) in He	Al/ZSM-5	Fixed Bed	550	97.6	25.1	Park 1997	[15]
2	n(C ₅) in He	Fe/ZSM-5	Fixed Bed	550	26.3	7.9	Park 1997	[15]
3	nC ₅ in He	Ni/ZSM-5	Fixed Bed	550	44.1	9.6	Park 1997	[15]
4	n(C ₆) in N ₂	Mo/ZSM-5	Fixed Bed	550	61.2	17.4	T.Thabalala 2015	[9]
5	n(C ₆)	V-MgO	Fixed Bed	525	73	31	Chetty 2017	[25]
6	(C ₃ -C ₁₂)	Cr-ZSM-5	Fixed Bed	550	45	29.3	Mohiuddin 2018	[26]
7	(C ₃ -C ₁₂)	Fe-ZSM-5	Fixed Bed	550	50	12	Mohiuddin 2018	[26]
8	n(C ₆) in H ₂	Cu-ZSM-5	Fixed Bed	550	99.5	85.4	Kuzmina 2010	[27]
9	n(C ₆) in H ₂	CuZHS-III-895	Fixed Bed	550	97	79.8	Kuzmina 2010	[27]
10	n(C ₆) in H ₂	Cu-ZHS-III-889	Fixed Bed	550	99.7	87	Kuzmina 2010	[27]

Besides Zinc, Gallium and Platinum, there are some metals that provide superior results in the aromatization reaction. In Table 2.5, different metals performance summary including Fe, Ni, Mo and others. Cu shows the best performance either conversion or yield. Different feed are used including heavy and light alkanes.

Table 2.6: Mixture performance summary for aromatization of light naphtha

Mixtures								
#	Feed	Catalyst Types	Reactor Type	Temperature (°C)	Conv. (%)	Aromatic Yield (%)	References	[#]
1	n(C ₆) in H ₂	Pt-Fe/KL	Fixed Bed	450	80	65.28	Song 2015	[17]
2	n(C ₆)in N ₂	ZnGa/ZSM-5	Fixed Bed	500	99	65	Hodala 2016	[11]
3	n(C ₇) in N ₂	ZnGa/ZSM-5	Fixed Bed	400	96.58	57.42	Li 2018	[12]
4	n(C ₆) in N ₂	Pt/GaZSM-11	Fixed Bed	540	70.1	26.5	Akhtar 2012	[22]
5	n(C ₆) in N ₂	Pt/Ga,AlZSM-5	Fixed Bed	540	55.3	6.12	Akhtar 2012	[22]
6	n(C ₆) in H ₂	PtCsMCM-41	Fixed Bed	450	34	11.9	Blanchard 2002	[19]
7	n(C ₆) in H ₂	Pt/FeKL	Fixed Bed	450	30	13.38	Song 2015	[17]
8	C ₃ in He	Pt-Pb/ZSM-5	Fixed Bed	550	94.5	45.4	Maggiore 1991	[20]
9	C ₃ in He	Pt-Ir/ZSM-5	Fixed Bed	550	99.8	61.2	Maggiore 1991	[20]
10	C ₃ in He	Pt-Re/ZSM-5	Fixed Bed	550	100	42.3	Maggiore 1991	[20]
11	C ₃ in He	Pt-La /ZSM-5	Fixed Bed	550	100	24.1	Maggiore 1991	[20]
12	(C ₂ -C ₄)	Ga-Pt/ZSM-5	Fixed Bed	600	47.6	30.1	Lapidus 2009	[14]

Sometimes, mixing two metals or more might affect the aromatization reaction in either ways. For example, mixing Zn and Ga provides results better than the metals alone supported on ZSM-5. The conversion and yield respectively are 99% and 65%. On the other hand, mixing metals with each other result in decreasing the performance. Moreover, the way and the order mixing might affect the aromatization. For instance, Pt and Fe show different results if the mechanism of addition changed as demonstrated in Table 2.6.

2.3 Catalyst Synthesis

There are many ways and producers to synthesize different types of zeolites in the literature and also commercial zeolites available in the market. In this section preparation of ZSM-5 and metal supported zeolites will be presented.

2.3.1 Synthesis of Conventional (Micro) H-ZSM-5

One commonly method that is used to prepare H-ZSM-5 is by hydrothermal treatment method [28, 29]. Increasing or decreasing the temperature of synthesis will yield samples with different degree of crystallinity and silica alumina ratio ($\text{SiO}_2/\text{Al}_2\text{O}_3$) can vary depending on the required producers. To examine the content different characterizations techniques are used. At the beginning, sodium aluminate source is gained via mixing amount of NaOH and $\text{Al}(\text{OH})_3$ or $\text{Al}(\text{NO}_3)_3$ with distilled water and the mixture is heated with continues stirring. Then, template solution is prepared via dissolving tetra-propyl-ammonium bromide (TPABr) in distilled water. Also, silica content is attained by mixing Areoisl 200 with D- H_2O and stirred until smooth gel content is obtained. After that the previous two solutions are added to the silica one with continues stirring to be ready to pour it to the auto-clave vessel to crystallize for amount of time (1-3) days. Next, the crystalline mixture is filtered and washed with distilled water and silver nitrate to get rid of bromide and hydroxide. In addition, the product is dried overnight in good oriented range of temperatures. Afterwards, resulting mixture is calcined at high temperature for some time to remove the template with product of the form Na-ZSM-5. To obtain the H-ZSM-5 particles, Na-ZSM-5 is treated with 1M NH_4Cl or NH_4NO_3 at room temperature

with continues stirring for some time. Finally, the mixture is washed and filtered then calcined to obtain the acidic form H^+ .

2.3.2 Synthesis of Metal Supported on Different Zeolites

In general, adding metals to the zeolites can affect the performance of the reaction. These metals supported catalysts are synthesized by wet impregnation method of different zeolites supports with specific Silica Alumina ratio for example 30, 50 or 70 etc. To obtain these metals supported catalyst, it necessary to have precursors that are added to the H-ZSM-5 support. After that, dissolved in mixture of distilled water then heated and dried overnight and next calcined. Examples are Ga/H-ZSM-5 from the precursor gallium nitrate $Ga(NO_3)_3 \cdot 8H_2O$ and Zn/H-ZSM-5 from zinc nitrate $Zn(NO_3)_2 \cdot 6H_2O$ precursor.

2.4 Chemistry and Mechanisms of Aromatization of Light Naphtha

The mechanisms and chemistry of light naphtha mainly C_6 includes several steps that are accompanied with Lewis-Brønsted acidic sites. Also, some reactions should be considered such as cracking and dehydrogenation reactions besides the synthesized zeolites. For instance, metal loaded catalysts increase the Lewis function of the catalyst [9]. Usually, the addition of the metal to the zeolite support enhances the selectivity towards the aromatics via preventing cracking reaction path of alkenes. Researches have been conducted to describe the rote of aromatization of light alkanes and this work summarized in which aromatization of light naphtha occur into two main steps. The first step is formation of alkenes from the initial alkane and the second step is the conversion of alkenes towards aromatics. Between these two steps other reaction may occur such as formation of cyclic rings by hydrogen transfer and isomerization of alkenes to form

cyclization then aromatics [30]. According to Nguyen research, mechanism of aromatization of light naphtha happens into three steps summarized in Figure 2.2 [31].

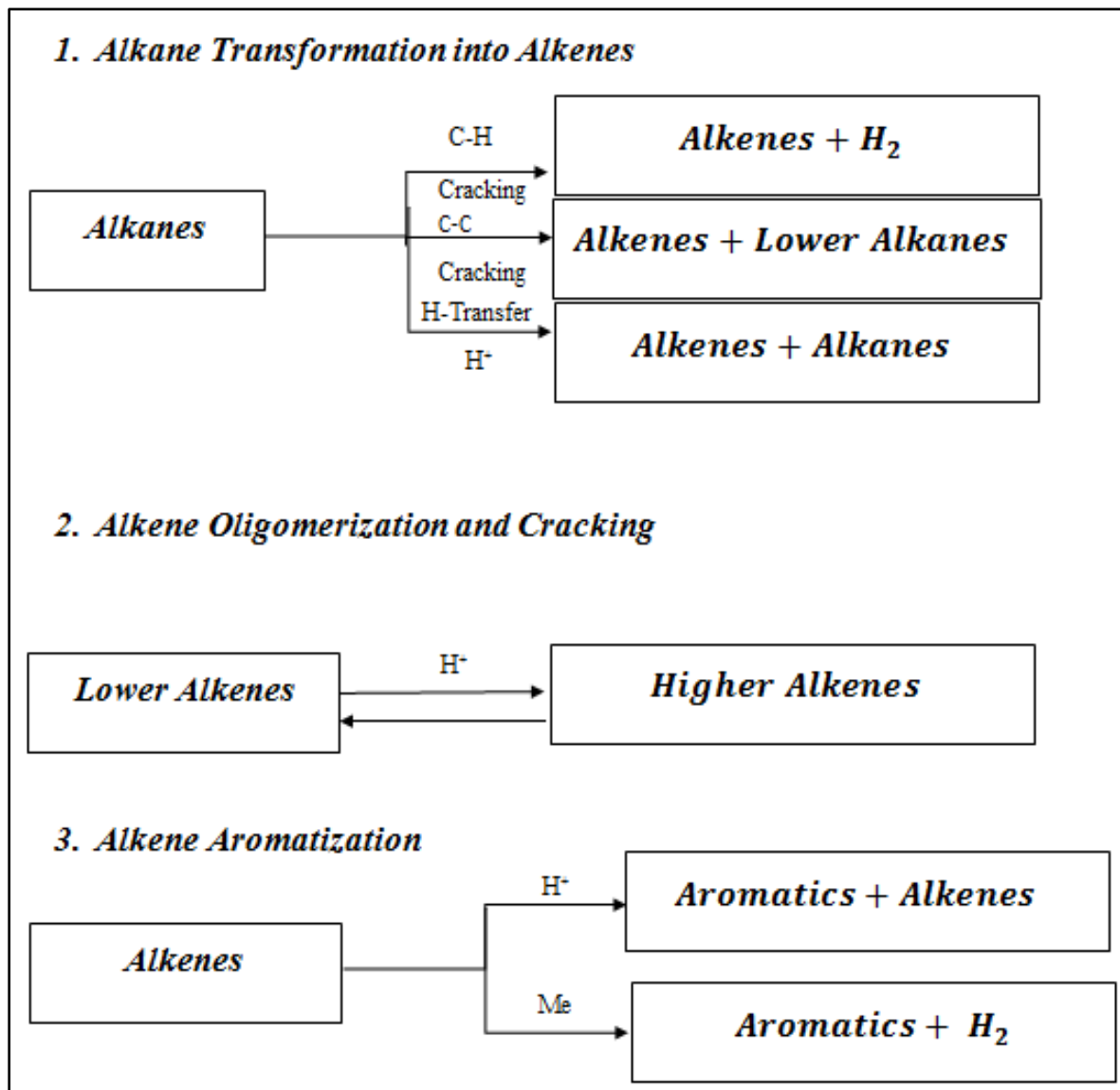


Figure 2.2: Aromatization of light naphtha three main mechanism steps [31]

Regarding Figure 2.2 the three main steps are as follow: alkanes to alkenes via cracking and hydrogen transfer (dehydrogenation), isomerization of alkenes and oligomerization stages, aromatics production through cyclization and dehydrogenation reactions. However, adding metals usually but not always increases the performance and there are some papers describing the mechanism over C₆ reaction. According to Kanai and Kawata et al research that aromatization of light alkanes (C₆) over Zn metal supported on H-ZSM-5 is categorized as bifunctional catalyst. Zinc metal acts as dehydrogenating material in the transformation from n-hexane to hexene and also in oligomerized olefins to blending gasoline components [32]. Furthermore, Gnep et al reported on the gallium (Ga) metal performance in the aromatization and it was concluded that Ga enhances the dehydrogenation reaction [33]. In addition, Inui et al investigated and examined the activity for Platinum (Pt) ion-exchanged with Gallium-silicate. The results indicated that platinum increased the reaction tendency toward olefins from paraffin and gallium enhanced the productions of aromatics and reduced coke formation [34]. Figure 2.3 presents the bifunctional catalyst possible mechanisms.

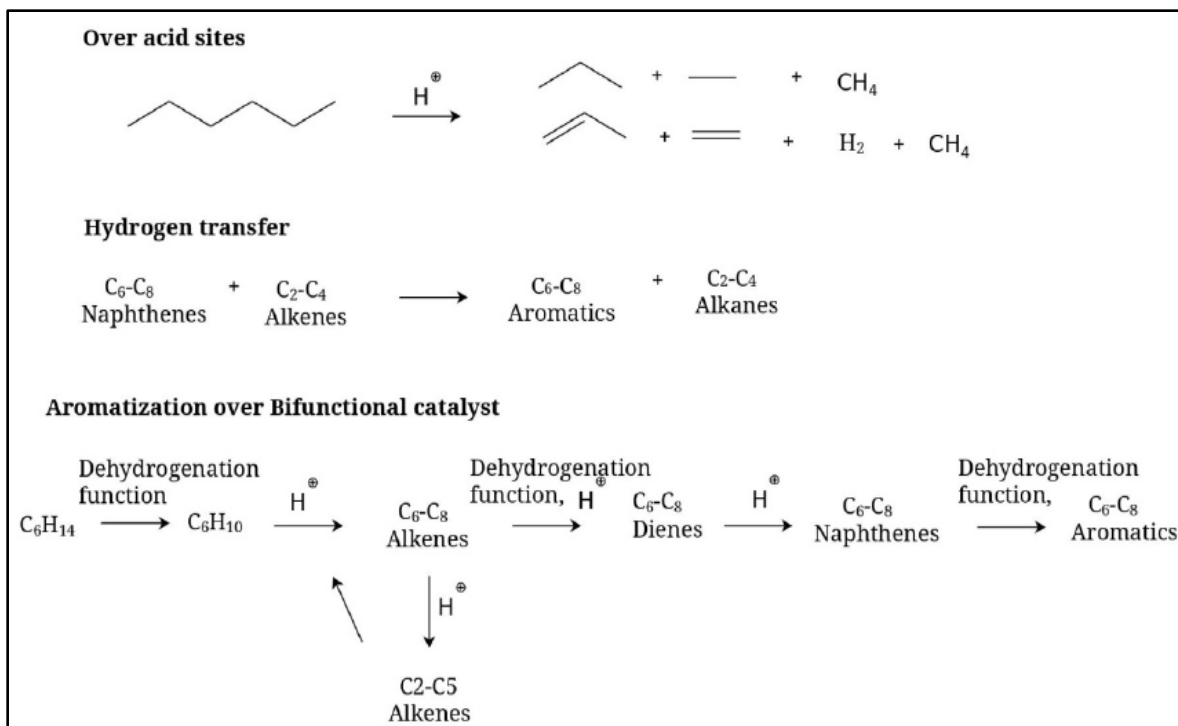


Figure 2.3: Aromatization of nC₆ over bifunctional catalyst possible mechanism route [11]

2.5 Characterization Techniques of Catalysts

Characterization of catalyst is an important tool to describe both chemical and physical properties. There are many instruments and characterization techniques to describe solid catalyst zeolites. Different characterizations have developed and used such as XRD (Powder-X-Ray Diffraction), Temperatures Programed Tests (TPD and TPR), and surface area test (BET) and Infrared Spectroscopy test (FT-IR). As a matter of fact, these tests provide useful information about crystallinity, structure, acid side strength.

2.5.1 Power X-ray Diffraction (XRD) Test

This method is a non-destructive method to examine crystalline behavior, phase identification and structure and conducted usually with the powder form. Usually different kinds of conventional and Nano materials are tested and examined by XRD such as organics, catalysts, metals and ceramics. In addition, useful information is extracted from this method like complication of crystal structure, size and impurities [35]. However, XRD is mainly described by Bragg's law where λ wavelength and d is the distance:

$$\lambda = 2d \sin\theta \quad \text{Equation 2-1}$$

For zeolites, XRD is simply used to find the degree of crystallinity and the phase of the sample to reference one. These diffraction patterns are well known as the finger print of the catalyst sample. Also, zones under the peaks are used to evaluate the crystallinity of the sample in comparison with a reference. In contrast, there is several aspects influence the XRD degree of crystallinity for example size and the shape of the catalyst. Another factor is amorphous phase affect the diffraction patterns which indicates difficulty in finding the crystallinity of the sample [36]. Figure 2.4 shows XRD sample's intensity curves.

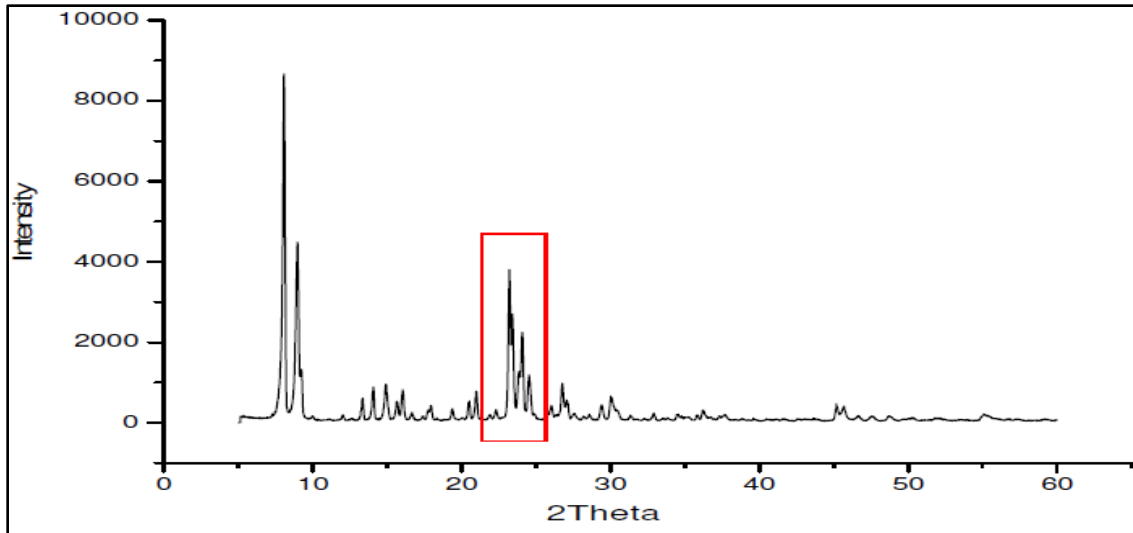


Figure 2.4: XRD sample's intensity curves [36]

2.5.2 Temperature Programed Desorption (TPD) Test

This test is also known as Thermal Desorption Spectroscopy (TDS) in which examine and investigates the interactions of catalyst surface with gas particles. It is mainly used to find the strength of acidic site of the catalyst. Additionally, maximum peaks indicate strong attach between the surface of the catalyst and adsorbents as presented in Figure 2.5 [37]. NH_3 and pyridine are the primary probes that used to investigate the acidic character of the catalyst via distinguishing between Lewis-Brønsted acid-base. Yet, Ammonia is more favorable than pyridine due to the limitations in the diffusion of the molecules associated with the pyridine like the case with ZSM-5.

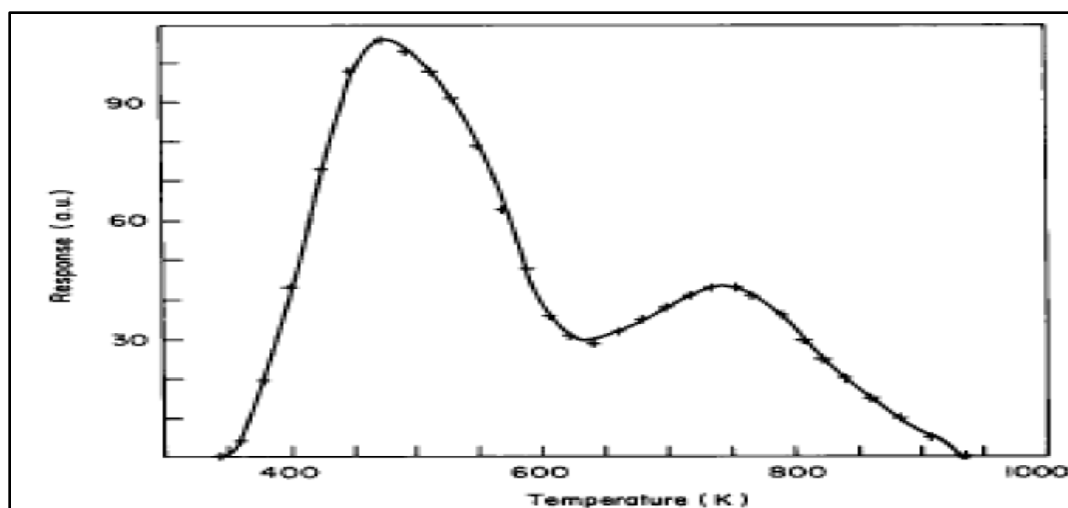


Figure 2.5: TPD Example with NH_3 [37]

The appearance of the peaks at high temperatures is due to the movement of the NH_3 from the Brønsted acid site. Also, IR test elaborates that there is interaction between the aluminum content and ammonia in the zeolite catalyst. Besides, N_2 formed from NH_3 has lone pair that enables him to attack any available orbitals by a covalent bond [55]. Figure 2.6 shows Brønsted and Lewis paths in zeolites.

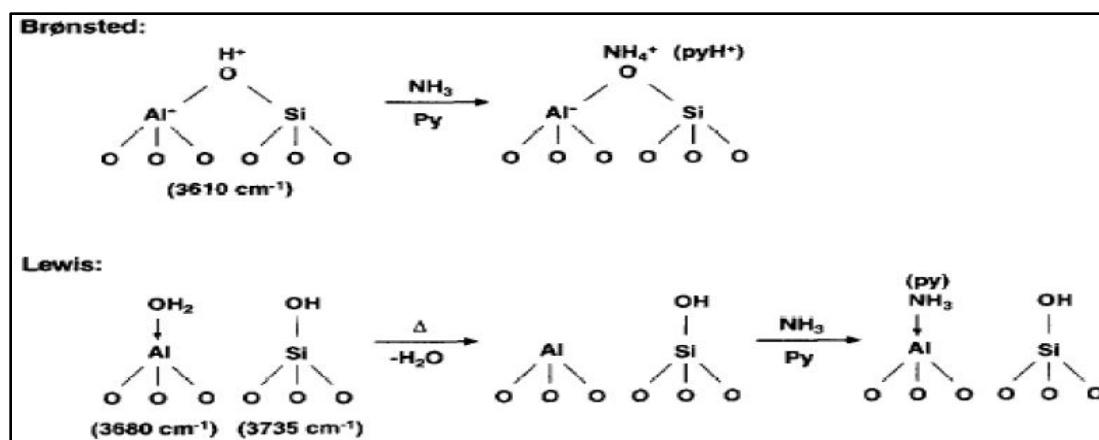


Figure 2.6: Brønsted and Lewis Paths in zeolites with NH_3 [38]

2.5.3 Temperature Programed Reduction (TPR) Test

In this technique, reduction kinetics of oxidic catalytic precursors is examined. In other words, catalyst precursor is examined and tested by TPR through a flow of a reducing gas mixture usually containing hydrogen (H_2) gas content like (N_2/NH_2 or Ar/H_2) in such a way temperature will raise linearly. Additionally, hydrogen gas consumption in TPR test will be used and measured to compute the degree of reduction and calculate the total depletion of Hydrogen. After that, Average Oxidation State is found for the specific catalyst or precursor [39]. Dissociative adsorption of hydrogen gas, which is very difficult step for oxides, is the first step of reductions reactions and concluding that reaction rate is dependent on hydrogen activation. Besides, degree of reduction increases as the time increases leading to proportional relation whereas temperature increases linearly. According to Hurst, reduction reaction rate is proposed and it is assumed that reduction of metals to oxides is impractical [40].

2.5.4 Surface Area (BET) Test

In general, catalysts that are used heterogeneous reactions are usually porous due to preparations method in the synthesis. An example of porous preparation method is hydrothermal method that produces crystalline molecular size. Frequently, the activity of the catalyst is somehow related to the total surface area so evaluating the surface area is extremely important in the characterization. It requires some knowledge about pore size and structure and other physical properties that may affect the catalytic reaction [41].

There are several practical methods to determine surface area and pores size and common used technique is gas adsorption. This method provides direct measurements of the pores size and structure depending on relative pressure and adsorbed volume besides other physical properties. In addition, there are different gases used in evaluating the adsorption such as Nitrogen, Argon and carbon dioxide. For instance, Nitrogen at 77 K is used to determine and investigate the adsorption for different catalysts due to its nature. Also, it is possible to estimate total surface area (Brunauer-Emmett-Teller) BET method, mesopores distribution to its size ratio Barrett-Joiner-Halenda (BJH) method and volume distributions. One of the best methods to determine and estimate the surface area from physisorption isotherm is the BET or (Brunauer-Emmett-Teller) method that is incorporated in Langmuir's model to maintain multilayers. Furthermore, there are some assumptions to be considered. Firstly, it considered that the first layer is set of equivalent sites of second layer as a base. Secondly, except for the first layer the conditions of adsorption-desorption are identical. Thirdly, the energy of adsorption-desorption site is equivalent the condensation energy. Finally, infinite thickness of the multi-layer is assumed and Figure 2.7 shows the BET Langmuir model [42].

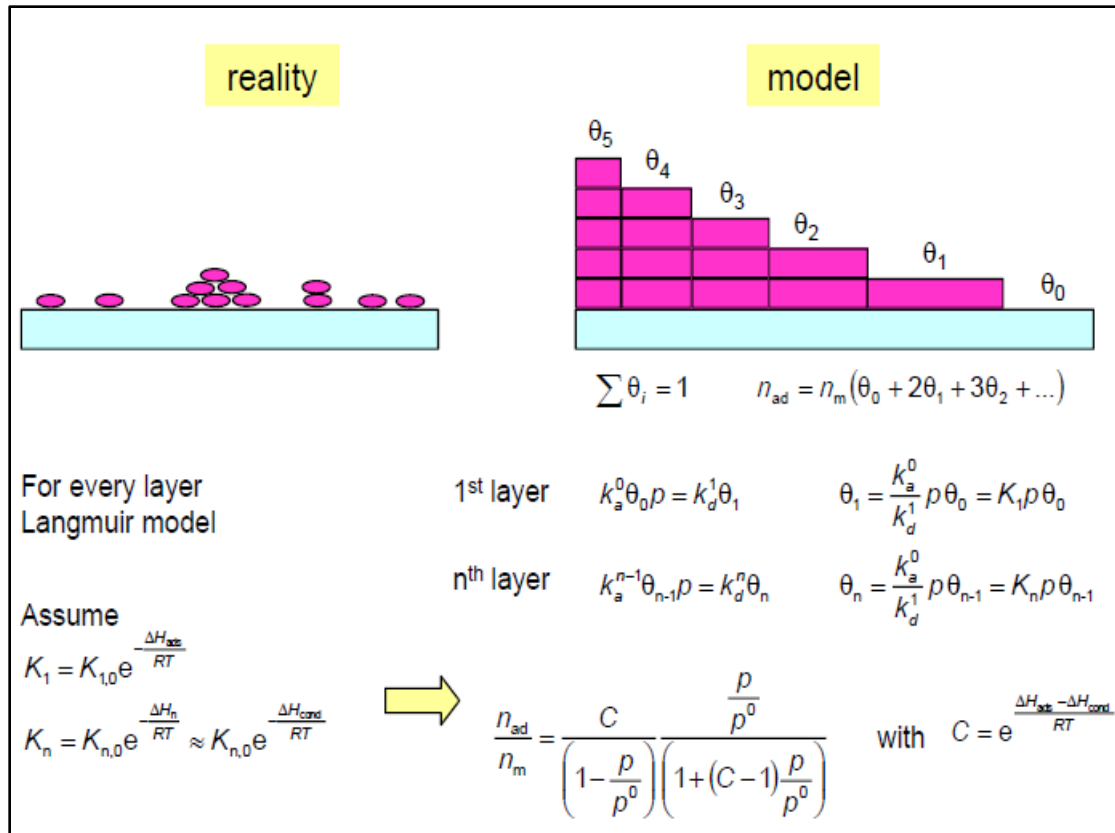


Figure 2.7: Langmuir's model equation and layers appearance [42]

2.5.5 Infrared Spectroscopy (FT-IR) Test

FT-IR is unique technique and commonly used upon all characterizations techniques and its main use is to determine the acidity of the zeolites. Actually, FT-IR is well thought-out to be a straight method to describe the (H^+) content of zeolites and focus on the OH stretch frequencies. Also, small spectroscopic changes that observed may affect the results and as result indicating beneficial data concerning zeolites samples that are examined. FT-IR test is quite similar to TPD technique in which it is possible to observe movement and interaction of (OH^-) group in basic probe molecular. These useful data will help to determine and investigate acidic sides and strength [43].

2.6 References

- [1] D.S. Coombs, A.J. Ellis, W.S. Fyfe and A.M. Taylor, *Geochimica et Cosmochimica Acta*, 17 (1957) 53.
- [2] R.M Barrer, *Hydrothermal Chemistry of Zeolites*, Academic Press, London (1982) p 35.
- [3] G. Gottardi and E. Galli, *Natural Zeolites*, Springer-Verlag Berlin Heidelberg (1985) p.1.
- [4] A. Chatterjee, D. Bhattacharya, M. Chatterjee and T.Iwasaki, *Microporous and Mesoporous Mater.*, 32 (1999) 189.
- [5] J. Wietkamp, *Solid State Ionics*, 131 (2000) 175.
- [6] D.H. Everett, *Pure Appl. Chem.*, 31 (1972) 585.
- [7] Miyaji A, Iwase Y, Nishitoba T, Long NQ, Motokura K, Baba T. Influence of zeolite pore structure on product selectivities for protolysis and hydride transfer reactions in the cracking of n-pentane. *Phys Chem Chem Phys*. 2015;17(7):5014-5032.
- [8] Smiešková A, Rojasová E, Hudec P, Šabo L. STUDY OF THE ROLE OF Zn IN AROMATIZATION OF LIGHT ALKANES WITH PROBE MOLECULES. 2004;82(2):227-234.
- [9] T. E. Tshabalala and M. S. Scurrrell, "Aromatization of n-hexane over Ga, Mo and Zn modified H-ZSM-5 zeolite catalysts," *Catal. Commun.*, vol. 72, pp. 49–52, 2015.

- [10] S. Tamiyakul, T. Sooknoi, L. L. Lobban, and S. Jongpatiwut, "Generation of reductive Zn species over Zn/HZSM-5 catalysts for n-pentane aromatization," *Appl. Catal. A Gen.*, vol. 525, pp. 190–196, 2016.
- [11] J. L. Hodala et al., "Aromatization of C₅-rich Light Naphtha Feedstock over Tailored Zeolite Catalysts: Comparison with Model Compounds (n-C₅ - n-C₇)," *ChemistrySelect*, vol. 1, no. 10, pp. 2515–2521, 2016.
- [12] Q. Li *et al.*, "Investigation on the light alkanes aromatization over Zn and Ga modified HZSM-5 catalysts in the presence of methane," *Fuel*, vol. 219, no. January, pp. 331–339, 2018.
- [13] H. Long, F. Jin, G. Xiong, and X. Wang, "Effect of lanthanum and phosphorus on the aromatization activity of Zn/ZSM-5 in FCC gasoline upgrading," *Microporous Mesoporous Mater.*, vol. 198, pp. 29–34, 2014.
- [14] A. A. Dergachev and A. L. Lapidus, "Catalytic aromatization of light alkanes," *Russ. J. Gen. Chem.*, vol. 79, no. 6, pp. 1244–1251, 2009.
- [15] Y. K. Park, D. H. Kim, and S. I. Woo, "Aromatization of pentane catalyzed over various metallosilicates," *Korean J. Chem. Eng.*, vol. 14, no. 4, pp. 249–256, 1997.
- [16] K. G. Azzam, G. Jacobs, W. D. Shafer, and B. H. Davis, "Aromatization of hexane over Pt/KL catalyst: Role of intracrystalline diffusion on catalyst performance using isotope labeling," *J. Catal.*, vol. 270, no. 2, pp. 242–248, 2010.
- [17] J. Song *et al.*, "The effect of Fe on Pt particle states in Pt/KL catalysts," *Appl. Catal. A Gen.*, vol. 492, pp. 31–37, 2015.

- [18] D. Xu *et al.*, “Controllable deposition of Pt nanoparticles into a KL zeolite by atomic layer deposition for highly efficient reforming of n-heptane to aromatics,” *Catal. Sci. Technol.*, vol. 7, no. 6, pp. 1342–1350, 2017.
- [19] J. Blanchard *et al.*, “Basic Cs-Pt/MCM-41 catalysts: Synthesis, characterization and activity in n-hexane conversion,” *Catal. Letters*, vol. 83, no. 3–4, pp. 221–229, 2002.
- [20] R. Maggiore, S. Scirè, S. Galvagno, C. Crisafulli, and G. Toscano, “Influence of iridium, rhenium and lanthanum on propane aromatization over platinum/ZSM-5 catalysts,” *Appl. Catal. A, Gen.*, vol. 79, no. 1, pp. 29–40, 1991.
- [21] K. Lee, S. Lee, Y. Jun, and M. Choi, “Cooperative effects of zeolite mesoporosity and defect sites on the amount and location of coke formation and its consequence in deactivation,” *J. Catal.*, vol. 347, pp. 222–230, 2017.
- [22] M. N. Akhtar, N. Al-Yassir, S. Al-Khattaf, and J. Čejka, “Aromatization of alkanes over Pt promoted conventional and mesoporous gallosilicates of MEL zeolite,” *Catal. Today*, vol. 179, no. 1, pp. 61–72, 2012.
- [23] T. Nitipan, S. Jongpatiwut, T. Rirksomboon, B. Kitiyanan, and T. Apphakvan, “Improved p-Xylene Selectivity of n-Pentane Aromatization over Silylated Ga-exchanged HZSM-5,” *World Acad. Sci. Eng. Technol.*, vol. 64, pp. 457–460, 2012.
- [24] T. Kimura, N. Hata, K. Sakashita, and S. Asaoka, “Production of aromatics from heavier n-paraffins on hybrid cracking-reforming catalyst,” *Catal. Today*, vol. 185, no. 1, pp. 119–125, 2012.

- [25] J. Chetty, V. D. B. C. Dasireddy, S. Singh, and H. B. Friedrich, “The oxidative aromatization of n-hexane over VMgO catalysts,” *React. Kinet. Mech. Catal.*, vol. 120, no. 1, pp. 307–321, 2017.
- [26] E. Mohiuddin, M. M. Mdleleni, and D. Key, “Catalytic cracking of naphtha: The effect of Fe and Cr impregnated ZSM-5 on olefin selectivity,” *Appl. Petrochemical Res.*, vol. 8, no. 2, pp. 119–129, 2018.
- [27] R. I. Kuz'mina, M. P. Frolov, V. T. Liventsev, T. K. Vetrova, and A. V Kovnev, “Development of zeolite-containing reforming catalysts,” *Catal. Ind.*, vol. 2, no. 4, pp. 329–333, 2010.
- [28] C. P. Nicolaidis, *Appl. Catal. A*, 185 (1999) 211-217.
- [29] N.P. Sicandu, PhD Thesis, University of the Witwatersrand, Johannesburg, 2003.
- [30] M. Guisnet and N.S. Gnep, *Appl. Catal. A: General*, 146 (1996) 33.
- [31] L.H. Nguyen, T.Vazhnova, S.T. Kolaczowski and D.B. Lukyanov, *Chem. Eng. Sci.*, 61 (2006) 5881.
- [32] J. Kanai and N. Kawata, “Aromatization of N-hexane over ZnO H-ZSM-5 catalysts,” *J. Catal.*, vol. 114, no. 2, pp. 284–290, 1988.
- [33] M.A. Kohler, M.S. Wainwright, D.L. Trimm, and N.W. Cant, *Ind. Eng. Chem. Res.*, 26 (1987) 652.
- [34] I. Nakamura and K. Fujimoto, *Catal. Today*, 31 (1996) 335.
- [35] B. Sulikowski and J. Klinowski, *Appl. Catal. A: General*, 89 (1992) 69.
- [36] W. Robert and F.R.S Cahn, Concise Encyclopedia of Material Characterization, 2nd Edition, Elsevier (2005), p. 983.
- [37] C.P. Nicolaidis, M.S. Scurrill, *Appl. Catal.*, 55 (1989) 259.

- [38] J.G. Post and J.H.C. van Hooff, *Zeolites*, 4 (1984) 9.
- [39] G.L. Woolery, G.H. Kuehl, H.C. Timken, A.W. Chester and J.C. Vartuli, *Zeolites*, 19 (1997) 288.
- [40] S Besselmann, C Freitag, O Hinrichsen and M Muhler, *Phys. Chem. Chem. Phys.*, 3 (2001) 4633.
- [41] N.W. Hurst, S.J. Gentry, A. Jones and B.D. McNicol, *Catal. Rev.-Sci. Eng.*, 24 (1982)233.
- [42] J.C. Groen, L.A.A Peffer and J Pérez-Ramírez, *Microporous and Mesoporous Mater.*, 60 (2003) 1.
- [43] M. Thommes, *Zeolites and Ordered Mesoporous Materials by Physical Adsorption*, Quantachrome Instruments, Boynton Beach, FL, USA, p 495-523.

CHAPTER 3

MATERIALS AND METHODS

3.1 Background

In this chapter, general information about the feed stocks that have been used in this study is presented. Also, synthesis of several catalyst that prepared by different methods especially ZSM-5 (MFI) and metal supported on it. Furthermore, evaluation of the catalyst for the aromatization reaction and the instrument that is used to analyze the products of aromatics is summarized.

3.2 Feed

Aromatization of light naphtha contains mainly (C_5 and C_6) normal and iso paraffin besides some small portions of naphthenes obtained from Saudi Aramco Ras Tanura refinery as presented in Table 3.1 below.

Table 3.1: Composition of light straight run naphtha feed

Component	normal-Paraffin wt. %	iso- Paraffin wt. %	Naphthenes wt. %	Aromatics wt. %
C₅	25.5	8.8	2.1	0
C₆	25.4	26.5	5.4	1.5
C₇	0.8	3.3	0.6	0.1
Total	51.7	38.6	8.1	1.6

3.3 Catalyst Synthesis

For the preparation of the zeolites catalyst, metal supported catalyst by wet Impregnation method and Nano ZSM-5 synthesis by emulsion method are presented below.

3.3.1 Preparation of Metal Supported Catalyst by Wet Co- Impregnation Method

There are several steps to prepare the metal supported catalyst. First of all, amount of catalyst is specified i.e. 4 g sample and 2 wt. % metal. Secondly, calculations are made to find out the amount of support and precursor needed. Then, support is dissolved in 50 ml distilled water flask under continues stirring. After some time, precursor is dissolved in in 10 ml D-H₂O and 40 ml distilled water is added to achieve a 100 ml solution. Keeping continues stirring is needed for uniform distribution. Next, the solution is dried overnight at temperature of 100 °C. Afterwards, solid formation is grinded to powder and calcined for 5 hours at 550 °C (5°C /min) to remove the template. Finally, metal supported catalyst is pelldized and ready to be loaded in the reactor.

3.3.2 Nano ZSM-5 Synthesis

To prepare Nano zeolite Mochizuki's method is used for (Si/Al) of 50 [1]. First of all, amount of Tetraethyl Orthosilicate (TEOS) is added to tetra-propyl-ammonium hydroxide (TPAOH) or tetra-propyl-ammonium bromide (TPABr) 98% with continues stirring for 24h and temperature 353K of. Secondly, solution of Aluminum Nitrate ($\text{Al}(\text{NO}_3)_3$) and Sodium Hydroxide (NaOH) with distilled water is added with stirring until mother gel solution is formed. Then, the gel is crystallized in an autoclave for 24h and temperature of 443 K. After wards, solid is collected by centrifugation in the form of Na-ZSM-5 then dried overnight and calcined for 10h at 823K temperature. The final molar ratio is $1\text{SiO}_2:0.01\text{Al}_2\text{O}_3:0.25\text{TPAOH}:0.05\text{Na}_2\text{O}:8.3\text{H}_2\text{O}$. Next , to obtain the acidic form the Na-ZSM-5 is treated with 1 M Ammonium Nitrate (NH_4NO_3) twice for 3 hours at 323K. Finally, the support is calcined at temperature of 823 K for 10h to replace Na^+ with the proton to produce Nano H-ZSM5.

3.4 Catalysts

For studying the Aromatization of Light Naphtha, different catalysts are investigated with different zeolites supports and metals:

- I. Different ZSM-5 (Conventional) support with several silica Alumina ratios.

- II. A number of metals that are supported on ZSM-5 prepared by wet impregnation method.
- III. Mixtures of metals on different Zeolites support with diverse weight percent loadings.

3.5 Evaluation of the Catalyst

The conversion reaction of light naphtha mainly (C₅-C₆) was evaluated and carried out in a cylindrical blast furnace, syringe (Plunger) pump and fixed bed quartz reactor at pressure of 1 atm. A 0.5 g weight catalyst sample is loaded to the reactor and volume is recorded preceded by cleaning step by acetone all parts of the reactor. Then, specific reaction recipe is used consisting of 4 steps. The first step is to preheat the sample with carrier gas (hydrogen (H₂) or nitrogen (N₂)) for almost 2 hours temperature set at 550 °C flowing at a rate set at 20 ml/minute .The main reason of the pretreatment is to remove immersed contaminations and the moistness from the catalyst sample and to activate it at temperature of 550°C before start passing the feed. The second step is where the feed passes through by the syringe pump and reaction taking place for 320 min. Also, the catalyst sample is exposed to the blend of light naphtha and nitrogen carrier gas at rate of 10 ml/min. In this step, five injections are obtained from the reactor to be investigated and examined by Shimadzu 2014 gas chromatograph but before that conditioning and blank runs are carried out. This is to make sure that the wires inside the gas chromatograph are clean and ready for the sample and method that examine the sample for 55 min each. The third and the fourth step are to stop the syringe pump and cool down

the reactor. Finally, Shimadzu 2014 gas chromatograph equipped with and FID packed column where the results are obtained.

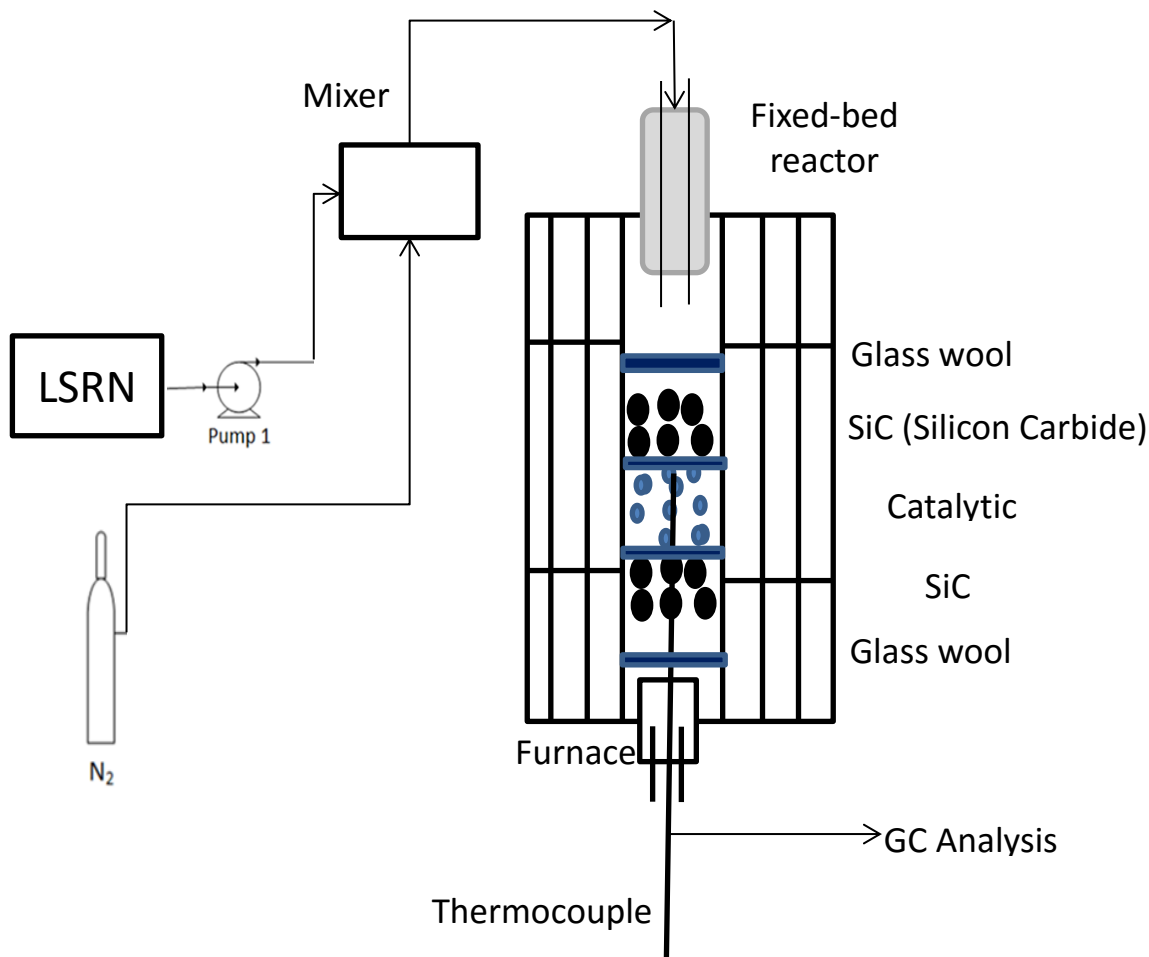


Figure 3.1: Micro fixed bed reactor set up scheme

3.6 References

- [1] Mochizuki H, Yokoi T, Imai H, et al. Facile control of crystallite size of ZSM-5 catalyst for cracking of hexane. *Microporous Mesoporous Mater.* 2011;145(1-3):165-171.

CHAPTER 4

EFFECT OF SiO₂/Al₂O₃ MOLAR RATIO OF MFI-TYPE

ZEOLITE CATALYST ON LIGHT NAPHTHA

AROMATIZATION

4.1 Background

In this chapter, the effect of SiO₂/Al₂O₃ ratio of MFI type zeolite catalyst on light naphtha aromatization is presented. A series of MFI zeolites with of SiO₂/Al₂O₃ (23, 30, 50, 280, and 1500) are examined. The activity of the aromatization reaction is carried in affixed bed reactor at 550 °C.

4.2 Introduction

Conversion of light naphtha into aromatics has gained significant attention in the past few decades owing to its large volume of paraffinic hydrocarbons produced from petrochemical refining processes [1, 2]. These aromatics compound (BTX) referred as Benzene, Toluene and Xylene have been categorized as important petrochemical intermediates for other chemicals and polymers. This is due to its application on the formation of high value-added chemicals as the fundamental building blocks [3-5]. Moreover, the relative demand for aromatics has increased due to the large-scale production of gasoline blending components in the Middle East and China, so more

efficient processes for the production of aromatics are highly desirable. In general, the remaining distillate of the catalytic reforming process is called raffinate oil which contains long branched chains of hydrocarbons mainly alkanes alkenes and cycloalkanes. Since the demand of aromatic is increasing in a dramatic way, raffinate oil is used as feedstock to produce various aromatics compounds mainly BTX products via suitable aromatization process. As (C₅-C₆) paraffins are the significant compositions in the raffinate oil, these alkanes are used to investigate the aromatization process over different suitable catalysts [6, 7].

Promising catalysts for light naphtha aromatization contain zeolites, which are crystalline aluminum-silicate materials with different properties, such as high acidity and high surface area, [8-10]. Zeolites contain intra-crystalline micro-pores similar to the molecular diameters of light hydrocarbons, thus providing impressive molecular sieving effects for light hydrocarbons and have been commonly used as selective form catalysts in various processes of hydrocarbons, such as aromatic alkylation [11, 12]. H-ZSM-5 (MFI) has been reported as the best catalyst for the production of gasoline blending components from the light naphtha feedstock [13]. Furthermore, it is reported that zeolites with MFI structure are the most stable among various zeolites [14, 15]. Still, coke formation is unavoidable as is always detected in light paraffinic hydrocarbons conversion on acidic zeolites that forms near the external surface of the, resulting in rapid blocking of the pores, leading to a short catalyst lifetime. [16]. For that reason, many efforts have been made for H-ZSM-5 to minimize the deactivation and to keep its initial performance in light naphtha aromatization [17–20].

In this research, the effect of $\text{SiO}_2/\text{Al}_2\text{O}_3$ molar ratio of MFI-type zeolite catalyst on light naphtha aromatization is investigated. Several Characterizations techniques were carried out to explain and elaborate the performance of light naphtha aromatization. MFI (30) exhibits excellent conversion and 59 wt. % selectivity towards total aromatics. In addition, varying $\text{SiO}_2/\text{Al}_2\text{O}_3$ affects the acidity of the MFI zeolite samples.

4.3 Experimental

4.3.1 Reagents

MFI zeolite with $\text{SiO}_2/\text{Al}_2\text{O}_3$ ratio 23, 30, 50, 280, and 1500 used were procured from Zeolyst. Light straight run naphtha (LSRN) feed was received from Ras Tanura Refinery, Saudi Arabia.

4.3.2 Catalyst Preparation and Light Straight Run Naphtha Feed

MFI zeolites with several $\text{SiO}_2/\text{Al}_2\text{O}_3$ molar ratio 23, 30, 50, 280, and 1500 were calcined at 550 °C for 5 h with heating rate of 5 °C/min in order to obtain the acidic form. The paraffins, *iso*-paraffins, olefins, naphthenes and aromatics (PIONA) content of light straight run naphtha (LSRN), received from Ras Tanura Refinery Saudi Arabia, was measured using a PIONA gas chromatograph. The PIONA composition (presented in Table 4.1) indicates high paraffinic nature of LSRN.

Table 4.1: Composition of light straight run naphtha feed

Component	Paraffin (wt.%)	<i>i</i>-Paraffin (wt.%)	Olefin s (wt.%)	Naphthenes (wt.%)	Aromatics (wt.%)
C₅	13.9	14.9	0.0	3.6	0.0
C₆	14.9	27.8	0.0	4.4	3.3
C₇	0.0	16.8	0.2	0.1	0.0
Total	28.8	59.5	0.2	8.1	3.3

4.3.3 Catalyst Characterization

MFI zeolite samples with several SiO₂/Al₂O₃ (23, 30, 50, 280, and 1500) molar ratios were characterized by XRD, BET, SEM, and NH₃-TPD, to investigate several physio-chemical and surface properties. XRD patterns are gained by Rigaku Miniflix II using CuK besides the following conditions of radiation [$\lambda = 1.54051 \text{ \AA}$, 30 kV and 15 mA and step size of 0.02° from 3° to 60° θ) and rate of 2°/min]. The surface area, pore volume, and pore diameter of the representative MFI zeolite samples with several SiO₂/Al₂O₃ molar ratios were determined by nitrogen adsorption at -195 °C with Micromeritics ASAP-2020 analyzer using the Brunauer-Emmett-Teller (BET) method based on the adsorption data in the partial pressure (P/P₀) range 0.05– 0.35. The pore-size distribution was determined by using the Barrett Joyner Halenda (BJH) adsorption model. Also, Micro pore volume was obtained by t-plot analysis. SEM of images of MFI zeolite samples were captured with a scanning electron microscope (NOVA FEISEM-450 equipped with EDX detector). The samples were loaded on the sample holder, held with

conductive copper tape and coated with a film of gold in a vacuum with a Cressington sputter ion-coater for 30 s with a 15 mA current. Temperature programmed desorption (NH₃-TPD) experiment were conducted to measure the acidity of MFI zeolite samples. This characterization test was conducted using Mettler Toledo. 15 mg of catalyst charged into the TPD apparatus was pretreated at 300 °C for 2 h with a stream of helium (25 mL/min). After cooling the catalyst to room temperature, ammonia (50 mL/min) was introduced into the reactor at 100 °C for 30 min to saturate acid sites of the catalyst. Physisorbed ammonia was removed at 120 °C for 2 h under a flow of helium (50 mL/min). After cooling down the sample, furnace temperature was increased from 100 °C to 600 °C at a heating rate of 10 °C/min under a flow of helium (25 mL/min). The desorbed ammonia was detected by the weight loss of the sample being analyzed.

4.3.4 Catalyst Evaluation

Catalyst performance evaluation screening tests were conducted in a laboratory-scale fixed-bed reactor system. In a typical experiment, the reactor (grade 316 stainless steel tube with an ID of 0.312 in., OD of 0.562 in., and a length of 8 in.) is charged with 0.5 g of the catalyst sieved to a particle size of 0.5-1.0 mm diameter. The catalyst is activated in a nitrogen stream at 550 °C for 2 h. The flow rate of the LSRN feed is varied by keeping the N₂ flow rate constant at 10 mL/min during the reaction. The reaction is carried out at 550 °C, WHSV (weight hourly space velocity) of 1 h⁻¹, 1-5 h time-on-stream (TOS), and atmospheric pressure. The quantitative analysis of the reaction products is carried out using an online DHA GC equipped with two FIDs and one TCD reactor.

4.4 Results and Discussion

4.4.1 Catalyst Characterization

The textural properties of MFI zeolite samples with several SiO₂/Al₂O₃ (23, 30, 50, 280, and 1500) molar ratios are shown in Table 4.2. The N₂ adsorption desorption isotherm is Type I with high up taking at low relative pressures no distinct hysteresis loop, confirming its micro porous character which is distinctive for zeolites based on Figure 4.1 and the *t*-plot method is used to obtain micro-pore volume [21]. The external surface area and pore diameter are decreasing as the SiO₂/Al₂O₃ increases. The specific areas for MFI (23) and MFI (30) are (299 m²/g, 351 m²/g) respectively. This variation of results is due to variation in the SiO₂/Al₂O₃ of the parent zeolite samples. Barrett, Joyner, and Halenda (BJH) pore size of MFI zeolite samples with several SiO₂/Al₂O₃ (23, 30, 50, 280, and 1500) molar ratios in Figure 4.2. Based on that, it can be concluded that the distribution of pores of ZSM5 parent are dominant in the micro-pore region.

Table 4.2: Textural properties of the MFI samples catalysts

Catalyst	S _{BET} (m ² /g)	Ext. SA by t-plot (m ² /g)	Pore Volume (cm ³ /g)	Pore Diameter (nm)
MFI(23)	299	222	0.076	3.61
MFI(30)	351	202	0.174	4.68
MFI(50)	294	198	0.075	3.23
MFI(280)	359	168	0.179	2.17
MFI(1500)	321	271	0.046	3.27

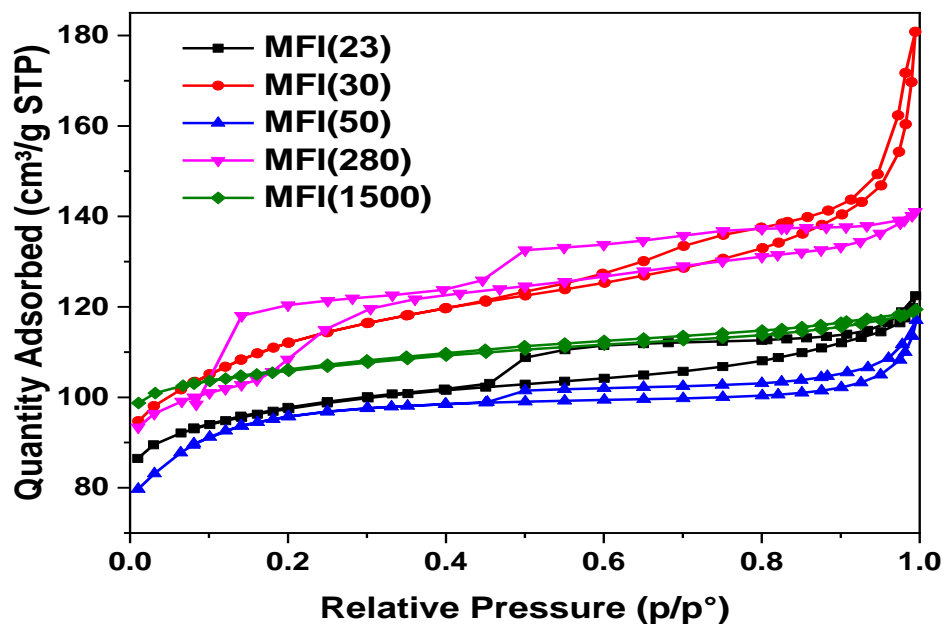


Figure 4.1: Nitrogen adsorption-desorption isotherms of the MFI zeolite samples with SiO₂/Al₂O₃ (23, 30, 50, 280, and 1500) molar ratios

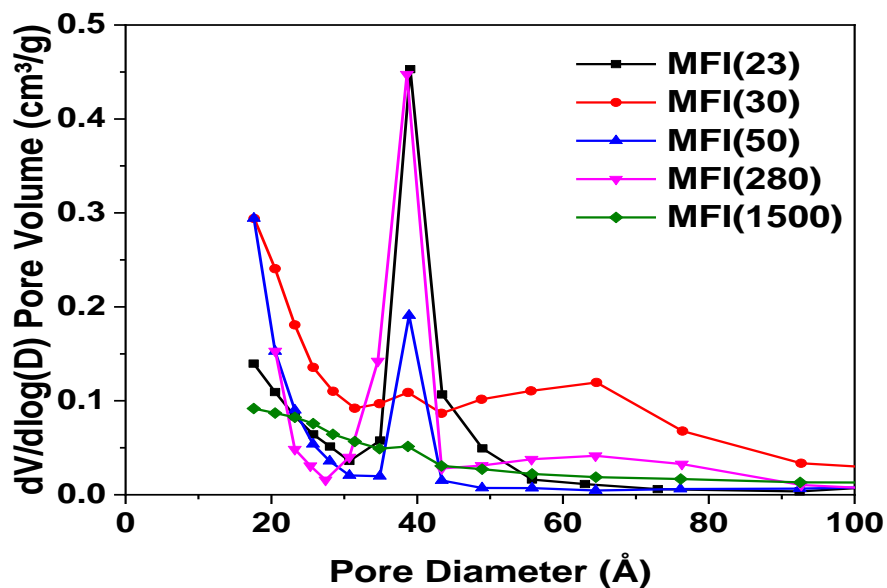


Figure 4.2: BJH pore size of the MFI zeolite samples with SiO₂/Al₂O₃ (23, 30, 50, 280, and 1500) ratios

XRD patterns for the parent MFI zeolite samples with several $\text{SiO}_2/\text{Al}_2\text{O}_3$ (23, 30, 50, 280, and 1500) molar ratios are presented in Figure 4.3. All the MFI zeolite samples shows the similar peak diffraction patterns compare to the literature that corresponded to zeolite ($7\text{--}9^\circ$ and $22^\circ\text{--}25^\circ$ 2θ). This indicates that $\text{SiO}_2/\text{Al}_2\text{O}_3$ has negligible impact on the MFI structure. However, the intensity of MFI (280) and MFI (1500) is slightly higher due to the variation in $\text{SiO}_2/\text{Al}_2\text{O}_3$.

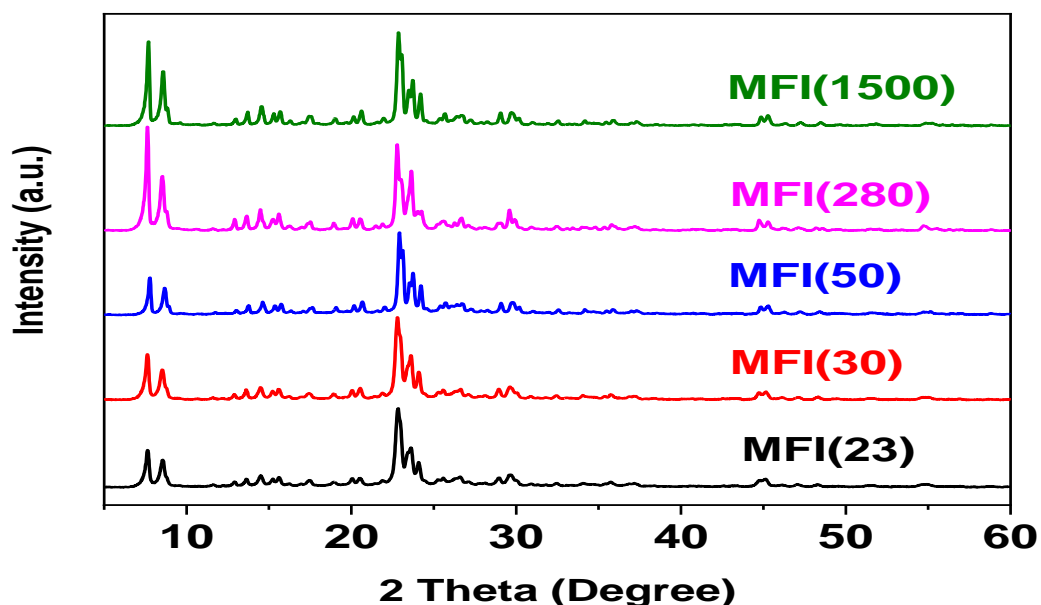


Figure 4.3: XRD patterns of the MFI zeolite samples with $\text{SiO}_2/\text{Al}_2\text{O}_3$ (23, 30, 50, 280, and 1500) molar ratios

The total acidity of the parent the parent MFI zeolite catalysts with several $\text{SiO}_2/\text{Al}_2\text{O}_3$ (23, 30, 50, 280, and 1500) molar ratios are shown in Table 4.3. The NH_3 -TPD profiles of the parent MFI samples catalysts and the relative deconvolution peaks are reported Figure 4.4. For parent MFI catalysts, NH_3 -TPD profiles is distributed in three peaks related to weak-medium, medium-strong, and strong acid sites, in the temperature range of $100\text{--}250^\circ\text{C}$, $250\text{--}400^\circ\text{C}$, and $400\text{--}600^\circ\text{C}$, respectively.

Table 4.3: NH₃ TPD profiles for MFI samples with SiO₂/Al₂O₃ (23, 30, 50, 280, and 1500) molar ratios

Catalyst	Area Distribution (mmol/g)		
	100-450 °C	above 450 °C	Total Area
MFI(23)	1.50	0.32	1.82
MFI(30)	1.64	0.43	2.06
MFI(50)	1.50	0.33	1.83
MFI(280)	0.43	0.16	0.59
MFI(1500)	0.13	0.11	0.24

All the samples have the similar behavior of the strong and low acid distributions. The low temperature region is attributed to the ammonia adsorbed on the weakly acidic sites that is influenced by the mobility of the proton, while the strong acid sites recognized by the surface hydroxyl group. As the SiO₂/Al₂O₃ molar ratio increase, the acidity of parent zeolite samples decrease due to shortage of alumina content.

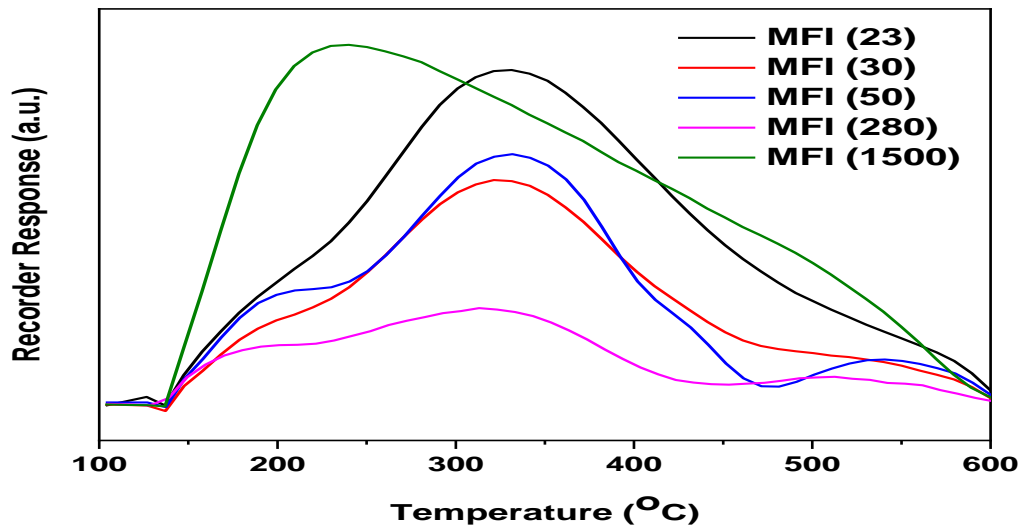


Figure 4.4: NH₃-TPD curves for the parent MFI zeolite samples with SiO₂/Al₂O₃ (23, 30, 50, 280, and 1500) ratios

SEM of images of the parent MFI zeolite samples with several $\text{SiO}_2/\text{Al}_2\text{O}_3$ (23, 30, 50, 280, and 1500) molar ratios catalysts were captured with a scanning electron microscope (NOVA FEISEM-450). SEM images of parent and MFI samples are shown in Figure 5. As can be seen in Figure 4.5, parent MFI (30) possesses a well-ordered a square-looking crystallite morphology with a large crystal size of about < 150 nm. As shown in figure 5 the surface morphology of MFI (23) is well ordered square shape and as the $\text{SiO}_2/\text{Al}_2\text{O}_3$ increases the shape of the MFI zeolite is becoming more cylindrical in shape.

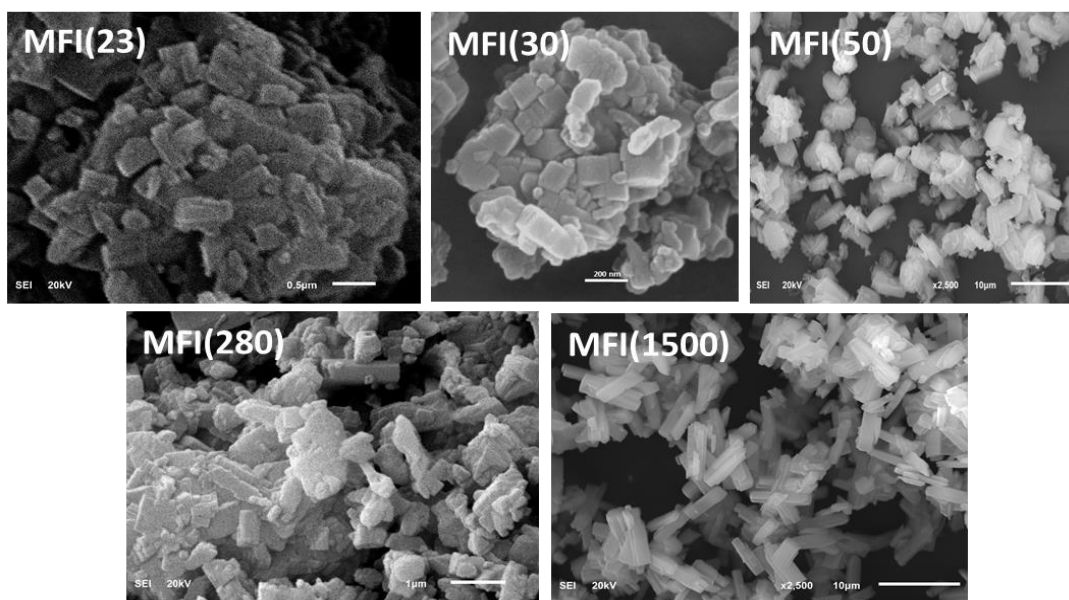


Figure 4.5: The SEM images of MFI zeolite samples with several $\text{SiO}_2/\text{Al}_2\text{O}_3$ (23, 30, 50, 280, and 1500) ratios

4.4.2 Catalyst Evaluation

Parent MFI zeolite samples with several $\text{SiO}_2/\text{Al}_2\text{O}_3$ (23, 30, 50, 280, and 1500) molar ratios catalysts were evaluated for the aromatization LSRN aromatization, results are summarized in Figure 4.6 and Table 4.4. The product distribution is divided mainly into liquid and gas yields. The liquid distribution includes BTX and C_{5+} paraffins and olefins while the gaseous products contains C_1 , C_2 , $\text{C}_2^=$ and C_3+C_4 . The conversion in general at 550 °C decreases as the $\text{SiO}_2/\text{Al}_2\text{O}_3$ increases. The conversion for the thermal, MFI (280) and MFI (1500) are 22 %, 65%, 35 % respectively. Other MFI samples are 100 % conversion. The zeolite provides the sufficient acidity to the reaction to carry out the oligomerization and cyclization over the acidic sites to produce aromatics. As the $\text{SiO}_2/\text{Al}_2\text{O}_3$ increases, the catalytic conversion activity of the MFI samples towards the production of aromatics decline dramatically. In specific, the total aromatics for MFI (30) catalyst are almost 59 wt. %. This high selectivity towards aromatics is attributed to acidic medium that is extremely effective in the conversion of small cracked products especially (C_3 , C_4) olefins that are frequently transformed into BTX by secondary reactions. Moreover, MFI (280) and MFI (1500) gave lower aromatics yield of 11 wt. % and 7 wt. % respectively. This is due to the lack of reaching the Brønsted acidic sites, cyclization of paraffins and high cracking rate [13].

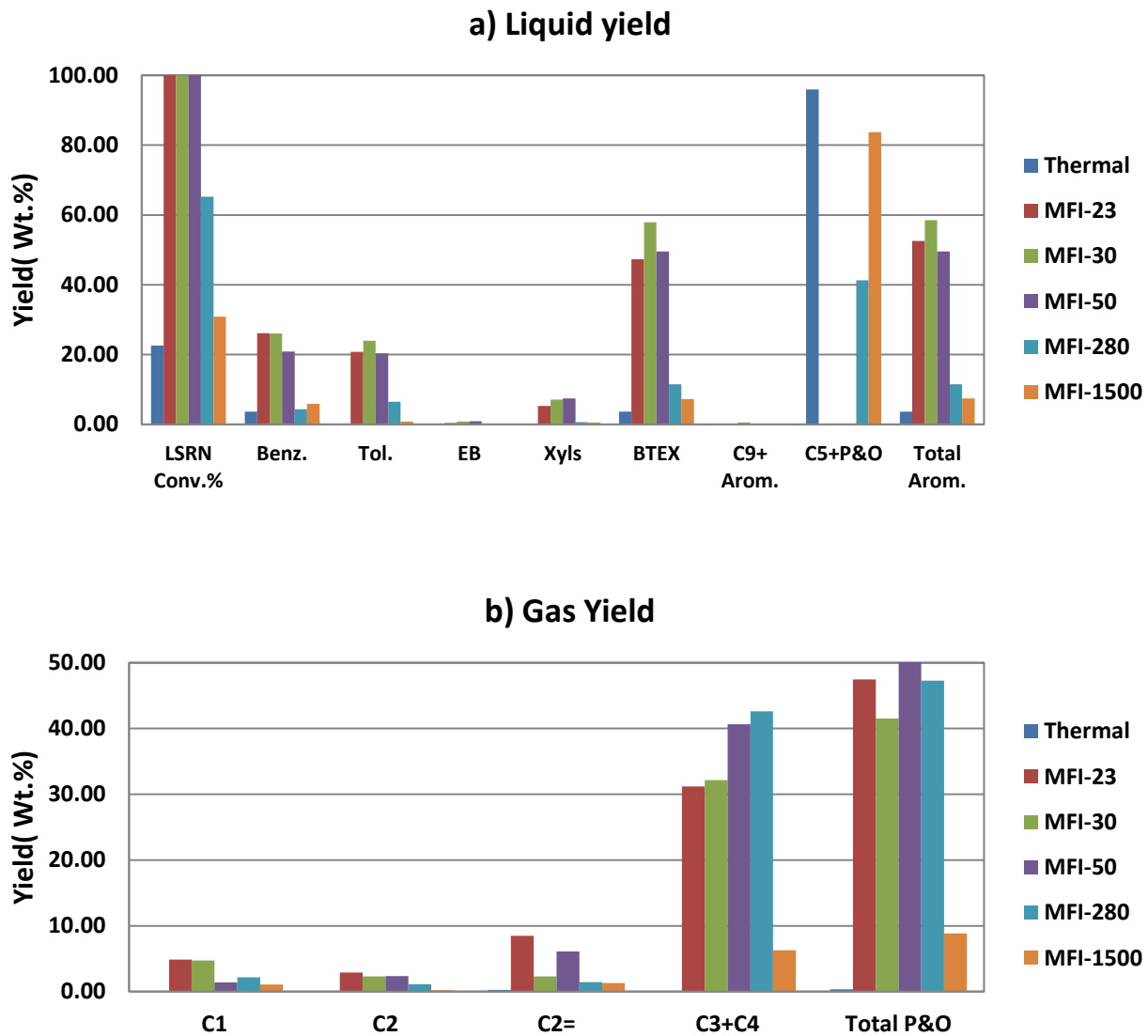


Figure 4.6: The effect of SiO₂/Al₂O₃ (23, 30, 50, 280, and 1500) molar ratios catalysts, in the conversion of LSRN at 550 °C and 1.0 h⁻¹ WHSV, Atmospheric pressure (a) Liquid yield, (b) Gas yield

Table 4.4: Catalytic performance of thermal and parent MFI with SiO₂/Al₂O₃ (23, 30, 50, 280, and 1500) ratios catalysts (Reaction conditions: Catalyst= 0.5 g, Feed= LSRN, Temp. = 550 oC, WHSV= 1 h⁻¹, N₂= 10 mL/min)

Catalyst	Thermal	MFI-23	MFI-30	MFI-50	MFI-280	MFI-1500
LSRN	22.55	100.00	100.00	100.00	65.20	30.86
Conv.%						
Benz.	3.69	26.10	26.03	20.88	4.35	5.87
Tol.	0.00	20.76	23.96	20.32	6.52	0.78
EB	0.00	0.41	0.81	0.91	0.00	0.10
Xyls	0.00	5.25	7.11	7.46	0.60	0.56
BTEX	3.69	47.27	57.91	49.57	11.47	7.30
C₉₊ Arom.	0.00	0.00	0.59	0.00	0.00	0.11
C₅₊P&O	95.97	0.00	0.00	0.00	41.25	83.76
Total Arom.	3.69	52.52	58.49	49.57	11.47	7.42
C₁	0.05	4.88	4.72	1.37	2.14	1.07
C₂	0.00	2.90	2.32	2.36	1.10	0.19
C₂₌	0.25	8.49	2.30	6.08	1.41	1.30
C₃+C₄	0.04	31.20	32.17	40.63	42.62	6.26
Total P&O	0.34	47.48	41.51	50.43	47.28	8.82
Sum	100.00	100.00	100.00	100.00	100.00	100.00

4.5 References

- [1] Song J, Ma HJ, Tian ZJ, Yan LJ, Xu ZS, Liu QH, et al. The effect of Fe on Pt particle states in Pt/KL catalysts. *Appl Catal A* 2015;492:31–7.
- [2] Ahuja R, Punji B, Findlater M, Supplee C, Schinski W, Brookhart M, et al. Catalytic dehydroaromatization of n-alkanes by pincer-ligated iridium complexes. *Nat Chem* 2011;3:167–71.
- [3] T. Inui, Y. Makino, F. Okazumi, S. Nagano, A. Miyamoto, *Ind. Eng. Chem. Res.*26 (1987) 647.
- [4] P. Meriaudeau, G. Sapaly, C. Naccache, *Stud. Surf. Sci. Catal.* 49 (1989) 1423.
- [5] R.L.V. Mao, L. Dufresne, *Appl. Catal.* 52 (1989) 1.
- [6] C.D. Gosling, F.P. Wilcher, L. Sullivan, *Hydrocarbon Process.* 12 (1991) 69.
- [7] G. Giannetto, R. Monque, R. Galiasso, *Catal. Rev. Sci. Eng.* 36 (1994) 271.
- [8] Magnoux, P., Cartraud, P., Mignard, S., Guisnet, M., *J. Catal.*,**106**, 242 (1987).
- [9] Corma, A., González-Alfaro, V., Orchillès, A. V., *Appl. Catal.A: General*, **129**, 203 (1995).
- [10] Katada, N., Kageyama, Y., Takahara, K., Kanai, T., Beguma, H. A., Niwa, M., *Catal. A Chem.*, **211**, 119 (2004).
- [11] Sugi, Y., Kubota, Y., Komura, K., Sugiyama, N., Hayashi, M., Kim, J. H., Seo, G., *Appl. Catal. A: General*, **299**, 157 (2006).
- [12] Inagaki, S., Kamino, K., Kikuchi, E., Matsukata, M., *Appl. Catal. A: General*, **318**, 22 (2007).
- [13] J.L.Hodala, AB. Halgeri, GV. Shanbhag, RS. Reddy, NV. Choudary, PV. Rao, *ChemistrySelect* 1 (2016) 2515–2521.

- [14] A. Corma, J. Mengual, P.J. Miguel, *Appl. Catal. A: Gen.* 417–418 (2012) 220–235.
- [15] M. Guisnet, P. Magnoux, *Appl. Catal.* 54 (1989) 1–27.
- [16] M. Guisnet, P. Magnoux, *Deactivation and Regeneration of Zeolite Catalysts*, Imperial College Press, London, 2011.
- [17] J. Lee, U.G. Hong, S. Hwang, M.H. Youn, I.K. Song, *Fuel Process. Technol.* 109(2013) 189–195.
- [18] H. Mochizuki, T. Yokoi, H. Imai, R. Watanabe, S. Namba, J.N. Kondo, T. Tatsumi, *Microporous Mesoporous Mater.* 145 (2011) 165–171.
- [19] H. Konno, T. Okamura, T. Kawahara, Y. Nakasaka, T. Tago, T. Masuda, *Chem. Eng.J.* 207–208 (2012) 490–496.
- [20] G. Zhao, J. Teng, Z. Xie, W. Jin, W. Yang, Q. Chen, Y. Tang, *J. Catal.* 248 (2007)29–37.
- [21] R.H. Perry, D.W. Green, *Perry's Chemical Engineers' Handbook*, 7th ed., McGraw-Hill, New York, 1997, p.2581.

CHAPTER 5

AROMATIZATION OF LIGHT NAPHTHA OVER BIMETALLIC Mo-M/ZSM-5 MODIFIED CATALYSTS

5.1 Background

In this chapter, the performance of the aromatization reaction of light alkanes is investigated over bi-metallic Mo-M/ZSM-5 catalyst. The catalytic reaction is carried out in affixed bed reactor at 550 °C, light naphtha feed (C₅, C₆) and atmospheric pressure. Also, several characterization methods are carried out. Finally, the stability of best performance catalyst toward the production of aromatics is summarized.

5.2 Introduction

Transforming light naphtha into greater significance products, particularly aromatization of linear alkanes into BTX aromatics (Benzene, Toluene, and Xylene) has been the focus of importance for preceding periods [1, 2]. They are generally manufactured via catalytically reforming of naphtha or light oil fraction pyrolysis and used as raw materials for the petrochemical industry to produce essential raw materials such as plastics, synthetic resins and purified acids like isophthalic and terephthalic acids, surrounded by supplementary materials [3-5]. In general, the remaining distillate of the catalytic reforming process is called raffinate oil which contains long branched chains of hydrocarbons mainly alkanes alkenes and cycloalkanes. Since the demand of aromatic is

increasing in a dramatic way, raffinate oil is used as feedstock to produce various aromatics compounds mainly BTX products via suitable aromatization process. As (C_5 - C_6) paraffins are the significant compositions in the raffinate oil, these alkanes are used to investigate the aromatization process over different suitable catalysts [6, 7]. It has been reported that HZSM-5 shows superior performance in selectivity and stability for transforming light naphtha into aromatics. In addition, Brønsted acid locations in ZSM-5 catalyze and improve the oligomerization of short chain olefins to C_{6+} paraffins and their following cyclization reactions. Furthermore, these factors of HZSM-5 could be promoted by implementing dehydrogenation cations agents such as Gallium, Zinc, Platinum [8–10]. These bifunctional catalysts contain metals that enhance the performance of the aromatization reaction besides the acidity from HZSM-5 and it includes dehydrogenation functions that convert olefins to aromatics [11-13]. Moreover, the metal function decreases cracking selectivity in the direction of olefins and yield hydrogen gas as side product. According to the literature, several metals display great performance to produce aromatics such as Zn [14–19], Ga [20–25], Pt [26–28] and La [29]. Tamiyakul et al. and his co-workers investigated the hydrogen treatment on Zn-MFI and studied the activity for normal Pentane for the aromatization reaction and concluded that the selectivity towards aromatics is increased [30]. Hodala et al. found that the Zn and Ga metals that supported on ZSM-5 improved the dehydrogenation function in the reaction and as a result increased the yield of aromatics formed from light alkanes [31]. Tshabalala et al. and his team reported that the aromatization reaction of normal Hexane (n - C_6) supported with several metals such as Zn and Ga displayed great performance in forming BTX compounds due to their extraordinary dehydrogenation capability [32].

Recently, Molybdenum has shown superior and high activities toward aromatics productions. Methane Dehydroaromatization (DHA) is a new attractive process for direct production of aromatics compounds over Mo/H-ZSM-5 and produces up to 70% benzene at high temperature [33]. It is demonstrated that much higher aromatics compounds are gained when using steam-dealuminated Mo/ZSM-5 in comparison with conventional catalysts. It is assumed that introducing the Molybdenum species, extracts easily the framework aluminum and enhancing the aromatics yield [34, 35]. In addition, Molybdenum oxides have shown effective performance in yielding aromatics as catalysts promoters over H-ZSM-5 [36-38]. Furthermore, Wang et al. investigated the aromatization over Mo-P/H-ZSM-5 in fluid catalytic cracking (FCC) of naphtha in a fixed bed reactor and the liquid yield of aromatics was 61% [39].

In this study, Bi-metallic effect of Mo-M-Z30 prepared via wet impregnation method are examined and investigated. Furthermore, the presence of Molybdenum (Mo) metal is evaluated with the other metals and how the aromatization reaction performance would change. In addition, Characterizations of several samples are carried out such as X-ray Diffraction (XRD), Surface area (BET), Temperature Programmed Desorption (TPD), and Scan Electron Microscopy (SEM). Also, Stability performance for 18 h is carried out for selective Mo-Zn/Z30 catalytic sample.

5.3 Experimental

5.3.1 Catalyst Synthesis

Zeolite based materials in the ammonium form with silica alumina ratio 30 is purchased and available in the market. The $\text{NH}_4\text{-ZSM-5}$ form is eliminated and converted to the hydrogen form (H-ZSM-5) by means of calcination of the sample at 550°C for 5 hours. This step is essential to obtain the acidic form of the zeolite. Several metals supported samples are synthesized using wet impregnation method of preparation with different metals loadings 2% Mo, 2% Fe, 2% Ga, 1% Pt, 2% Ce and 1% Zn. Many precursors are used and utilized in the synthesis process such as $\text{Pt}(\text{NH}_3)_4(\text{NO}_3)_2$, $\text{Fe}(\text{NO}_3)_3 \cdot 9\text{H}_2\text{O}$, $\text{Ga}(\text{NO}_3)_3 \cdot 9\text{H}_2\text{O}$, $\text{Ce}(\text{NO}_3)_3 \cdot 6\text{H}_2\text{O}$, $(\text{NH}_4)_6\text{Mo}_7\text{O}_{24} \cdot 4\text{H}_2\text{O}$ and $\text{Zn}(\text{NO}_3)_2 \cdot 6\text{H}_2\text{O}$. These precursors are used to prepare different Bi-metallic supported zeolites Mo-M-Z30. 4g batch is prepared by dissolving the parent support ZSM-5(30) in specific amount of distilled water and keep it for stirring for some time. Next, the precursor is dissolved in small amount of DI- H_2O and then added to the solution for stirring to obtain uniform distribution. Afterwards, the combined solution is heated at 70°C overnight and dried at 100°C for 24 hours. Finally, the sample is crushed and calcined at 550°C for 5 hours at ramp of $10^\circ\text{C}/\text{min}$ to convert the metals to the oxide form and to remove the remaining of the precursors mainly nitrates. The metal supported samples on the zeolites are characterized through different characterizations methods.

5.3.2 Catalyst Characterization

X-ray diffraction (XRD) patterns are collected by means of a Rigaku Miniflix II using CuK as a radiation source in addition to [K ($\lambda = 1.54051 \text{ \AA}$), 30 kV and 15 mA and step size of 0.02° from 3° to 90° θ] and rate of $2^\circ/\text{min}$]. The textural properties of the metal supported catalyst are analyzed via A Micromeritics ASAP-2020 analyzer by the usage of Nitrogen gas adsorption at 77K. The samples are heated under vacuum pressure for 2 hours at 220°C . Then, the surface area of the sample is calculated from the desorption data ranged between 0.06 up to 0.3 (P/P_0). In addition, Ammonia Temperature Programmed Desorption (NH_3 -TPD) is used to investigate the acidity of the metal supported samples using Mettler Toledo instrument. In this individual analysis, 100mg of the sample is preheated at 300°C using Helium gas (He) at flow rate of 50cc/min for 2 hours. Then, a mixture of 5% NH_3 -He is adsorbed on the sample at a temperature of 100°C for 30 minutes. After that, the ammonia is removed using a purge of helium gas flowing on the sample at 120°C for 2 hours. As a final step, the catalytic samples are heated from (120 to 600) $^\circ\text{C}$ at ramp of $10^\circ\text{C}/\text{min}$ and helium flow of 30cc/min. In the heating period, the ammonia adsorbed is observed. Furthermore, the morphology and crystalline size of specific selected catalytic samples are investigated through Scanning Electron Microscopy recorded by Philips XL30 SEM.

5.3.3 Catalyst Evaluation

The conversion reaction of light naphtha into blending gasoline components is carried out into micro stainless steel fixed bed reactor under atmospheric pressure. Before the reaction, the catalyst is pelldized and sieved to size of 0.5–1.00 mm diameter. In a normal experiment, a pelldized 0.5 g catalyst is loaded to the reactor bounded with silicon carbide to make sure that the sample is in the middle of the reactor. The light alkanes feed is mixed with nitrogen as a carrier gas with flow of 10 ml/min. Moreover, the feed is preheated for 2 hours at 550°C to activate the catalyst. After that, the feed is introduced through the reactor using syringe pump at flow rate of 0.01 ml/min. The reaction conditions are T=550°C, WHSV=1 h⁻¹, TOS= 5 hrs. The BTEX compounds are collected and analyzed by online gas chromatograph (GC SHIMADZU 2014 GC-14B, OV-1 capillary column 50 m ×0.20 mm, flame ionization detector). Light Naphtha conversion is evaluated by the presence of (C₅ and C₆) in product distribution. Furthermore, specific distribution of the aromatics compound is achieved by PIONA and Detailed Hydrocarbon Analysis (DHA) to obtain the yield in a % mass basis. The composition of the light naphtha feed contains mainly C₅ and C₆ normal and Iso- paraffins and other hydrocarbons as minor portions as shown in Table 5.1.

Table 5.1: Composition of light naphtha feed (100% Total)

Component	normal-Paraffin, wt. %	iso-Paraffin, wt. %	Olefins wt. %	Naphthenes, wt. %	Aromatics, wt. %
C₅	13.9	14.9	0.0	3.6	0.0
C₆	14.9	27.8	0.0	4.4	3.3
C₇	0.0	16.8	0.2	0.1	0.0
Total	28.8	59.5	0.2	8.1	3.3

5.4 Results and Discussion

5.4.1 Catalyst Characterization

The crystallinity of the parent zeolite and metal supported catalysts are analyzed using XRD characterization patterns as shown in Figure 5.1. All the metallic samples have the same crystalline patterns of the parent zeolite and the ranges are (7° – 9° and 22° – 25°) 2θ correspondingly because the crystal growth in the samples. The small diffraction angle ($2\theta = 7.8$ and $2\theta = 9.8$) refer to the crystal planes (011) and (200) respectively [40]. The presence of the active metals may possibly not change the parent zeolite framework. Moreover, significant peaks of the metal oxides are not detected in the XRD which could be due to the great dispersion of the metals on the zeolite surface [41]. However, in comparison with the parent zeolites, the peak intensity of the metallic samples is slightly lower. This is due to mainly the intermixing of the metals into the support without any effect on the crystalline structure and the attribution of the X-ray absorption coefficient of impregnated metal species [42, 43].

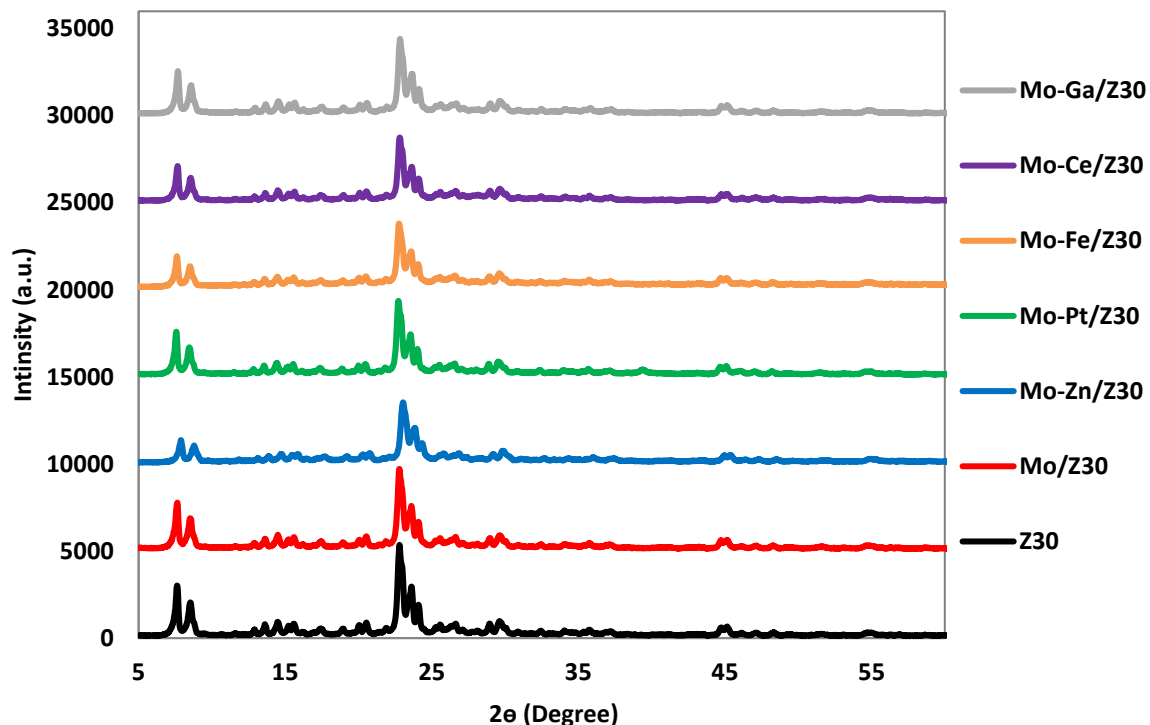


Figure 5.1: XRD patterns of H-ZSM-5 and other metal modified catalysts

The textural properties of the parent zeolite and metal supported samples are achieved using BET characterization technique to investigate surface area and pore volume as shown in Table 5.2. The N_2 adsorption desorption isotherm is Type I which is distinctive for zeolites as demonstrated in Figures 5.2 and 5.3 and the t-plot method is used to obtain micro-pore volume. Deposition of the metal species decreases of the S_{BET} for all the metallic samples and increase in the pore diameter. This is due to the interaction of the metal particles that results in elevating the pore diameter. These micro-porous features may possibly be important and accountable for the enhanced of light naphtha aromatization performance [44]. The S_{BET} of parent H-ZSM-5 is $351(m^2/g)$.

Table 5.2: Textural properties of ZSM-5 and bi-metallic modified catalysts

Catalyst	S_{BET} (m^2/g)	Pore Volume (cm^3/g)	Pore Diameter (nm)
Z30	351	0.174	4.68
Mo/Z30	330(-6%)	0.177(+2%)	5.46 (+17%)
Mo-Ga/Z30	307(-13%)	0.155(-11%)	5.53(+18%)
Mo-Zn/Z30	325(-7%)	0.177(+2%)	5.59(+19%)
Mo-Pt/Z30	317(-10%)	0.171(-11%)	5.64(+21%)
Mo-Fe/Z30	328(-7%)	0.173(-1%)	5.40(+15%)
Mo-Ce/Z30	321(-9%)	0.174(0%)	5.61(+20%)

Loaded amount: Pt and Zn 1.0 wt. %; Fe, La, Ga and Mo 2.0 wt. %, numbers in the parenthesis describe % difference in textural properties of catalysts after metal(s) impregnation.

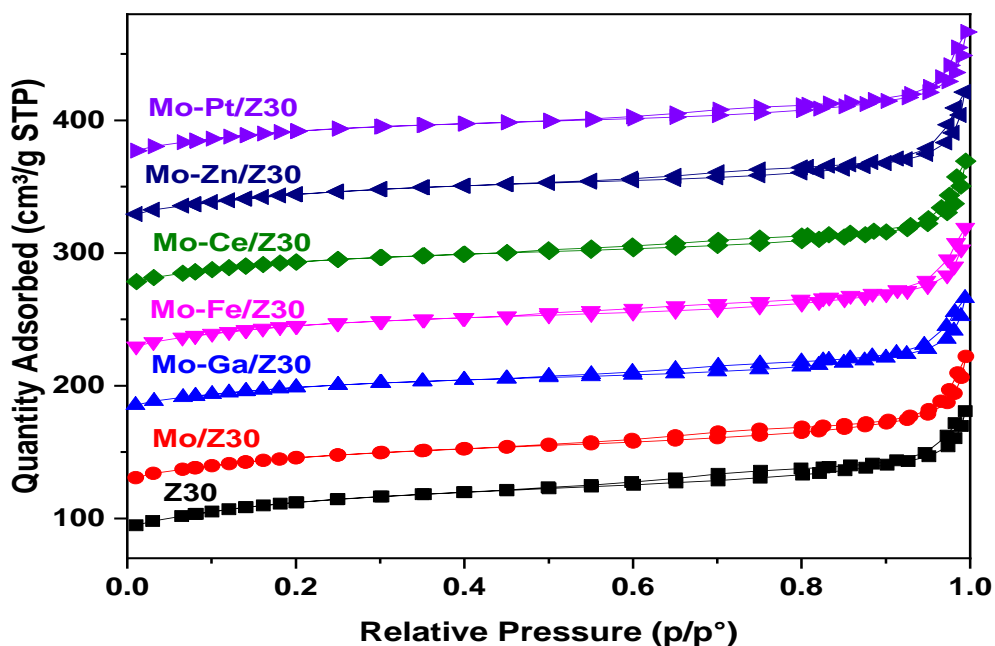


Figure 5.2: N_2 adsorption-desorption isotherms for parent and modified ZSM-5

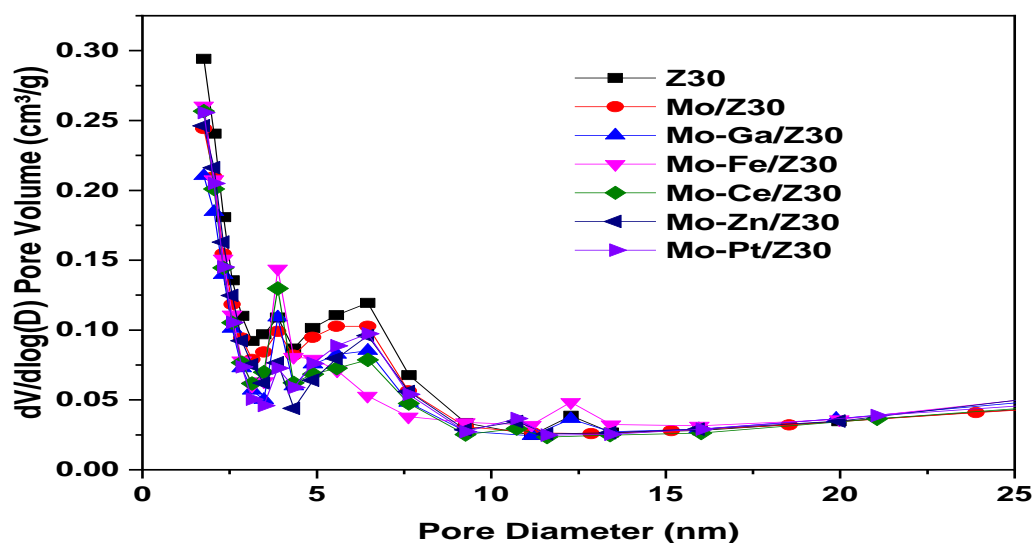


Figure 5.3: BJH pore size distribution for parent and modified ZSM-5

The strength of accessible surface acidic sites of the zeolite samples are examined and characterized using NH_3 -TPD analysis. There are main characteristics temperature regions which is low temperature peak that is related with weak acid sites (250°C) and strong acidic sites (above 400°C) and in between is the medium region as shown in Table 5.3. The low temperature region is ascribed to the ammonia adsorbed on the weakly acidic that is influenced by the movement of the proton whereas the strong acid sites acknowledged by the surface hydroxyl group [45, 46]. The metals supported catalysts have similar behavior as the parent zeolite where the acidity locations are the same. The introduction of the metals into the zeolite support, as illustrated in Figure 5.4, results in significant loss of acidic sites. This decrease will cause suppress acidic sites and accordingly stops the cracking side reaction towards olefins and force the reaction to produce aromatics. This suppression in the acidic sites particularly in the strong acidic sites by the metals is observed by NH_3 -TPD in which is demonstrated by the variation of

BTX and gaseous products. Conversely, lesser acidic sites produce heavier cracked (C_3+C_4) products [31].

Table 5.3: (NH_3 -TPD) and strong acidic sites for parent and modified ZSM-5

Catalyst	Area Distribution (mmol/g)			Total Area
	100-250 °C	250-400 °C	Above 400 °C	
Z30	1.00	0.51	0.56	2.06
Mo/Z30	1.04	0.47	0.42	1.93
Mo-Ga/Z30	0.98	0.53	0.44	1.95
Mo-Zn/Z30	1.06	0.59	0.49	2.14
Mo-Ce/Z30	1.01	0.73	0.63	2.37
Mo-Pt/Z30	1.03	0.63	0.51	2.17
Mo-Fe/Z30	1.02	0.54	0.48	2.04

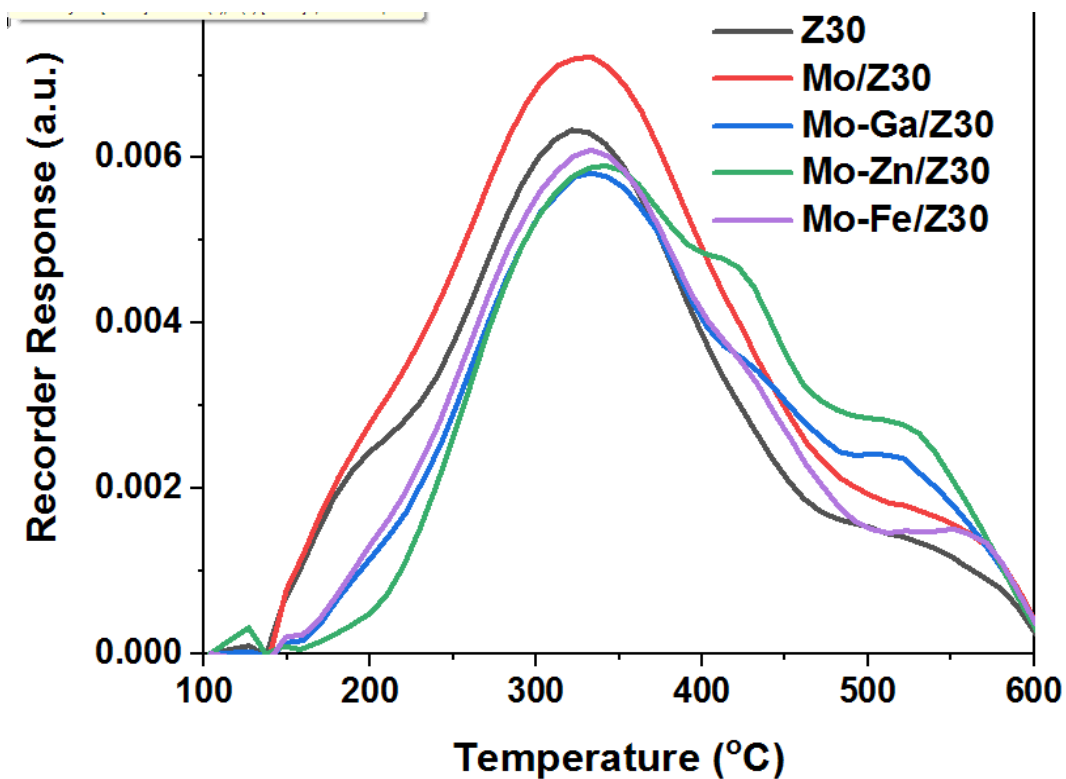


Figure 5.4: NH_3 -TPD patterns for ZSM-5 and bi-metallic modified catalysts

The morphology and crystallinity of the parent zeolite and metallic supported catalytic samples are analyzed using Scanning Electron Microscopy (SEM). Figure 5.5 illuminates the morphology of the samples and it is without doubt that all samples are crystalline and have the similar morphology for the zeolite and metallic supported samples. What is more, mapping of the metals on H-ZSM-5 is shown in Figure 5.6 to exhibit the dispersion of the Bi-metallic Mo-Zn on ZSM-5 support and it is clear the smoothness of the surface of zeolite increase the dispersion of the metals. Furthermore, as the metals are more dispersed the better the aromatization yield is.

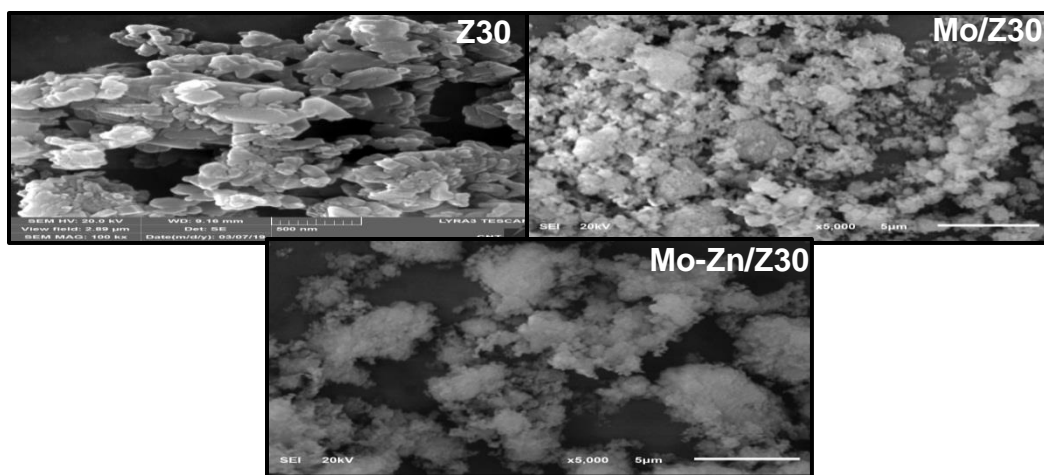


Figure 5.5: SEM images for parent Z30 and modified Mo/Z30 and Mo-Zn/Z30

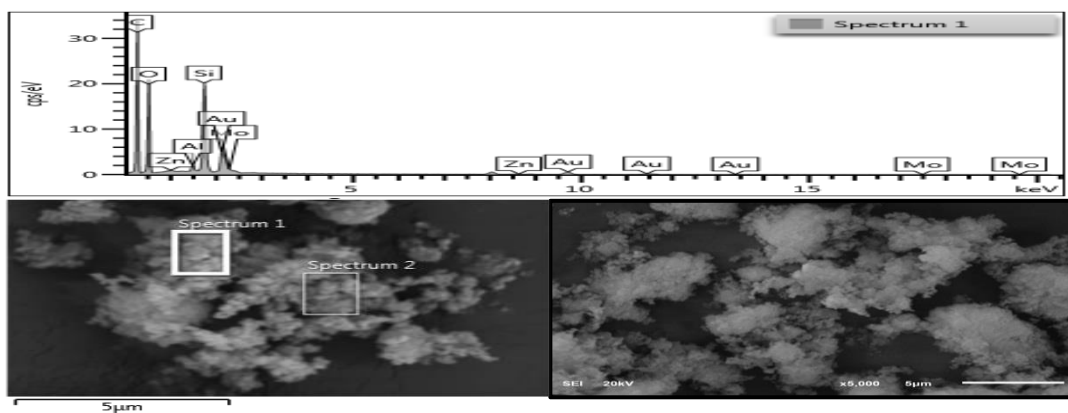


Figure 5.6: Elemental mapping for modified Mo-Zn/Z30 catalyst

5.4.2 Catalytic Performance

The aromatization reaction of light naphtha is evaluated over fixed bed reactor at 550°C and atmospheric pressure. The performance of zeolite and bi-metallic samples impregnated over H-ZSM-5 with SAR 30 is summarized in Table 5.4. The product distribution is categorized as liquid and gas yield where the liquid yield includes the aromatics and C₅₊ Paraffins whereas the gas yield contains Methane, Ethane and C₃+C₄. The conversion of all samples varies from (97-100) % except for the sample Mo-Fe/Z30 which is 81 %. In comparison with parent zeolite, adding metal species enhance the catalytic performance of light naphtha towards aromatics. Bi-metallic catalyst samples could activate alkanes through dissociative chemisorption and as a result BTX products are formed via further dehydrogenation and cyclization [31, 47]. The catalytic performance of light naphtha is more effective when two main factors are considered: acidity and dehydrogenation function. Zeolite provides sufficient acidity to the reaction and the pore volume to increase the internal surface area and to carry out the oligomerization and cyclization over the acidic sites to produce aromatics while the metal enhances the dehydrogenation function. Furthermore, the dispersion of the metals into the support elevates the performance of aromatics production. In individual, total aromatics for Mo-Ga/Z30 and Mo-Zn/Z30 are 61.75 wt. % and 61.38 wt. % correspondingly. This high selectivity towards BTX compounds is indorsed to the dehydrogenation activity of the metals which is in effect in transformation of small cracked products particularly (C₃, C₄) olefins that are commonly converted into BTX by secondary reactions. Contrariwise, the low aromatic yield of Mo-Fe/Z30 is 30.86 wt. % .This is because the deficiency of getting the Brønsted acidic sites, cyclization of paraffins and high cracking rate [31]. On

the other hand, the gas yield comprises total paraffin and olefins from (C₁ to C₄). Mo-Ga/Z30 and Mo-Zn/Z30 show total P& O which is 38 wt. % for both whereas total P&O for Mo-Ce/Z30, Mo-Pt/Z30 and Mo-Fe/Z30 is 54 wt. %, 42 wt. % and 48 wt. % consistently. This is because less density of acidic sites that causes some cracking formation of C₃+C₄ fractions. Yield is demonstrated in Figure 5.7.

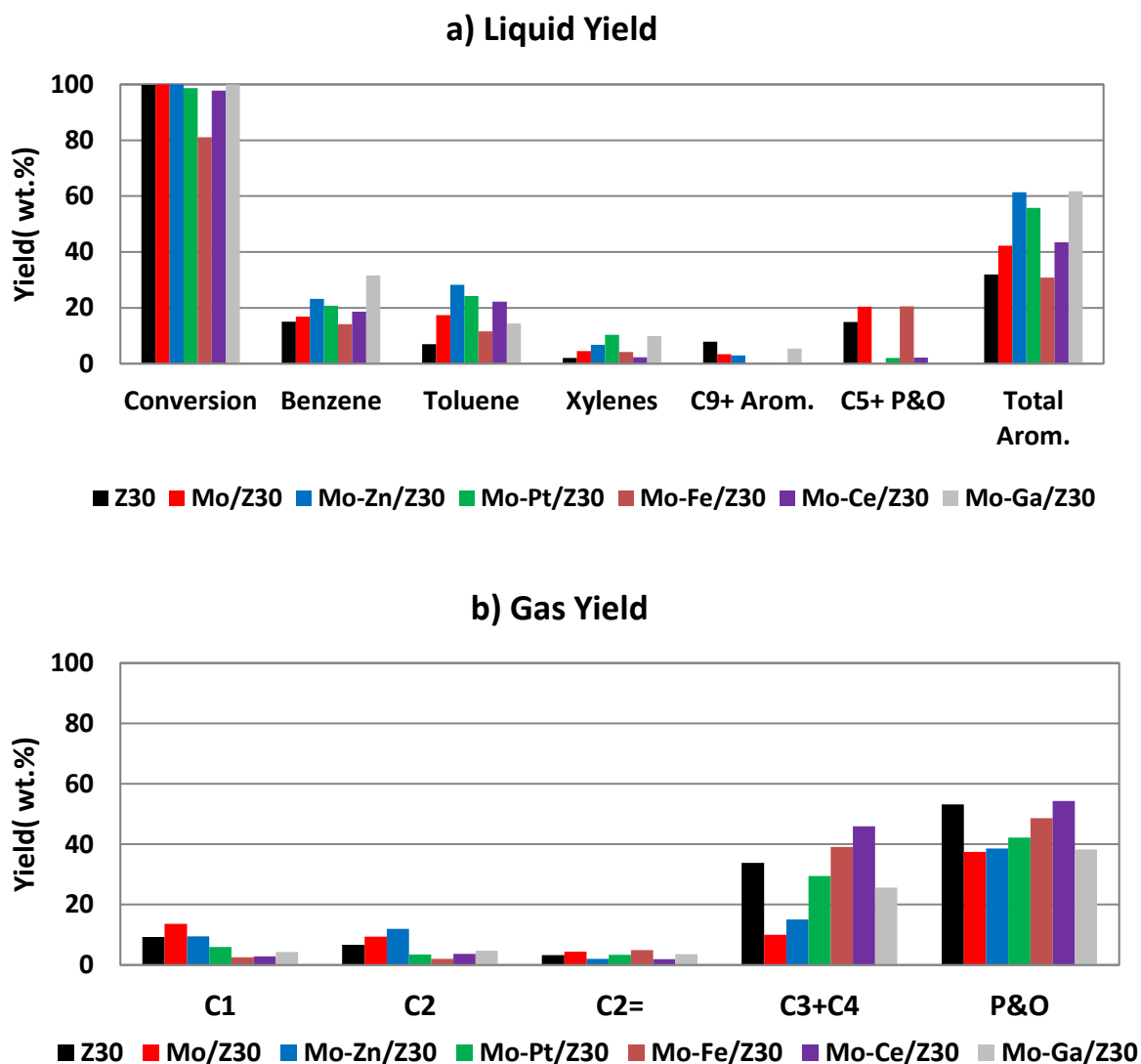
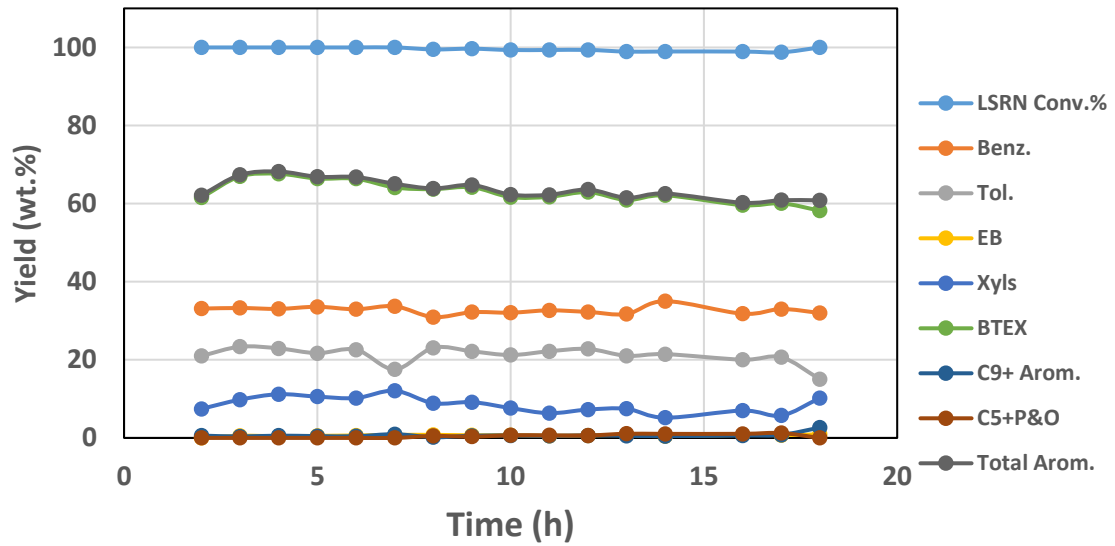


Figure 5.7: The effect of the parent and Mo or Mo-M modified Z30 catalysts, prepared by the co-impregnation method, in the conversion of LSRN at 550 °C and 1.0 h⁻¹ WHSV. (a) Liquid yield, (b) Gas yield

5.4.3 Effect of Time-On-Stream

Time on stream study is conducted under the same optimized conditions for the best performance catalyst Mo-Zn-Z30 in order to investigate the stability of the catalytic sample in the direction of deactivation as shown in Figure 5.8. In this analysis, the conversion is nearly (98-100) % whereas the aromatics differ in distribution. In the first 6h TOS, the aromatics yield 66.82 wt. % however after 16h analysis the aromatics yield dropped to 60.23 wt. %. Furthermore, although the conversion remained almost unchanged, the aromatics yield fell by 6%. On the other hand, C₁, C₂ and C₃+C₄ distribution of gaseous products showed slight variation over the 18h period. Throughout the 24h study, a marginal decrease in methane (4.01 wt. % to 3.16 wt. %), and ethane (7.17 wt. % to 1.85 wt. %) while C₃+C₄ increased from 18.68 wt. % to 31.66 wt. % Overall, coke formation usually results in a decrease the acidic sites and accordingly minor cracked products decreased however longer C₃+C₄ hydrocarbon increased. Also reproducibility test for Mo-Zn/Z30 is shown in Figure 5.9.

a) Liquid Yield



b) Gas Yield

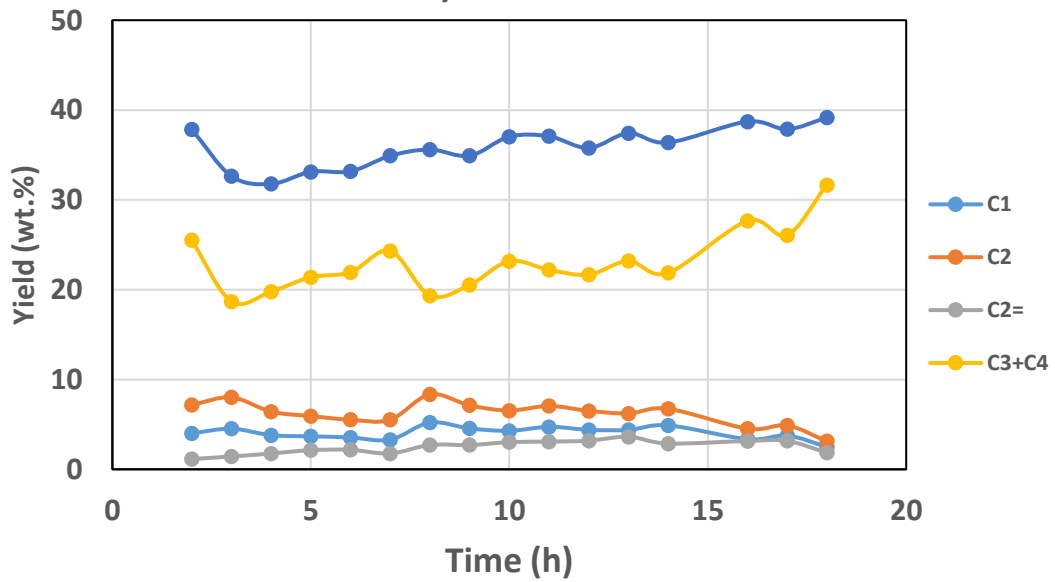


Figure 5.8: Time-on-stream for aromatization of LSRN over the Mo-Zn/Z30 liquid and gaseous product distribution (WHSV= 1h⁻¹, feed=0.01 mL/min, N₂=10 mL/min, T=550 °C). (a) Liquid yield, (b) Gas yield

Table 5.4: Catalytic performance of parent ZSM-5 and bi-metal modified ZSM-5 (Reaction conditions: Catalyst= 0.5 g, Feed= LSRN, Temp. = 550 °C, WHSV= 1 h⁻¹, N₂= 10 mL/min)

Catalyst	Z30	Mo/Z30	Mo-Zn/Z30	Mo-Ga/Z30	Mo-Pt/Z30	Mo-Ce/Z30	Mo-Fe/Z30
Conversion	99.77	100.00	100.00	100.00	98.71	97.82	81.08
	Yield (wt. %)						
C₁	9.26	13.64	9.51	4.26	5.96	2.84	2.54
C₂	6.73	9.39	11.99	4.72	3.43	3.67	2.05
C₂₌	3.30	4.38	2.00	3.59	3.35	1.96	4.89
C₃+C₄	33.85	10.02	15.12	25.68	29.42	45.88	39.10
P&O	53.14	37.43	38.62	38.25	42.16	54.35	48.58
Benzene	15.02	16.88	23.24	31.59	20.76	18.58	14.16
Toluene	6.96	17.43	28.20	14.41	24.20	22.15	11.52
Xylenes	2.02	4.49	6.70	9.91	10.32	2.24	4.21
BTX	24.00	38.81	58.38	56.31	55.83	43.47	30.48
C₉₊ Arom.	7.91	3.40	2.99	5.45	0.00	0.00	0.38
C₅₊ P&O	14.94	20.36	0.00	0.00	2.02	2.18	20.56
Total Arom.	31.91	42.21	61.38	61.75	55.83	43.47	30.86
Total P & O	68.08	57.79	38.62	38.25	44.18	56.53	69.14
Total	100.0	100.0	100.0	100.0	100.0	100.0	100.0

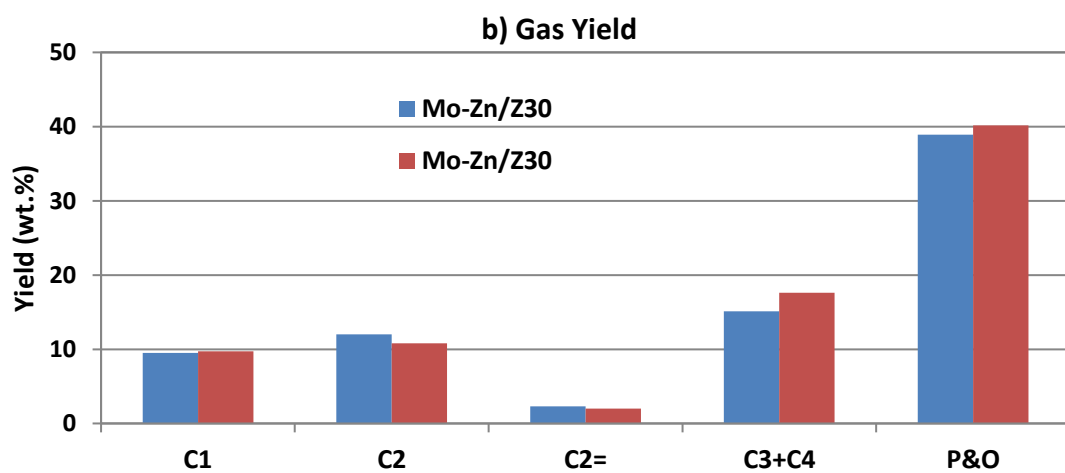
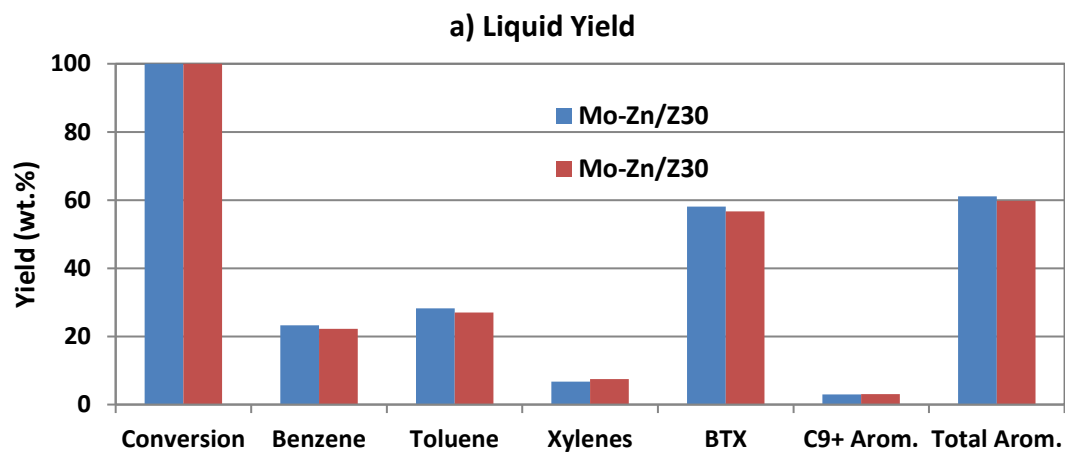


Figure 5.9: Reproducibility test for Mo-Zn/Z30 a) Liquid Yield b) Gas yield

5.5 References

- [1] Song J, Ma HJ, Tian ZJ, Yan LJ, Xu ZS, Liu QH, et al. The effect of Fe on Pt particle states in Pt/KL catalysts. *Appl Catal A* 2015;492:31–7.
- [2] Ahuja R, Punji B, Findlater M, Supplee C, Schinski W, Brookhart M, et al. Catalytic dehydroaromatization of n-alkanes by pincer-ligated iridium complexes. *Nat Chem* 2011;3:167–71.
- [3] T. Inui, Y. Makino, F. Okazumi, S. Nagano, A. Miyamoto, *Ind. Eng. Chem. Res.* 26 (1987) 647.
- [4] P. Meriaudeau, G. Sapaly, C. Naccache, *Stud. Surf. Sci. Catal.* 49 (1989) 1423.
- [5] R.L.V. Mao, L. Dufresne, *Appl. Catal.* 52 (1989) 1.
- [6] C.D. Gosling, F.P. Wilcher, L. Sullivan, *Hydrocarbon Process.* 12 (1991) 69.
- [7] G. Giannetto, R. Monque, R. Galiasso, *Catal. Rev. Sci. Eng.* 36 (1994) 271.
- [8] D. Seddon, *Catal. Today* 6 (1989) 351.
- [9] I. Inui, F. Okazumi, *J. Catal.* 90 (1984) 366.
- [10] Y. Ono, K. Kanae, *J. Chem. Soc. Faraday Trans.* 87 (1991) 669.
- [11] M. Miyamoto, K. Mabuchi, J. Kamada, Y. Hirota, Y. Oumi, N. Nishiyama, S. Uemiya, *J. Porous. Mater.* 22 (2015) 769–778.
- [12] K. Frey, L.M. Lubango, M.S. Scurrrell, L. Guzzi, *React. Kinet. Mech. Catal.* 104 (2011) 303–309.
- [13] Y. Wang, T. Yokoi, S. Namba, J.N. Kondo, T. Tatsumi, *Appl. Catal. A* (2014).
- [14] Q. Li *et al.*, “Investigation on the light alkanes aromatization over Zn and Ga modified HZSM-5 catalysts in the presence of methane,” *Fuel*, vol. 219, no. January, pp. 331–339, 2018.

- [15] H. Long, F. Jin, G. Xiong, and X. Wang, "Effect of lanthanum and phosphorus on the aromatization activity of Zn/ZSM-5 in FCC gasoline upgrading," *Microporous Mesoporous Mater.*, vol. 198, pp. 29–34, 2014.
- [16] A. A. Dergachev and A. L. Lapidus, "Catalytic aromatization of light alkanes," *Russ. J. Gen. Chem.*, vol. 79, no. 6, pp. 1244–1251, 2009.
- [17] Y. K. Park, D. H. Kim, and S. I. Woo, "Aromatization of pentane catalyzed over various metallosilicates," *Korean J. Chem. Eng.*, vol. 14, no. 4, pp. 249–256, 1997.
- [18] Smiešková A, Rojasová E, Hudec P, Šabo L. STUDY OF THE ROLE OF Zn IN AROMATIZATION OF LIGHT ALKANES WITH PROBE MOLECULES. 2004;82(2):227-234.
- [19] C.G. Yang, M.H. Qiu, S.W. Hu, X.Q. Chen, G.F. Zeng, Z.Y. Liu, Y.H. Sun, Stable and efficient aromatic yield from methanol over alkali treated hierarchical Zn-containing HZSM-5 zeolites, *Microporous Mesoporous Mater.* 231 (2016) 110–116.
- [20] M. N. Akhtar, N. Al-Yassir, S. Al-Khattaf, and J. Čejka, "Aromatization of alkanes over Pt promoted conventional and mesoporous gallosilicates of MEL zeolite," *Catal. Today*, vol. 179, no. 1, pp. 61–72, 2012.
- [21] K. Lee, S. Lee, Y. Jun, and M. Choi, "Cooperative effects of zeolite mesoporosity and defect sites on the amount and location of coke formation and its consequence in deactivation," *J. Catal.*, vol. 347, pp. 222–230, 2017.
- [22] E. Lalik, X. Liu, J. Klinowski, Role of gallium in the catalytic activity of zeolite [Si,Ga]- ZSM-5 for methanol conversion, *J. Phys. Chem.* 96 (1992) 805–809.

- [23] T. Nitipan, S. Jongpatiwut, T. Rirksomboon, B. Kitiyanan, and T. Apphakvan, "Improved p-Xylene Selectivity of n-Pentane Aromatization over Silylated Ga-exchanged HZSM- 5," *World Acad. Sci. Eng. Technol.*, vol. 64, pp. 457–460, 2012.
- [24] T. Kimura, N. Hata, K. Sakashita, and S. Asaoka, "Production of aromatics from heavier n-paraffins on hybrid cracking-reforming catalyst," *Catal. Today*, vol. 185, no. 1, pp. 119–125, 2012.
- [25] P.C. Lai, C.H. Chen, H.Y. Hsu, C.H. Lee, Y.C. Lin, Methanol aromatization over Gadoped desilicated HZSM-5, *RSC Adv.* 6 (2016) 67361–67371.
- [26] K. G. Azzam, G. Jacobs, W. D. Shafer, and B. H. Davis, "Aromatization of hexane over Pt/KL catalyst: Role of intracrystalline diffusion on catalyst performance using isotope labeling," *J. Catal.*, vol. 270, no. 2, pp. 242–248, 2010.
- [27] J. Song *et al.*, "The effect of Fe on Pt particle states in Pt/KL catalysts," *Appl. Catal. A Gen.*, vol. 492, pp. 31–37, 2015.
- [28] D. Xu *et al.*, "Controllable deposition of Pt nanoparticles into a KL zeolite by atomic layer deposition for highly efficient reforming of n-heptane to aromatics," *Catal. Sci. Technol.*, vol. 7, no. 6, pp. 1342–1350, 2017.
- [29] Y. Ni, W. Peng, A. Sun, W. Mo, J. Hu, T. Li, G. Li, High selective and stable performance of catalytic aromatization of alcohols and ethers over La/Zn/HZSM-5 catalysts, *J. Ind. Eng. Chem.* 16 (2010) 503–505.
- [30] Tamiyakul, S.; Sooknoi, T.; Lobban, L.L., Jongpatiwut, S. (2016). Generation of reductive Zn species over Zn/HZSM-5 catalysts for n-pentane aromatization. *J. Appl. Catal. A, Gen.* 525, 190-196.

- [31] Hodala JL, Halgeri AB, Shanbhag GV, Reddy RS, Choudary NV, Rao PV, et al. Aromatization of C5-rich Light Naphtha Feedstock over Tailored Zeolite Catalysts: comparison with Model Compounds (n-C5-n-C7). *ChemistrySelect* 2016;1:2515–21.
- [32] Tshabalala TE, Scurrrell MS. Aromatization of n-hexane over Ga, Mo and Zn modified H-ZSM-5 zeolite catalysts. *Catal Commun* 2015;72:49–52.
- [33] Z.R. Ismagilov, E.V. Matus, L.T. Tsikoza, *Energy Environ. Sci.*, 1 (2008) 526–541.
- [34] Lu Y., Ma D., Xu Z., Tian Z., Bao X., Lin L., *Chem. Comm.* 2048 (2001).
- [35] Liu W., Xu Y., Wong S.-T., Wang L., Qiu J., Yang N., *J. Mol. Catal.* 120:257 (1997).
- [36] J. P. Tessonier, B. Louis, S. Rigolet, M. J. Ledoux and C. Pham-Huu, *Appl. Catal., A*, 2008, 336, 79–88
- [37] Y. D. Xu, X. H. Bao and L. W. Lin, *J. Catal.*, 2003, 216, 386–395.
- [38] W. Ding, S. Li, G. D. Meitzner and E. Iglesia, *J. Phys. Chem. B*, 2001, 105, 506–513.
- [39] Wang, K., Wang, H., Wei, M., Bai, Y. Study on the hydroaromatization of FCC naphtha over MoP/HZSM-5 catalyst. *Petrol. Proc. Petrochem* (2008).. 39, 26-29.
- [40] Velu S, Wang L, Okazaki M, Suzuki K, Tomura S. Characterization of MCM-41 mesoporous molecular sieves containing copper and zinc and their catalytic performance in the selective oxidation of alcohols to aldehydes. *Microporous Mesoporous Mater* 2002;54:113–26.

- [41] Niu X, Gao J, Miao Q, Dong M, Wang GF, Fan WB, et al. Influence of preparation method on the performance of Zn-containing HZSM-5 catalysts in methanol-to aromatics. *Microporous Mesoporous Mater* 2014;197:252–61.
- [42] Y.M. Ni , W.Y. Peng , M.Sun A , W.L. Mo , J.L. Hu , T. Li , G.X. Li , *J. Ind. Eng. Chem.* 16 (2010) 503–505 .
- [43] H.A. Zaidi , K.K. Pant , *Catal. Today.* 96 (2004) 155–160.
- [44] Wang AG, Austin D, Karmakar A, Bernard GM, Michaelis VK, Yung MM, et al. Methane upgrading of acetic acid as a model compound for a biomass-derived liquid over a modified zeolite catalyst. *ACS Catal* 2017;7:3681–92.
- [45] Franke ME, Simon U. Solvate-supported proton transport in zeolites. *ChemPhysChem*, 2004;5:465–72.
- [46] Ni Y, Sun A, Wu X, Hai G, Hu J, Li T, et al. The preparation of nano-sized H [Zn, Al] ZSM-5 zeolite and its application in the aromatization of methanol. *Microporous Mesoporous Mater* 2011;143:435–42.
- [47] Ono Y. Transformation of lower alkanes into aromatic hydrocarbons over ZSM-5 zeolites. *Catal Rev Sci Eng* 1992;34:179–226.

CHAPTER 6

AROMATIZATION OF LIGHT PARAFFINIC NAPHTHA OVER Pt-M/ZSM-5 TRI-COMPOSITED CATALYSTS

6.1 Background

This chapter is mainly about the effect of bimetallic Pt-M/ZSM-5(MFI) (Z30) modified catalyst prepared by wetness co-impregnation method. The catalytic activity of transforming light naphtha (C₅-C₆) is presented. Also, several characterization methods are carried out. Finally, the stability of best performance catalyst toward the production of aromatics is summarized.

6.2 Introduction

The main utilization of C₅/C₆ paraffinic naphtha has been as a feedstock for steam cracking (60 %) plants for ethylene production and as an isomerate for gasoline blending (30 %). However, currently light naphtha components find less use as gasoline blending because of their high vapor pressure and low-octane number [1]. While the current global demand for light naphtha is estimated at 8.8 million barrel per day (bpd), the global demand for gasoline is 26.1 million bpd or about the 26 % of global refined products demand [1,2]. The aromatization of light naphtha into BTX aromatics (benzene, toluene, and xylenes) has received attention from both industry and academia. Aromatics, especially benzene and para-xylene are important basic petrochemicals used in the

production of several value-added chemicals and polymers. In 2018, the global demand for benzene was 48 million tons whereas that for paraxylene was 43 million tons with growth projections at above 3.5% per annum through 2021 [3].

Several zeolites have been identified for the aromatization of light naphtha such as ZSM-5, Y, mordenite, and beta zeolite [1]. Studies show that ZSM-5 catalyst improves the selectivity toward some desired products such as methanol to gasoline [4], cracking [5] and alkylation [6]. ZSM-5 is also been used to transform light naphtha into aromatics because of its excellent properties high surface area, stability and intra-crystalline microspores properties [7–9]. Impregnation of metals into the ZSM-5 structure enhances the aromatization selectivity in such a way that acidity of ZSM-5 provides the cracking, while metallic sites are responsible for the dehydrogenation, which converts olefins finally into aromatics [10–12]. Also, the metal function reduces severe cracking selectivity toward lower paraffins and produces hydrogen as byproduct.

Several research groups have studied the effect of gallium and zinc modified H-ZSM-5 catalysts for the aromatization n-hexane and light naphtha [13, 14]. The aromatization of n-hexane on ZSM-5 modified with different Zn and Ga catalysts displayed good catalytic activity in producing aromatics due to their high dehydrogenation ability [15]. The effect of hydrogen treatment on Zn/H-ZSM-5 and their activity in n-pentane aromatization were investigated showing that the formation of H₂-chemisorbed Zn species remarkably increased BTX selectivity to 31% [16]. It was also reported that the H₂-chemisorbed Zn species deactivated in the absence of hydrogen gas and hydrogen treatment for regeneration is required to activate the catalyst [16].

Hodala et al. investigated light naphtha aromatization over Zn-Ga/ZSM-5 yielding 65% aromatics due to dissociative chemisorption of alkanes resulting in dehydrogenation/aromatization [17]. There have been extensive studies in developing new catalysts for transforming naphtha (C₆-C₈ alkanes) into gasoline blending components such as catalytic reforming on chlorinated Re-Pt/Al₂O₃ catalyst [18, 19]. This catalyst is not selective for light alkane conversion into aromatics, as it leads to significant side reactions such as skeletal isomerization and hydrocracking. Pt supported-alumina mixed along with other metals was used for the catalytic reforming to produce aromatics; however, the conversion towards BTX compounds was limited [20]. Initially, Pt supported over non-acidic KL zeolite has also gain a great attention in aromatization of hexane [21, 22]. Bernard et al. found that Pt modified over KL zeolites exhibit good catalytic performance for light alkanes aromatization [23]. The aromatization of n-hexane over 1%Pt/KL at 500 °C and 1 atm displayed high activity and selectivity towards benzene and excellent stability during hexane dehydrocyclization [24]. It was proposed that the controlled entry of hexane into the lobes of L-zeolite containing active sites was the reason for the exceptional Pt/KL catalytic performance. The narrow windows of the L-zeolite channels inhibited the occurrence of bimolecular reactions which was responsible for coke formation and catalyst deactivation [24]. Jacobs et al. explored the effect of Pt particles distribution on KL support for the stability of Pt/KL catalyst. It was found that Pt size distribution is more critical on activity and stability for n-hexane aromatization [25].

Alternative approaches have been presented to further improve the aromatization of n-hexane with partial substitution of Al by Ga/Fe into zeolite crystals, which would shorten the contact time of reaction intermediates. Akhtar et al. [26] investigated the aromatization of n-hexane and propane over Pt promoted mesoporous gallium-containing HZSM-11 zeolite with controlled mesoporosity generated by desilication. The better conversion and selectivity over Pt/mesoporous GaZSM-11 were attributed to the improved accessibility to the active extra-framework Ga species owing to the generation of mesopores inside the zeolite particles and shortening the contact time necessary for the reactions. Song et al. [27] prepared two types of Fe-containing Pt/KL catalysts and tested for the aromatization of n-hexane. Pt/FeKL contained framework Fe, which was incorporated through hydrothermal synthesis, and Pt-Fe/KL contained non-framework Fe, which was introduced through impregnation. Electron-rich platinum species ($\text{Pt}^{\delta-}$) were detected with non-framework Fe, which favored higher Pt dispersion and smaller Pt particle size. Whereas, partial substitution of Al by Fe in the KL zeolite framework favored formation of electron-deficient platinum species ($\text{Pt}^{\delta+}$) with lower dispersion and bigger particle size. These differences in Pt dispersion and electronic states affected the Fe-containing Pt/KL catalysts aromatization performances and the order of n-hexane aromatization is, Pt-Fe/KL > Pt/KL > Pt/FeKL. However, in many of these methods, the size and dispersion of Pt particles cannot be well controlled, which resulted in aggregation, rapid deactivation, and decrease in selectivity of Pt/KL catalysts during the operation [28, 29].

In this study Pt and modifier M (modifier M= Zn, Fe, La, and Ga) are combined with HZSM-5[(Z30) Si/2Al=30] to form, tri-composited catalysts by wet co-impregnation method and investigated in the catalytic conversion of light paraffinic naphtha to aromatics. As the result of tri-component catalyst system, the selected mesoporous catalyst Pt-Ga/Z30 exhibited excellent conversion and 60 wt. % selectivity towards total aromatics with low toluene/benzene ratio of about 0.5. Furthermore, the short-term stability (24 h) of the best performing catalyst (Pt-Ga/Z30) was also investigated.

6.3 Experimental

6.3.1 Catalyst Preparation

All precursors of Pt and modifiers [i.e. tetra ammine platinum(II) nitrate $\text{Pt}(\text{NH}_3)_4(\text{NO}_3)_2$, zinc nitrate hexahydrate $\text{Zn}(\text{NO}_3)_2 \cdot 6\text{H}_2\text{O}$, iron(III) nitrate nonahydrate $\text{Fe}(\text{NO}_3)_3 \cdot 9\text{H}_2\text{O}$, lanthanum(III) nitrate hydrate $\text{La}(\text{NO}_3)_3 \cdot x\text{H}_2\text{O}$, and gallium(III) nitrate hydrate $\text{Ga}(\text{NO}_3)_3 \cdot x\text{H}_2\text{O}$] $\text{Pt}(\text{NH}_3)_4(\text{NO}_3)_2$, $\text{Zn}(\text{NO}_3)_2 \cdot 6\text{H}_2\text{O}$, $\text{Fe}(\text{NO}_3)_3 \cdot 9\text{H}_2\text{O}$, $\text{La}(\text{NO}_3)_3 \cdot x\text{H}_2\text{O}$, and $\text{Ga}(\text{NO}_3)_3 \cdot x\text{H}_2\text{O}$] were purchased from Sigma-Aldrich and used as received. ZSM-5 zeolite with $\text{SiO}_2/\text{Al}_2\text{O}_3$ ratio 30 used was procured from Zeolyst International. A series of tri-composited catalysts were prepared by wet co-impregnation of the 1.0 wt. % Pt-M/ZSM-5[Si/2Al=30] (modifier M= 1 wt. % Zn, 2 wt. % of Fe, La, and Ga). The ZSM-5 was calcined at 550 °C for 5 h with heating rate of 5 °C/min before impregnation. In a typical procedure, certain amounts of the precursors and zeolite were added to 100 mL water in a 250 mL round bottom flask, stirred with a magnetic stirrer (500 rpm) for 1 h to obtain a homogenous mixture. Subsequently, water was removed using a hot plate under

stirring at 50 °C. The catalyst precursor was then dried in air at 100 °C overnight and calcined in air at 550 °C for 5 h.

6.3.2 Catalyst Characterization

The parent and Pt-M modified ZSM-5 catalysts were characterized by XRD, BET, SEM, and NH₃-TPD, to investigate several physio-chemical and surface properties. Powder XRD patterns are gained by Rigaku Miniflix II using Cu K α radiation ($\lambda = 1.5405 \text{ \AA}$) besides the following conditions of 30 kV, 15 mA, step size of 0.02° from 5° to 60° θ and rate of 2°·min⁻¹. The surface area, pore volume, and pore diameter were determined by nitrogen adsorption at -195 °C with Micromeritics ASAP-2020 analyzer using the Brunauer-Emmett-Teller (BET) equation. SEM of images was captured with a scanning electron microscope (NOVA FEISEM-450 equipped with EDX detector). The samples were loaded on the sample holder, held with conductive copper tape and coated with a film of gold in a vacuum with a Cressington sputter ion-coater for 30 s with a 15 mA current. Temperature programmed desorption (NH₃-TPD) experiment were conducted to measure the acidity using BEL-CAT-A-200, chemisorption apparatus. This apparatus was consisting of a gas mixing unit, quartz micro reactor and a thermal conductivity detector (TCD). Samples were pretreated at 500 °C for 2 h with a stream of helium (50 mL/min). After cooling the catalyst to room temperature, ammonia (50 mL/min) was introduced into the reactor at 100 °C for 30 min to saturate acid sites of the catalyst. Physisorbed ammonia was removed at 120 °C for 2 h under a flow of helium (50 mL/min). After cooling down the sample, furnace temperature was increased from 100

°C to 600 °C at a heating rate of 10 °C/min under a flow of helium (25 mL/min). The desorbed ammonia was detected using a thermal conductivity detector (TCD).

6.3.3 Catalyst Characterization

The parent and modified ZSM-5(30) catalysts were characterized by XRD, BET, SEM, and NH₃-TPD, to investigate several physio-chemical and surface properties. XRD patterns are gained by Rigaku Miniflix II using CuK besides the following conditions of radiation [$\lambda = 1.54051 \text{ \AA}$, 30 kV and 15 mA and step size of 0.02° from 5° to 60° θ] and rate of 2°/min]. The surface area, pore volume, and pore diameter of the representative ZSM-5(30) zeolite and metal modified catalysts, synthesized by metal impregnation using the wet co-impregnation method, were determined by nitrogen adsorption at -195 °C with Micromeritics ASAP-2020 analyzer using the Brunauer-Emmett-Teller (BET) equation. SEM of images of the parent and modified ZSM-5(30) catalysts were captured with a scanning electron microscope (NOVA FEISEM-450 equipped with EDX detector). The samples were loaded on the sample holder, held with conductive copper tape and coated with a film of gold in a vacuum with a Cressington sputter ion-coater for 30 s with a 15 mA current. Temperature programmed desorption (NH₃-TPD) experiment were conducted to measure the acidity of parent and modified ZSM-5(30) catalysts. This characterization test was conducted using BELCAT, Japan. 100 mg of catalyst charged into the TPD apparatus was pretreated at 300 °C for 2 h with a stream of helium (25 mL/min). After cooling the catalyst to room temperature, ammonia (50 mL/min) was introduced into the reactor at 100 °C for 30 min to saturate

acid sites of the catalyst. Physisorbed ammonia was removed at 120 °C for 2 h under a flow of helium (50 mL/min). After cooling down the sample, furnace temperature was increased from 100 °C to 600 °C at a heating rate of 10 °C/min under a flow of helium (25 mL/min). The desorbed ammonia was detected using a thermal conductivity detector (TCD).

6.3.4 Catalyst Evaluation

A gas chromatograph equipped with detailed hydrocarbon analysis (GC-DHA), manufactured by Shimadzu was used for analysis of feed as well as of reaction products. Light straight run naphtha (LSRN) feed was received from Ras Tanura Refinery, Saudi Arabia. The paraffins, *iso*-paraffins, olefins, naphthenes and aromatics (PIONA) content of light straight run naphtha (LSRN), received from Ras Tanura Refinery Saudi Arabia was measured using a GC-DHA. The PIONA composition is presented in Table 6.1. The table indicates highly paraffinic nature of LSRN (90 wt. %).

Table 6.1: Composition of light straight run naphtha feed (wt. %)

Component	n-Paraffins	<i>iso</i>-Paraffins	Olefins	Naphthenes	Aromatics	Total
C₅	25.5	8.8	0.0	2.1	0.0	36.4
C₆	25.4	26.5	0.0	5.4	1.5	58.8
C₇	0.8	3.3	0.0	0.6	0.1	4.8
Total	51.7	38.6	0.0	8.1	1.6	100.0

Catalyst evaluation tests were conducted in a laboratory-scale fixed-bed flow-type reactor system. In a typical experiment, the reactor (grade 316 stainless steel tube with ID of 7.9 mm, OD of 14.3 mm, and L of 203 mm) was charged with 0.5 g of the catalyst sieved to a particle size of 0.5-1.0 mm diameter. The catalyst was activated in a nitrogen stream at 550 °C for 2 h. The hydro treated naphtha feed contains 42.6 ppm sulfur, and has a density of 0.6764 g/cm³. The flow rate of the LSRN feed was (0.01 to 0.5) mL/min and controlled under N₂ flow rate of 10 mL/min during the reaction. The reaction was carried out at 550 °C, weight hourly space velocity (WHSV) of 1 h⁻¹, 1-5 h time-on-stream (TOS), and atmospheric pressure. The quantitative analysis of the reaction products was carried out using an online GC-DHA equipped with one FID and one TCD detector. The conversion was obtained using the following equation.

$$\text{Conversion of light naphtha} = 100\% - \text{Unreacted } (C_5, C_6) \quad \text{Equation 6-1}$$

6.4 Results and Discussion

6.4.1 Catalyst Characterization

The textural properties: specific surface area, pore volume and average pore diameter of parent and modified ZSM-5 samples are shown in Table 6.2. The specific surface area, pore volume and average pore diameter of the parent ZSM-5 catalyst are 351 m²·g⁻¹, 0.174 cm³·g⁻¹, and 4.7 nm were found to change -5 %, +44 % and +66 % respectively after Pt impregnation. The mesoporosity without large decrease of surface area was added to Pt/ZSM-5 catalyst. The Pt-impregnation added mesoporosity was reserved to some extent even after M modification. The modifier M of Pt-M bi-component on the zeolite makes the surface area decrease further and reduces the increase degree of pore volume and pore diameter. The obtained result for Pt-Ga/ZSM-5 catalyst shows the mesoporosity kept well. The mesoporosity is supposed mainly due to desilication by cooperation of NH₃ and NO₃⁻ during the impregnation and calcining of precursor species with the zeolite. The noted mesoporous characteristics could be accountable for their performance in light naphtha aromatization [30].

Table 6.2; Textural properties of parent and modified ZSM-5 catalysts

Catalyst	S _{BET} (m ² ·g ⁻¹)	Pore Volume (cm ³ ·g ⁻¹)	Average Pore Diameter (nm)
Z30	351	0.174	4.7
Pt/Z30	332(-5%)	0.250(+44%)	7.8(+66%)
Pt-Zn/Z30	332(-5%)	0.219(+26%)	7.1(+51%)
Pt-Fe/Z30	307(-13%)	0.185(+6%)	7.2(+53%)
Pt-La/Z30	290(-17%)	0.168(-3%)	6.9(+47%)
Pt-Ga/Z30	306(-13%)	0.217(+25%)	7.7(+64%)

Loaded amount: Pt and Zn 1.0 wt. %; Fe, La, and Ga 2 wt. %, numbers in the parenthesis describe % difference in textural properties of catalysts after metal(s) impregnation.

Nitrogen adsorption-desorption isotherms and Barrett, Joyner, and Halenda (BJH) pore size distribution presented in Figures 6.1 and 6.2, respectively predict more for the mesoporosity. The N₂ adsorption desorption isotherm is Type I, which is distinctive for zeolites and the *t*-plot method is used to obtain micro-pore volume. While the shapes of the isotherms as well as the hysteresis loops of the catalysts are almost similar, the pore size distribution of Pt-Ga/ZSM-5 catalyst compared with those of the parent zeolite and the Pt/ZSM-5 shows increased mesopore at 4 nm instead of decreased mesopore at 7 nm. The results suggest that Ga species is well dispersed to form nano-sized particles inside the mesopore.

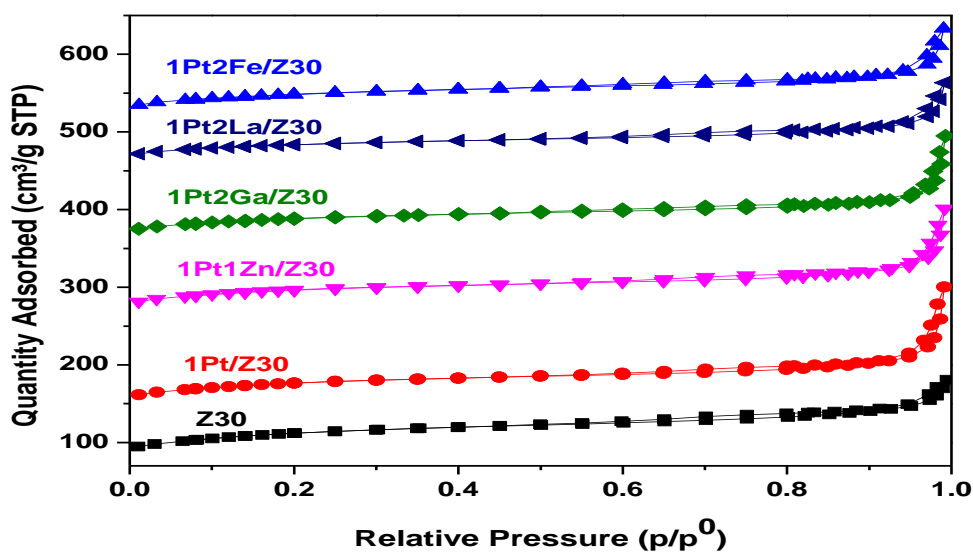


Figure 6.1: Nitrogen adsorption-desorption isotherms of parent and modified ZSM-5(30) catalysts

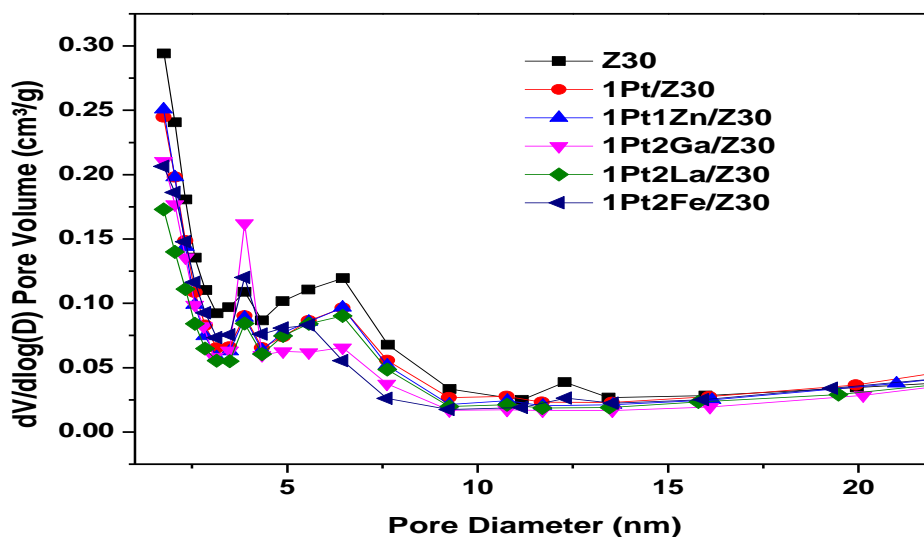


Figure 6.2: The BJH pore size of parent and modified ZSM-5(30) catalysts

XRD patterns for the parent ZSM-5 and Pt-M/ZSM-5 catalysts are presented in Figure 6.3. While the peak intensities of the Pt/ZSM-5 and Pt-M/ZSM-5 catalysts are only slightly weaker than the parent ZSM-5 zeolite, all the Pt-M/ZSM-5 catalysts show the similar peak diffraction patterns compare to the parent at 2θ : $7-9^\circ$ and $22^\circ-25^\circ$. The fact indicates that the loading and loaded components on the ZSM-5 have negligible impact on the zeolite structure except or mesoporosity formation. Moreover, no significant peaks of any metal or metal oxide species are observed. This is due to the high dispersion species as nano-sized particles into the parent ZSM-5 mesopores developed with Pt-impregnation. The lower intensity of P-M catalysts is due to the attribution of the high X-ray coefficient of impregnated nano-sized particles and well intermixing of metal species into ZSM-5 [31-32].

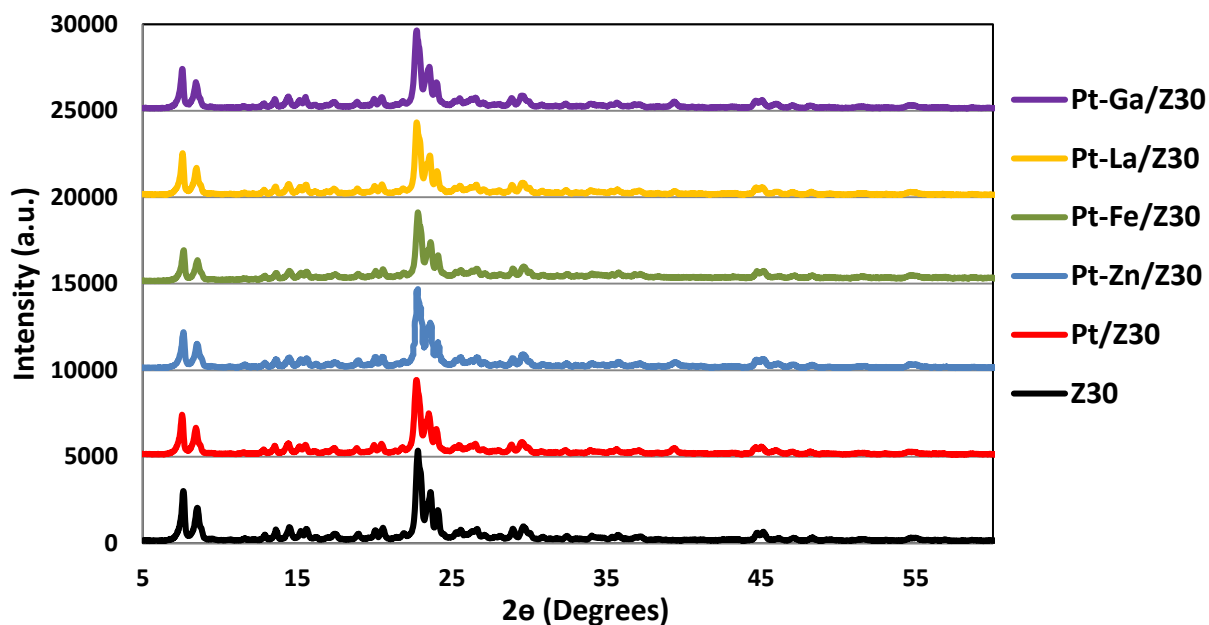


Figure 6.3: XRD patterns of the parent and modified ZSM-5(30) catalysts

SEM images of the parent and modified ZSM-5 samples are shown in Figure 6.4. As can be seen in Figure 6.4 (a), the parent ZSM-5 possesses well-ordered sharp-edges and square-looking crystallite morphology with a large crystal size of about < 150 nm. As shown in Figure 6.4 (b-f) the surface morphology of the Pt/ZSM-5 and Pt-M/ZSM-5 catalysts changed into the sharp-less and grained after impregnating components. The Pt-La/ZSM-5 catalyst as shown in Figure 6.4 (d) has the most sharp-less and grained morphology among the Pt-M/ZSM-5 catalysts, while the others are similar to the Pt/ZSM-5. This agrees with textural properties in Table 6.2. Figure 6.5 shows the SEM image and the corresponding elemental maps for the Pt-Ga/ ZSM-5 catalyst. The map confirms the homogeneous nature of the elemental (Si, Al, O, Ga, Pt) dispersion on the ZSM-5.

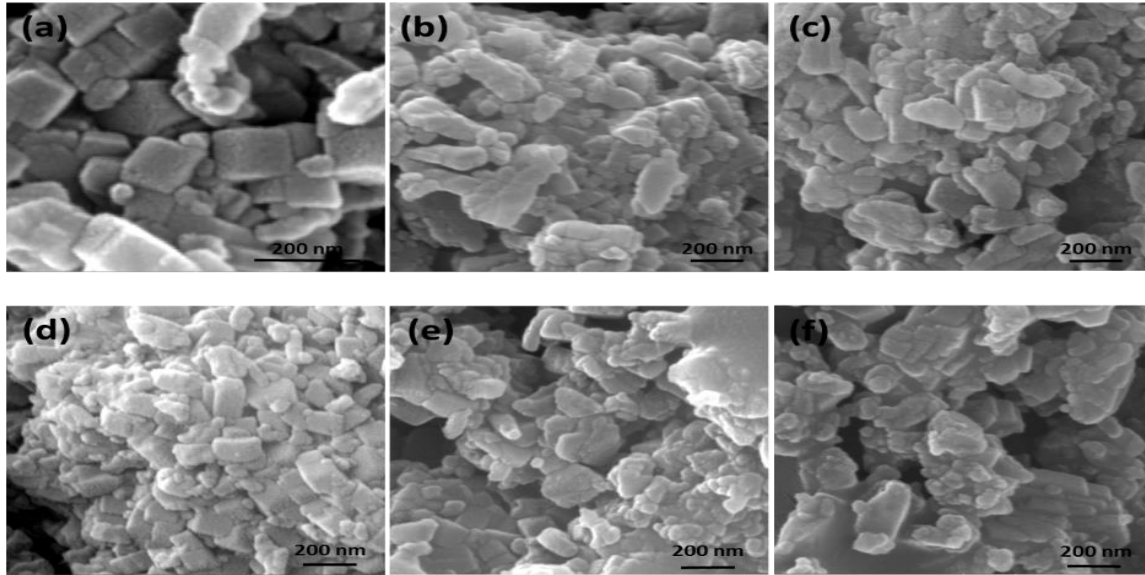


Figure 6.4: The SEM images of (a) Z30, (b) Pt/Z30, (c) Pt-Zn/Z30, (d) Pt-La/Z30, (e) Pt-Ga/Z30, and (f) Pt-Fe/Z30 catalysts

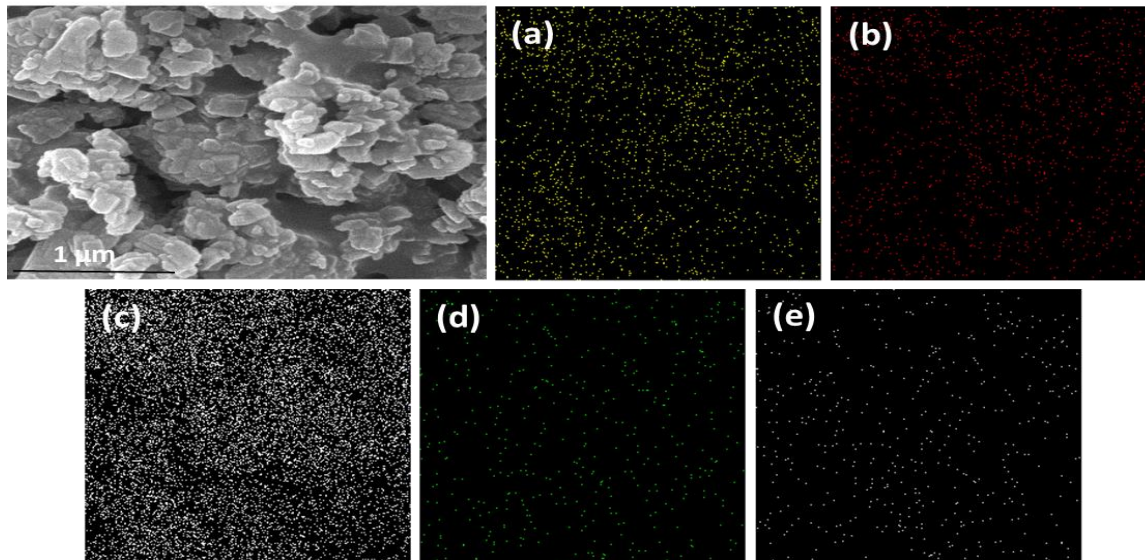


Figure 6.5: The homogeneous elemental dispersion of (a) O (b) Al, (c) Si, (d) Ga and (e) Pt in Z30 revealed by EDXS mapping of the Pt-Ga/Z30 catalyst

The NH₃-TPD profiles of the parent ZSM-5 and Pt-M/ZSM-5 catalysts are reported Figure 6.6. For the parent ZSM-5 and Pt-M/ZSM-5 catalysts, NH₃-TPD profiles is distributed in the three deconvoluted peaks related to weak–medium, medium–strong, and strong acid sites, in the temperature range of 100–250 °C, 250–400 °C, and 400–600 °C, respectively. The acidity of the parent and Pt or Pt-M modified ZSM-5 catalysts is shown in Table 6.3. The Pt-M/ZSM-5 catalysts except for the strong acid-less Pt-Ga/ZSM-5 have the similar distributions of the weak–medium, medium–strong, and decreased strong acid, which works for severe cracking and hydrogen transfer reaction from ring compounds to lower olefins. The low-medium temperature peak was recognized by the ammonia adsorbed on the weak acidic sites, which was anticipated to effectively influence the proton mobility [33]. However, the medium-high temperature peak was related to the strong adsorption site belonging to the surface of hydroxyl groups in the catalytic samples, representing the presence of strong Brønsted acidic sites [34].

Table 6.3: Total acidity and acid strength distribution of the parent and Pt or Pt-M modified ZSM-5 catalysts from NH₃-TPD

Catalyst	Amount NH ₃ desorbed (mmol/g)			
	100-250 °C	250-400 °C	Above 400 °C	Total
Z30	0.038	0.018	0.156	0.212
Pt/Z30	0.020	0.016	0.065	0.101
Pt-Zn/Z30	0.085	0.019	0.010	0.114
Pt-Fe/Z30	0.087	0.045	0.035	0.167
Pt-La/Z30	0.121	0.037	0.010	0.168
Pt-Ga/Z30	0.059	0.031	0.001	0.091

It is been reported that, impregnating metals oxides into the parent ZSM-5 suppresses the weak and strong acidic sites. These metal(s) impregnated zeolites are supposed to occupy and fill the pores with non-framework Al, resulting in inaccessible NH_3 chemisorption and blockage of the strong acidic sites [17]. Furthermore, it is shown that the suppression of the strong acidic sites of ZSM-5 in such a way inhibits the hydrogen transfer reaction with result of reduced alkane's formation and more aromatics yield [35].

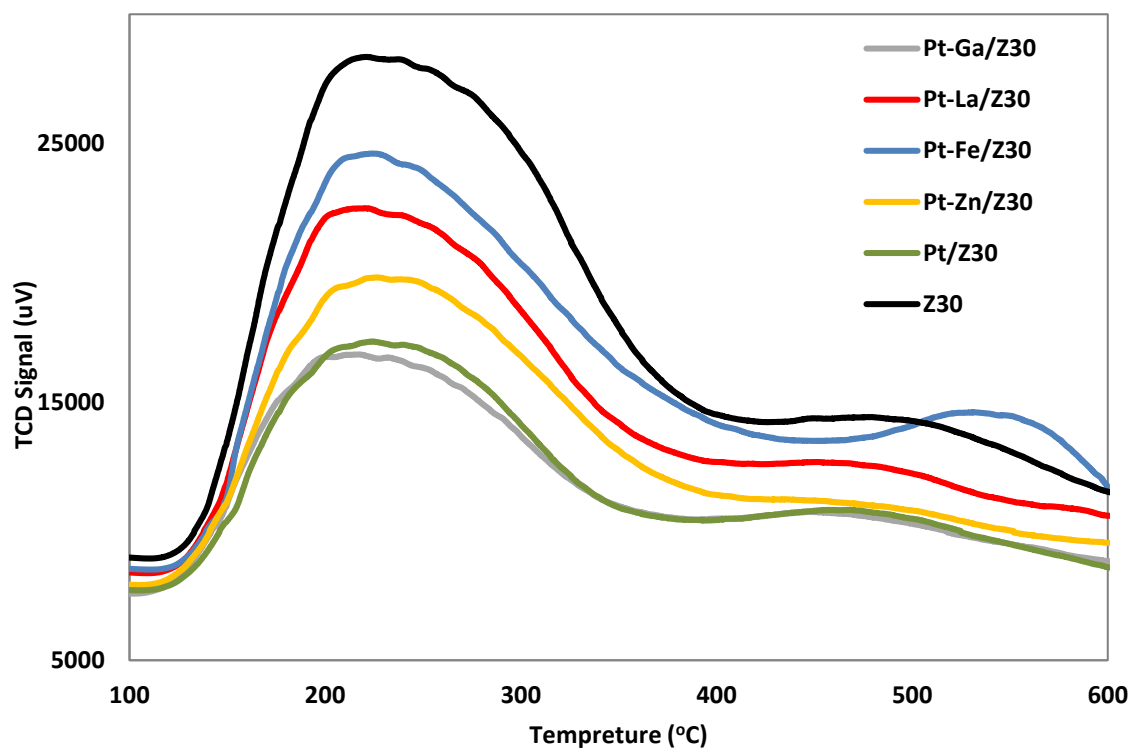


Figure 6.6: NH_3 -TPD curves obtained for the parent and modified ZSM-5(30) catalysts

6.4.2 Catalyst Evaluation

The parent and Pt or Pt-M modified ZSM-5 catalysts were evaluated for the aromatization LSRN using a fixed bed reactor at 550 °C, WHSV of 1 h⁻¹, and atmospheric pressure. The results are summarized in Figure 6.7 (Table 6.4). The product distribution is divided mainly into liquid and gas yields. The liquid distribution includes BTEX and C₅₊ paraffins and olefins, while the gaseous products contain C₁, C₂, C₂= and C₃+C₄ paraffins and olefins. Almost all the parent and Pt or Pt-M modified ZSM-5 catalysts showed complete conversion of LSRN at 550 °C (99-100 %). The parent and Pt sole modified ZSM-5 catalysts showed lower yields of aromatics 32 wt. % and 37 wt. % respectively. Whereas modifiers M were observed to enhance the aromatization in a significant way. This is due to two important factors, acidity of zeolites and dehydrogenation function of Pt and modifier M, as they act together effectively to convert the light naphtha into aromatics. The addition of the modifiers enhanced the aromatization performance in such a way. It converts the alkanes into olefins through dissociative chemisorption, as alkenes undergo oligomerization and cyclization over the acid sites to yield aromatics [17]. Furthermore, the dispersion of the modifiers over zeolite elevates the aromatization reaction to prevent over-cracking into lower olefins. In particular, the total aromatics from the Pt-Ga modified ZSM-5 and Pt-Zn modified catalysts are 60 wt. % and 45 wt. % with toluene/benzene ratio = ~0.5 respectively. This high selectivity towards aromatics is attributed to the dehydrogenation activity of the two components Pt and the modifier, which are effective in the conversion of small cracked intermediates especially (C₃, C₄) paraffins that are frequently transformed into aromatics by secondary reactions. On the other hand, the Pt-La modified ZSM-5 and Pt-Fe

modified catalysts gave lower aromatics yield 35 wt. % and 36 wt. % respectively. This is due to the lack of the dehydrogenation activity with the Brønsted acidic sites, high olefin dimerization rate and cyclization of paraffins [17]. Also reproducibility test is carried out to examine the consistency of the results for Pt-Ga/Z30 and they are within ± 2 % error. As shown in Figure 6.8.

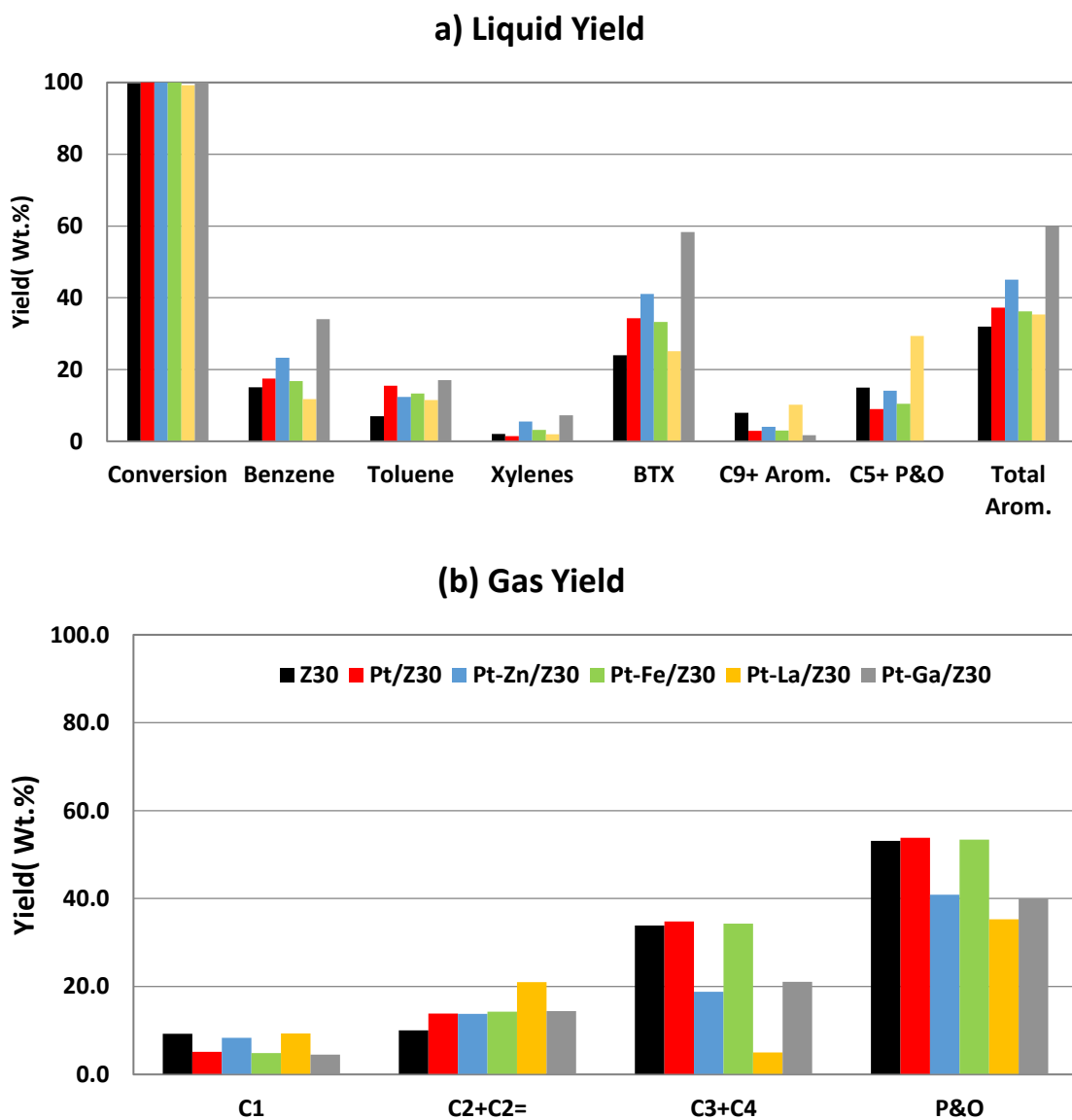


Figure 6.7: The effect of the parent and Pt or Pt-M modified Z30 catalysts, prepared by the co-impregnation method, in the conversion of LSRN at 550 °C and 1.0 h⁻¹ WHSV. (a) Liquid yield, (b) Gas yield

Table 6.4: Catalytic performance of parent and modified ZSM-5 (Reaction conditions: Catalyst= 0.5 g, Feed= LSRN, Temp. = 550 °C, WHSV= 1 h⁻¹, N₂= 10 mL/min).

Catalyst	Z30	Pt/Z30	Pt-Fe/Z30	Pt-Ga/Z30	Pt-Zn/Z30	Pt-La/Z30
Conversion	99.77	100.00	100.00	100.00	100.00	99.23
	Yield (wt. %)					
C₁	9.26	5.15	4.83	4.54	8.33	9.34
C₂	6.73	12.68	13.33	14.04	12.59	20.09
C₂₌	3.30	1.14	0.92	0.38	1.16	0.90
C₃+C₄	33.85	34.83	34.31	21.05	18.79	4.99
P&O	53.14	53.80	53.39	40.01	40.87	35.32
Benzene	15.02	17.44	16.76	34.06	23.28	11.76
Toluene	6.96	15.44	13.32	17.03	12.32	11.45
Xylenes	2.02	1.44	3.15	7.23	5.48	1.91
BTX	24.00	34.32	33.24	58.32	41.08	25.12
C₉₊ Aromatics	7.91	2.91	2.96	1.67	3.99	10.20
C₅₊ P&O	14.94	8.97	10.42	0.00	14.05	29.35
Total Arom.	31.913	37.23	36.19	59.99	45.08	35.33
Total P & O	68.09	62.77	63.81	40.01	54.92	64.67
Total	100.00	100.00	100.00	100.00	100.00	100.00

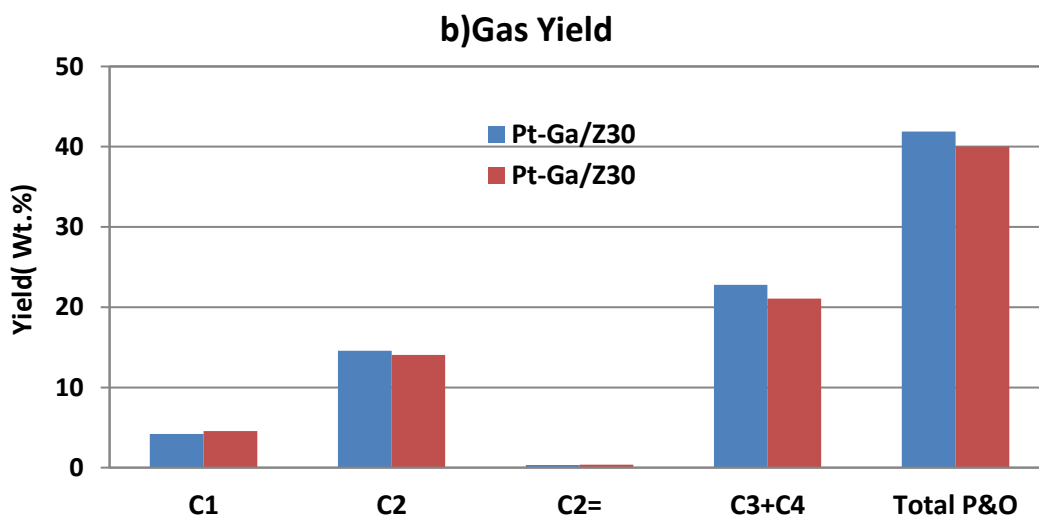
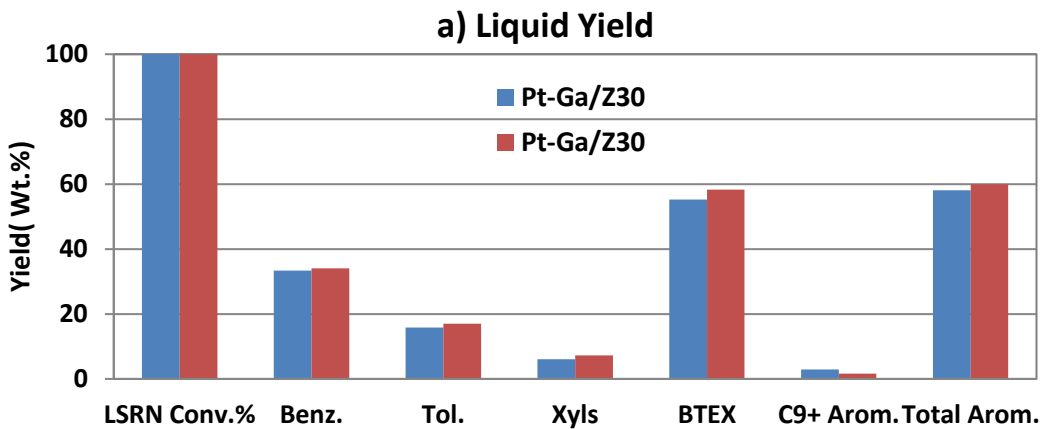


Figure 6.8: Repeatability results for Pt-Ga/Z30 a) liquid b) gas yield

6.4.3 Effect of Time-on-Stream

Time-on-stream study as shown in Figure 6.9 was carried out for the best performance catalyst Pt-Ga/ZSM-5 under the constant reaction conditions, in order to analyze stability of the catalyst against deactivation. During the test of time-on-stream: 24 h at 550 °C, LSRN conversion was kept in 99-100 % without decreasing. For the 24 h on stream, the total aromatics yield (nearly equal to liquid yield) remained almost 60 wt. %. Also, benzene and toluene yields with toluene/benzene ratio = ~0.5 were nearly constant at around 34 wt. % and around 17 wt. % respectively. The C₉₊ aromatics yield, in general reflecting to coke formation was kept around 2-3 wt. % without increasing. On the other hand, gaseous paraffins and olefins products C₁, C₂, C₂⁼ and C₃+C₄ showed marginal variation without both trends of increasing and decreasing. During 24 h on stream, methane and ethane were observed constantly at around 5 wt. % and 14 wt. % respectively, while C₃+C₄ yield effecting total gas yield at around 40 wt. % changed mainly at around 21 wt. %. Overall these results direct that the Pt-Ga/ZSM-5 catalyst is effectively well stable for LSRN conversion to aromatics.

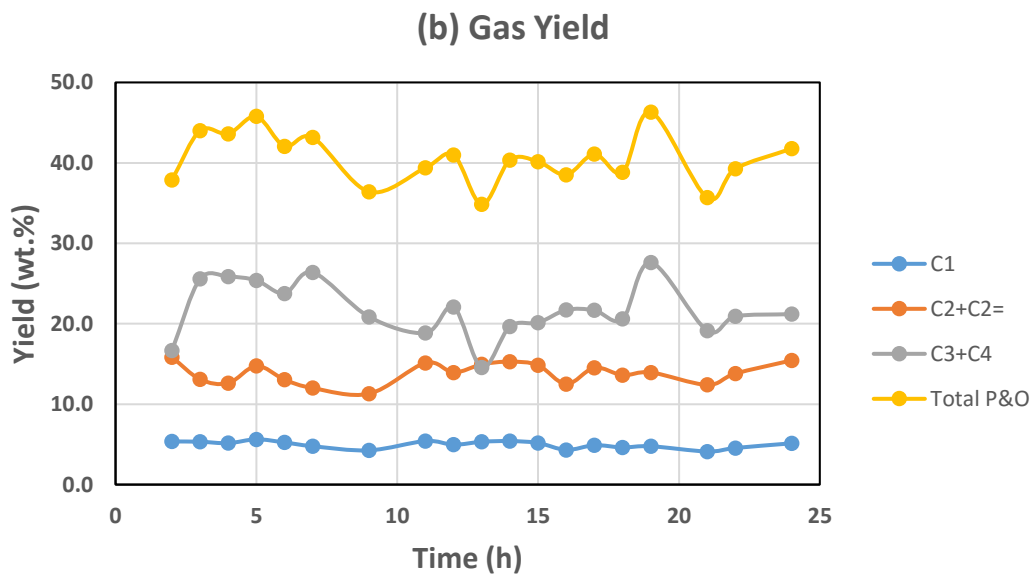
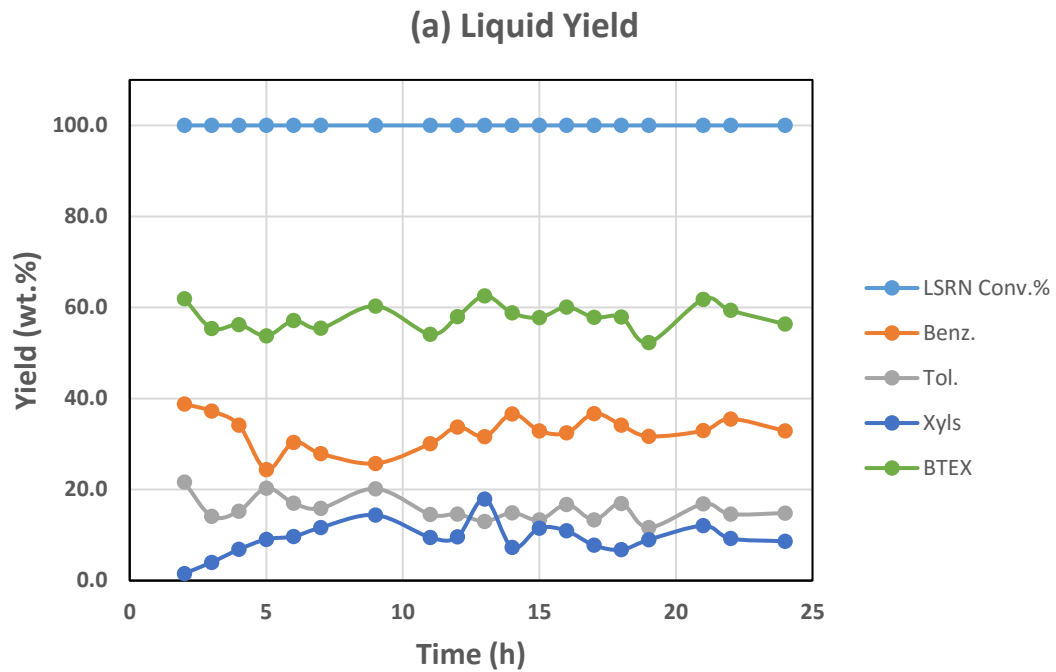


Figure 6.9: Time-on-stream for aromatization of LSRN over the Pt-Ga/Z30 liquid and gaseous product distribution (WHSV=1 h⁻¹, feed=0.01 mL/min, N₂=10 mL/min, T=550 °C). (a) Liquid yield, (b) Gas yield

6.5 References

- [1] A. Aitani, M.N. Akhtar, S. Al-Khattaf, Y. Jin, O. Koseoglu, Catalytic upgrading of light naphtha to gasoline blending components: A mini review. *Energy Fuels* 33 (2019) 3828-3843.
- [2] J. Glauser, *Petroleum Liquid Feedstocks: Naphtha and Gas Oil*, Chemical Economics Handbook, IHS Markit, 2016, London.
- [3] D. Dickson, A. Hussain, B. Kumpf, *The Future of Petrochemicals: Growth Surrounded by Uncertainty*, Deloitte, 2019, New York.
- [4] X. Chen, S. Huang, D. Cao, W. Wang, Optimal feed ratio of benzene–propylene binary mixtures for alkylation in ZSM-5 by molecular simulation. *Fluid Phase Equilib.* 260 (2007) 146–152.
- [5] X. Wang, H. Carabineiro, F. Lemos, M.A. Lemos, F. Ramôa Ribeiro, Propane conversion over a H-ZSM5 acid catalyst: Part 1. Observed kinetics *J. Mol. Catal. A, Chem.* 216 (2004) 131–137.
- [6] T.C. Tsai, I. Wang, C.-K. Huang, S.-D. Liu, Study on ethylbenzene and xylene conversion over modified ZSM-5. *Appl. Catal. A* 321 (2007) 125–134.
- [7] M. Guisnet, N.S. Gnep, F. Alario, Aromatization of short chain alkanes on zeolite catalysts. *Appl. Catal. A* 89 (1992) 1–30.
- [8] A. Bhan, W.N. Delgass, Propane Aromatization over HZSM-5 and Ga/HZSM-5 Catalysts. *Catal. Rev. Sci. Eng.* 50 (2008) 19–151.

- [9] T. Mole, J.R. Anderson, G. Creer, The reaction of propane over ZSM-5-H and ZSM-5-Zn zeolite catalysts. *Appl. Catal.* 17 (1985) 141–154.
- [10] M. Miyamoto, K. Mabuchi, J. Kamada, Y. Hirota, Y. Oumi, N. Nishiyama, S. Uemiya, para-Selectivity of silicalite-1 coated MFI type galloaluminosilicate in aromatization of light alkanes. *J. Porous. Mater.* 22 (2015) 769–778.
- [11] K. Frey, L.M. Lubango, M.S. Scurrall, L. Guzzi, React. Light alkane aromatization over modified Zn-ZSM-5 catalysts: characterization of the catalysts by hydrogen/deuterium isotope exchange. *Kinet. Mech. Catal.* 104 (2011) 311–312.
- [12] Y. Wang, T. Yokoi, S. Namba, J.N. Kondo, T. Tatsumi, Catalytic cracking of n-hexane for producing propylene on MCM-22 zeolites. *Appl. Catal. A* 504 (2015) 192-202.
- [13] K. Lee, S. Lee, Y. Jun, M. Choi, Cooperative effects of zeolite mesoporosity and defect sites on the amount and location of coke formation and its consequence in deactivation. *J. Catal.* 347 (2017) 222–230.
- [14] M. Guisnet, N.S. Gnep, Ethylbenzene transformation on bifunctional Pt/Al₂O₃-NaHMOR catalysts: Influence of Na exchange on their activity and selectivity in ethylbenzene isomerization. *Appl. Catal. A, Gen.* 89 (2002) 253–262.
- [15] T.E. Tshabalala, M.S. Scurrall, Aromatization of n-hexane over Ga, Mo and Zn modified H-ZSM-5 zeolite catalysts. *Catal. Commun.* 72 (2015) 49–52.

- [16] S. Tamiyakul, T. Sooknoi, L. Lobban, S.J. Jongpatiwut, Generation of reductive Zn species over Zn/HZSM-5 catalysts for n-pentane aromatization. *Appl. Catal. A, Gen.* 525 (2016) 190–196.
- [17] J.L. Hodala, A.B. Halgeri, G.V. Shanbhag, R.S. Reddy, N.V. Choudary, P.V. Rao, Aromatization of C5-rich light naphtha feedstock over tailored zeolite catalysts: comparison with model compounds (n-C5 - n-C7). *Chemistry Select* 1 (2016) 2515–2521.
- [18] C.T.O. Connor, in: G. Ertl, H. Knözinger, F. Schüth, J. Weitkamp (Eds) *Handbook of Heterogeneous Catalysis Vol. VII* Wiley-VCH Verlag GmbH & Co, Germany, 2008, pp. 3123–3133.
- [19] A. Corma, Transformation of hydrocarbons on zeolite catalysts. *Catal. Lett.* 22 (1993) 33–52.
- [20] N.K. Mal, M. Sasidharan, M. Matsukata, S. Sivasanker, A.V. Ramasawamy, *Stud. Reforming of n-hexane over Pt-Tin silicalite-1. Surf. Sci. Catal.* 154 (2004) 2403–2410.
- [21] S.J. Tauster, J.J. Steger, Molecular die catalysis: Hexane aromatization over Pt/KL. *J. Catal.* 125 (1990) 387–389.
- [22] M. Kumar, A.K. Saxena, B.S. Negi, N. Viswanadham, Role of pore size analysis in development of zeolite reforming catalyst. *Catal. Today* 130 (2008) 501–508.
- [23] J.R. Bernard, D.W. Ward, *Proc. 5th Int. Conf. on Zeolites*, Heyden, London, (1980) 686–695.

- [24] K.G. Azzam, G. Jacobs, W.D. Shafer, B.H. Davis, Aromatization of hexane over Pt/KL catalyst: Role of intracrystalline diffusion on catalyst performance using isotope labeling. *J. Catal.* 270 (2010) 242–248.
- [25] G. Jacobs, W.E. Alvarez, D.E. Resasco, Study of preparation parameters of powder and pelletized Pt/KL catalysts for n-hexane aromatization. *Appl. Catal. A* 206 (2001) 267–282.
- [26] M.N. Akhtar, N. Al-Yassir, S. Al-Khattaf, J. Čejka, Aromatization of alkanes over Pt promoted conventional and mesoporous gallosilicates of MEL zeolite. *Catal. Today* 179 (2012) 61–72.
- [27] J. Song, The effect of Fe on Pt particle states in Pt/KL catalysts. *Appl. Catal. A, Gen.* 492 (2015) 31–37.
- [28] G. Jacobs, F. Ghadiali, A. Pisanu, A. Borgna, W.E. Alvarez, D.E. Resasco, Characterization of the morphology of Pt clusters incorporated in a KL zeolite by vapor phase and incipient wetness impregnation. Influence of Pt particle morphology on aromatization activity and deactivation. *Appl. Catal. A*, 188 (1999) 79–98.
- [29] V.R. Anderson, N. Leick, J.W. Clancey, K.E. Hurst, K.M. Jones, A.C. Dillon, S.M. George, Atomic layer deposition of platinum nanoparticles on titanium oxide and tungsten oxide using Platinum(II) hexafluoroacetylacetonate and formalin as the reactants. *J. Phys. Chem. C*, 118 (2014) 8960–8970.

- [30] Q. Li, Investigation on the light alkanes aromatization over Zn and Ga modified HZSM-5 catalysts in the presence of methane. *Fuel*, 219 (2018) 331–339.
- [31] Y. Ni, W. Peng, A. Sun, W. Mo, J. Hu, T. Li, G. Li, High selective and stable performance of catalytic aromatization of alcohols and ethers over La/Zn/HZSM-5 catalysts. *J. Ind. Eng. Chem.* 16 (2010) 503–505.
- [32] H.A. Zaidi, K.K. Pant, Catalytic conversion of methanol to gasoline range hydrocarbons. *Catal. Today* 96 (2004) 155–160.
- [33] M.E. Franke, U. Simon. Solvate-supported proton transport in zeolites. *ChemPhysChem* 5 (2004) 65–72.
- [34] Y. Ni, A. Sun, X. Wu, G. Hai, J. Hu, T. Li, The preparation of nano-sized H[Zn, Al]ZSM-5 zeolite and its application in the aromatization of methanol. *Microporous Mesoporous Mater.* 143 (2011) 435–442.
- [35] Y. Ono, Transformation of lower alkanes into aromatic hydrocarbons over ZSM-5 zeolites. *Catal. Rev. Sci. Eng.* 34 (1992) 179–226.

CHAPTER 7

CONCLUSIONS AND RECOMMENDATIONS

7.1 Background

In this chapter all the findings of this work are summarized and recommendations for future work in the field of aromatization of light naphtha are listed.

7.2 Conclusions

To sum up, the aromatization reaction of low hydrocarbons paraffins (C_5-C_6) is investigated over parent and modified metal species loaded zeolite catalysts (H-ZSM-5) with (Si /Al is 30). These metals include Mo, Zn Ga, Pt, Ce and Fe with co-impregnation method of synthesis. The conversion for parent zeolite and most of bi-metallic samples is unchanged. Aromatics yield and activity of Bi-metallic is high due to two main factors acidity and dehydrogenation function of the catalytic samples which called bi-functional mechanism. H-ZSM-5(30) is responsible for the acidic medium while the metal is accountable for the dehydrogenation achievability. Based on the intellectual capacity of the catalytic characterizations, XRD patterns show crystallinity for all samples and similar to the zeolite which indicates that there is no significant presence of the metal oxides and highly dispersed metals on the support. Moreover, S_{BET} of the bi-metallic samples exhibits enhancement in the pore volume and micropores structure that is considered for the great for BTX compounds productions. In addition, NH_3 -TPD of the samples shows the behavior of the zeolite impregnated bi-metallic samples and strong acid sites appear

at high temperature range. The suppression of acidic sites enhances the production of gasoline blending component. Furthermore, the SEM shows the images and the morphology of the all samples. Among the prepared catalysts bimetallic Pt-Ga/ Z30, Mo-Ga/ Z30 and Mo-Zn/Z30 showed highest yield of aromatics (68 wt. %) (62 wt. %) with (32 wt. %) and (39 wt. %) yield of gaseous C₁-C₄ hydrocarbons respectively. Bimetallic Pt-Ga/ Z30 supported catalyst also shows a good stability towards the selective production of aromatics 58 wt. % for 24 h time on stream. Also, Mo-Zn/ Z30 exhibited excellent stability into the formation of aromatics 60 wt. % for 18 h time on stream. Furthermore, a series of parent MFI zeolite catalysts with several SiO₂/Al₂O₃ (23, 30, 50, 280, and 1500) molar ratios catalysts were investigated. The parent commercialized catalysts were evaluated for the production of aromatics. Between the all samples, MFI (30) showed highest yield of aromatics (59 wt. %) with 42 wt. % yield of gaseous C₁-C₄ hydrocarbons while MFI(280) & MFI(1500) were the lowest 11 wt. % & 7 wt. % yields of aromatics respectively. It is demonstrated that the high aromatization activity of MFI (30) is associated with nature of MFI zeolites due to acidity medium that elevate the production of aromatics. As the SiO₂/Al₂O₃ increases, the acidity of the MFI decreases dramatically. Therefore, the aromatization of light alkanes could produce effortlessly high BTX compounds over metal oxide based catalysts and a substantial alternative route to consume petrochemical and natural gas resources reforming rather than isomerization in the conversion of n-hexane feed. However, it is necessary to competence the interaction of the metal species and the acidic sites formation mechanisms of aromatics to optimize the well-performing catalyst.

7.3 Recommendations

Since the aromatization of light paraffinic naphtha is growing and evolving, several improvements could be applied to enhance desired products selectivity. First of all, tri-metallic combination of ZSM-5(SAR 30), effect of pressure and effect of the carrier gas could be studied for the light naphtha aromatization. In addition, kinetic modeling of selective catalyst sample shall be studied. Furthermore, modifications could be effective such as other supports investigations or hierarchical analysis on ZSM-5 support that might be implied in future work.

Vitae

Name	: Mohammed Osama Ellouh
Nationality	: Jordanian
Date of Birth	: 3/21/1994
Email	: mohammed.os.ellouh@gmail.com
Address	: Ba-Khashab Street Jeddah, Saudi Arabia Zip code 22331
Academic Background	: B.Sc. Chemical Engineering, (2012-2017), KFUPM, Dhahran, Saudi Arabia M.S Chemical Engineering, (2017 - 2019), KFUPM, Dhahran, Saudi Arabia
Published Papers	: M. Ellouh, H. Al-Asiri, Z. S. Qureshi, A. Aitani, M. N. Akhtar, Y. Jin, O. Koseoglu, Aromatization of light paraffinic naphtha over Pt-M/ZSM-5 tri-composited catalysts : M. Ellouh, H. Al-Asiri, Z. S. Qureshi, A. Aitani, M. N. Akhtar, Y. Jin, O. Koseoglu, Aromatization of light naphtha over Mo-M/ZSM-5 bimetallic catalysts
Achievements	: M. Ellouh, H. Al-Asiri, Z. S. Qureshi, A. Aitani, M. N. Akhtar, Y. Jin, O. Koseoglu. The effect of SiO ₂ /Al ₂ O ₃ of MFI type zeolite on light naphtha aromatization, 29th Annual Saudi- Japan Symposium, 2-3 November 2019 (Poster Session)